"RESTRAINED METAL COLUMNS"

by

Wm. B. Cranston, B.Sc.,

A Thesis Submitted for the Degree of Doctor

of Philosophy to the Faculty of Engineering of

the University of Glasgow

September 1963

ProQuest LLC.
789 East Eisenhower Parkway
P.O. Box 1346
Ann Arbor, MI 48106 – 1346

"Restrained Metal Columns"

SYNOPSIS

A review of previous research into column behaviour is made.

A general method of analysis for elastically restrained columns bent about one axis of symmetry and held against sway is described. The method was developed specifically for use on the English Electric 'DEUCE' computer, for which programmes have been prepared. In the method the column cross-section is considered as a number of strips, in which the stresses are assumed to be uniform. The stress/strain curve for the column material is approximated by a series of straight lines, while proper account is taken of the unloading of fibres strained into the plastic range. The analysis considers particular columns, studying their behaviour as loading is applied up to and through collapse.

The validity of the method is checked by comparisons with analytical and theoretical work by other authors, excellent agreement being obtained.

Tests carried out by the author on pinned steel columns, pinned aluminium columns, and restrained aluminium columns are described. Analysis of these tests is shown to give results in good agreement with the experiments, confirming the general validity of the analysis.

The results of a comprehensive series of analyses of rectangular columns of ideal elastic-plastic material are then presented. The variables considered are slenderness, degree of restraint, and magnitude and ratio of end moments. The general behaviour during loading is described. Detailed plots of collapse load values are given along with working load values calculated according to B.S. 449-1959. The load factors according to B.S. 449 are shown to be slightly below 2·0 in some cases. In most cases, however, the load factors are well above 2·0, while in some cases they are above 4·0.

Finally the major conclusions of the thesis are stated and suggestions for future research given.

CONTENTS

Acknowledgements

This thesis was prepared at the University of Glasgow under the supervision of Professor W. T. Marshall, to whom the author is most grateful for encouragement and guidance.

The work of the engineering laboratory staff in fabricating test equipment and test specimens is gratefully acknowledged, along with the assistance given by the staff of the Computing Laboratory.

The author is especially indebted to Mr H. M. Nelson of the Civil Engineering Department, discussions with whom were invaluable in solving many of the problems associated with the work, and also to Dr L. D. Savage of the Mechanical Engineering Department, who ran some of the work on the computer and gave considerable assistance in the programming details.

Finally the author thanks his wife, whose unselfishness and encouragement only he can appreciate.

INTRODUCTION

The behaviour of metal columns has been the subject of research for many years. Despite this the problem is still not fully understood, and design methods are for the most part based on empirical formulae. The development of ultimate load design methods has centred attention on the actual behaviour of structures at collapse. It is therefore necessary for a full explanation of column behaviour to be obtained before a complete ultimate load design method can be formulated.

The object of this thesis is thus to extend the knowledge of column behaviour. In view of the complexity of the problem the main emphasis of the work has been on developing a general analytical approach suitable for use on an electronic digital computer. The use of a computer has enabled a far wider range of variables to be studied than would have been practical in an experimental approach.

Chapter 1 of the thesis contains a review of previous work on columns, leading to the conclusion that the restrained column in particular requires further study.

In Chapter 2 a general method of analysis for restrained columns, developed by the author for use on an electronic computer, is described. The method has been fully developed for analysis of elastically restrained columns held against sway and bent about one axis of symmetry, and has been programmed for the English Electric 'DEUCE' computer. The stress-strain curve for the column material is dealt with in a general manner by approximating it as a series of straight lines. The cross-section of the column is divided into a series of strips, which are considered small enough for the stress in them to be assumed uniform. This enables any cross-sectional shape to be catered for, and by keeping a "strain history" for each strip, proper account is taken of material strained into the plastic range. The method also takes account of variable cross-section along the column, initial curvature, various end moment and end eccentricity combinations, and varying degrees of end restraint. Pinned columns are analysed by this method using a very low value for the restraint stiffness.

In Chapter 3 results calculated by the author's method are

checked against those calculated by the methods of other authors. The author's method is also used to analyse tests carried out by other authors. Agreement is generally excellent.

In Chapter 4 tests carried out by the author on pinned steel columns, pinned aluminium columns, and restrained aluminium columns are described. The experimental results are compared with those calculated and good agreement demonstrated.

Chapter 5 contains the results of analysis of a comprehensive range of pinned and restrained columns of ideal elastic-plastic material. The variables considered are slenderness, degree of restraint, and magnitude and ratio of end moment loading. The collapse loads are presented in interaction diagram form, while salient features of behaviour are demonstrated by detailed plots of information for some of the columns. A comparison with design criteria given in B.S.449-1959[1] is made. This shows that the load factor against collapse is in some cases below the nominal 2·0 implied in these criteria. In most cases it is above 2·0, and in many cases above 4·0.

Chapter 6 contains the conclusions of the thesis and suggestions for further research work.

CHAPTER 1

1. Review of previous work

The immense amount of work which has been carried out on columns makes it necessary to consider a selection from the more important contributions.

One of the first contributions was made by EULER[2], who in 1759 developed the simple formula which bears his name. This formula applies to centrally loaded columns in the elastic range. Since that time there have been many studies of column behaviour both in the elastic and plastic ranges. The work in each range is reviewed separately below, and a further classification is made in that pinned and restrained columns are considered separately for each range.

1.1. Pinned columns in the elastic range

Following on Euler's work it was realised that the practical column could be subjected to eccentric load, or could possess initial curvature.

SCHEFFLER[3] gave the solution for straight eccentrically loaded columns, now known as the secant formula. AYRTON and PERRY[4] proposed a method of analysis based on the assumption of an initial curvature in the column, taking the load at which the yield stress was reached as the collapse load.

ROBERTSON[5] continued this work, considering a large number of experimental tests under central axial load. He found suitable values for initial curvature which when substituted in Perry's formula indicated that the yield stress was just reached at the experimental collapse load. This formula, incorporating the values of initial curvature suggested by Robertson, has since been adopted for design use in this country. It is used on a load factor basis, the working load being a specified fraction of the load calculated to cause yield to be reached.

YOUNG[6] has developed an analysis considering the column as initially straight, with the axial load applied at unequal eccentricities at each end. STEPHENSON and CLONINGER[7] have extended this work to deal with initial curvature in addition to unequal eccentricity.

1.2. Restrained columns in the elastic range

ROBERTSON[5] has suggested the extension of his method to the restrained column, by considering it as equivalent to a pinned column of reduced or equivalent length.

The behaviour of the restrained column has been studied experimentally by BAKER[8] for the Steel Structures Research Committee (S.S.R.C.). He concluded that columns in steel building frames could be subjected to much higher bending moments than those usually considered in design at that time. Extensive theoretical studies have been carried out by BAKER & HOLDER[9] and BAKER & WILLIAMS[10, 11], again for the S.S.R.C., resulting in a design method to take proper account of the moment loading. A basic assumption in this work was that the axial load did not significantly reduce the column stiffness.

STEPHENSON[12] has presented some rigorous solutions for fixed and restrained columns, along with suggestions for design procedures. The formulae developed are complex and reference must be made to various tables when obtaining solutions.

WOOD, LAWTON & GOODWIN[13] have resolved the complexity of the problem by presenting nomograms from which solutions can be obtained. The nomograms are entered with values of the out-of-balance fixed-ended moments on the column ends, along with the ratios of the column stiffness to the stiffness of all the members framing into the column end. The value of the maximum moment in the column is then read directly from the nomogram. Nomograms are given for a range of axial load to Euler load. Several design examples are presented which illustrate the simplicity and convenience of this method.

1.3. Pinned columns in the plastic range.

One of the first contributions in this field was made by ENGESSER[14], who proposed the tangent modulus formula for centrally loaded straight columns. Following an objection by JASINSKI[15], ENGESSER[16] modified his theory to give the reduced modulus formula. VON KARMAN[17, 18] derived the reduced modulus formula independently and carried out a series of experiments which gave reasonable correlation. He also described how solutions for eccentrically loaded columns could be obtained by calculating the deflection curves of the column for various central deflections and axial loads. To obtain the deflection curves, the moment/curvature relations for specified axial loads were determined graphically and then integrated. Several

methods of integration were presented.

CHWALLA[19] continued along the lines proposed by von Karman, determining theoretically the collapse loads of a large range of eccentrically loaded steel columns, considering the effects of different types of cross-section[20], and various ratios of end eccentricity[21], Chwalla used for all his work a stress-strain diagram considered typical of mild steel. (Figure 3.6)

JEZEK[22, 23] presented an approach for rectangular section columns of ideal elastic-plastic material (Figure 3.1). He derived analytical expressions for the moment/curvature relations, and obtained solutions from the differential equations governing the deflected shape of the columns. From these solutions he derived the collapse loads for a range of pinned eccentrically loaded columns. JEZEK[24, 25] also obtained solutions assuming the deflected shape of the column to be a half-sine wave, and showed that this gave results very close to his exact solutions.

ROS[26] also adopted the assumption of a half-sine wave for the deflected shape of the column, but continued to use von Karman's approach to derive the moment/curvature relation.

WESTERGAARD & OSGOOD[27] and HARTMANN[28] adopted essentially the same approach as Ros, with the slightly different assumption of a partial cosine curve for the deflected shape of the column.

An extensive experimental and theoretical investigation was carried out by KOLLBRUNNER[29], who compared experimental results for eccentrically loaded steel and aluminium columns with analysis by the methods of Chwalla, Hartmann, and Ros. The theoretical results differed very little from each other, and agreed well with the test results.

HORNE[30] has developed techniques based on column deflection curves. By plotting properties of different wavelengths he has obtained collapse loads of rectangular columns of ideal elastic-plastic material. Another deflection curve approach, using an electronic computer for calculation, has been presented by ELLIS[31].

KETTER, KAMINSKY & BEEDLE[32] have developed a different approach to column analysis using an iterative technique due to NEWMARK[33]. The influence of residual stresses is taken into account. GALAMBOS & KETTER[34] have used this analytical approach

to obtain theoretical collapse loads of wide flange I section columns over a range of slenderness ratio and end moment ratio. They compare these theoretical results with experimental results of tests carried out at Cornell University[35], Lehigh University[36, 37], the University of Liege[38], and the University of Wisconsin[39]. Agreement is excellent in all cases except where serious lateral-torsional buckling took place. GALAMBOS[40] has provided a solution which deals with lateral-torsional buckling. KETTER[41] has presented additional results for the wide flange I section, including the case where equal end moments deflect the column into a symmetrical S shape.

While all these studies on eccentrically loaded columns were being made, a lively controversy persisted over the validity of the tangent modulus and reduced modulus formulae for centrally loaded straight columns. SHANLEY[42] has resolved this controversy, showing that for such columns the collapse load lies between the loads given by the two formulae.

The considerable difficulties in most of the analytical work referred to above have led several authors to propose various types of interaction formulae, aiming at a simple approach for the designer. CLARK[43], MASSONET[38], and AUSTIN[44], have presented studies and show that very good agreement can be obtained with test results.

1.4. Restrained columns in the plastic range

CHWALLA[45] presented the first studies in this range, using a similar approach to that used in his studies of pinned columns. He presented a small number of theoretical results for columns with varying degrees of end-restraint, and various eccentricities of applied loading.

In Great Britain the work of the Steel Structures Research Committee on a design method for steel columns[9, 10, 11] stimulated an extensive investigation of the restrained column. The results of this investigation have been summarised by BAKER, HORNE & HEYMAN[46].

The first stage was the study of columns bent about one axis only. Tests were carried out by BAKER & RODERICK[47, 48, 49] on rectangular and I section steel columns with beams welded to them. Loading was applied first to the beams which were arranged to apply either single or double curvature bending about the minor axis.

Axial loading was then applied. The beams were designed to remain elastic up to and through collapse. It was found that variation in beam loading affected the collapse loads very little, and also that the yield stress could be reached well below the maximum axial load.

An analysis for some of the tests was carried out, using theory developed by RODERICK & HORNE[50] and BAKER, RODERICK & HORNE[51] The results are presented in Chapter 14 of reference 46. The main features of the tests were explained by the theory. The theory was then used to calculate thecollapse loads about the minor axis for a range of rectangular and I section columns, making use of the EDSAC I electronic computer at Cambridge. An account of this computer work has been given by EICKHOFF[52], who has also presented some studies[67] where plasticity developed in the restraining beams. Approximate design methods suggested by RODERICK[53] were checked against this range of solutions, and one method was found to be satisfactory. This method requires that the beams of the structure be designed elastically to provide restraint for the columns which are designed on a load factor basis, the collapse load taking full advantage of plasticity in the column. Collapse is assumed to take place about the minor axis and the effects of bending about the major axis are ignored.

At this stage in the investigation the behaviour of columns bent about both axes was considered. RODERICK[54] carried out a short series of tests on I sections with restraining beams about both axes. A variety of combinations of beam loads were applied. Collapse always occurred about the minor axis, suggesting that the design method mentioned above might be suitable. However it was found that the influence of major axis beam loading could be considerable. A detailed analytical study was not attempted for these tests since the development of ultimate load design methods had made it necessary to consider the behaviour of columns when the beams had plastic hinges in them.

Where plastic hinges are present in the beams of a structure the columns may be called upon to carry all or part of the full plastic moment of the beam. In a preliminary series of tests by HEYMAN[55], I section columns were tested with major axis bending moments applied through cantilevers, simulating beams with plastic

hinges. It was found that major axis plastic hinges could form at the ends of columns.

At this point HORNE[56] made a thorough review of the problem from the ultimate load design point of view, coming to the conclusion that further progress could not be made until a basic underlying theory was developed. The work described above had shown the complexity of column behaviour in the plastic range, and that there was little immediate prospect of a satisfactory plastic design method being developed. Horne therefore proposed an elastic design method for I section columns, assuming that the beams of the structure would be determined by plastic design.

In this method it is assumed that the bending moments and axial loads can be assessed first. The column length is then checked to see that the yield stress is not exceeded under this loading. Bending about both axes is considered along with torsional instability effects. The amount of work involved in carrying out the check is consistent with design office use. In correspondence[57] on this method CAMPUS & MASSONET compared the collapse loads obtained from their tests on I section columns[38] with the loads at which first yield was forecast by Horne's theory. The comparison was satisfactory in that the collapse loads were on average 15% higher than the theoretical yield loads, although in 4 out of 63 cases they were slightly below the theoretical. It is plain therefore that this method will give an economical design provided the bending moments and axial load can be accurately assessed. Very little detail on this aspect was given but in a subsequent paper HORNE[58] has put forward specific proposals.

HORNE[59] later produced a method which allowed the development of plastic hinges at the ends of columns. A series of tests were carried out by HORNE, GILROY, NEILE & WILSON[60] which confirm the validity of this method. Curves showing allowable axial loading and slenderness ratios compatible with end plastic hinges are given in Chapter 15 of reference 46. These can be used in design.

A less comprehensive investigation has been carried out in America. BIJLAARD[61] developed an approximate theoretical approach for both equal and unequal eccentricity of axial loading, using material originally presented by CHWALLA[45]. Results from his approach gave close correlation with those of Chwalla. BIJLAARD, FISHER & WINTER[62] used a simplified version of this approximate

method to analyse experimental tests on I and square section columns. The axial load in these tests was applied at equal eccentricities at each end, bending the columns in single curvature. The experimental results confirmed Baker and Roderick's conclusion that a considerable reserve of strength could remain after first yield had been reached in the column. The theoretical collapse loads were in good agreement with those found in the experiments.

More recently a paper by OJALVO[63] presents methods of analysis for unequal eccentricities of loading, based on the column deflection curve approach.

1.5 Conclusions

The behaviour of columns in the elastic range has been almost completely explored. Rational methods[12, 13] have been developed to apply the limiting stress concept of design to pinned and restrained columns.

The behaviour of pinned columns in the plastic range, bent about one axis, is now almost fully understood. A design method for wide-flange I section columns has been proposed[64], based on work by GALAMBOS & KETTER[34]. A design method for I section columns with end plastic hinges has been proposed by BAKER, HORNE & HEYMAN[46].

The behaviour of the restrained column in the plastic range is still, however, not fully understood, and it is only recently that much attention has been centred on it. BLEICH[65] in a review of research on column behaviour (published in 1952) pointed out the need for research in this field. His remarks prompted the work of BIJLAARD, FISHER & WINTER[62]. A reflection of the lack of knowledge of the restrained column can be found in a recent (1960) publication[66] by the Column Research Council (U.S.A.) in which only 3 pages out of 83 are devoted to columns in frames.

Two basic conclusions can be drawn from the work already carried out on restrained columns. The first is that the presence of restraint can greatly enhance the carrying capacity of the column. The second is that restrained columns can possess a marked reserve of strength beyond the point at which first yield is reached. It follows therefore that elastic design procedures may be excessively conservative.

The most recent proposals[56], however, recommend that columns in framed buildings be designed on an elastic basis.

The major effort of this thesis is directed at the behaviour of the restrained column, in order to make a thorough assessment of what can be gained by providing restraint, and what is demanded of the restraining members. The approach is predominantly analytical, although experiments have been carried out to check the validity of the analysis.

CHAPTER 2

2. General method of analysis for restrained columns

A review of existing methods of column analysis is made, followed by a description of the work leading to the analysis developed by the author. A description of this analysis is then given with a discussion of the particular case where the column is bent in symmetrical double curvature. Some remarks on convergence of the analytical procedures are made. The chapter concludes with some details of the computer programmes which were written to carry out the analysis. Further details of the analysis and the programmes are given in Appendix 2.

2.1. Review of existing analytical methods

The first stage in any rigorous method of analysis is to find the moment/curvature relation for the column cross-section. The curvature is a linear function of the moment in the elastic range, but in the plastic range it becomes a complicated function of the moment and axial load. Analytical expressions can be derived[22] for simple geometric shapes and stress-strain diagrams, but in general graphical or numerical methods must be employed. In reference 19 a typical method is shown. The results of these graphical methods are usually presented as plots of curvature against moment, for specific values of axial load. By interpolation the curvature due to a given moment and axial load can be found.

When the moment/curvature relation is known the differential equations governing the shape of the column can be set up. Where analytical expressions for the moment/curvature relation have been obtained the differential equations can sometimes be solved by formal mathematics[22, 30]. In general this is not the case, and the solutions must be obtained by numerical procedures. Two distinct methods have been developed.

The first is due to VON KARMAN[18] and is based on column deflection curves. Column deflection curves are obtained by numerical or graphical integration of the moment/curvature relation, assuming different boundary conditions, and integrating along the curve by a step by step process. By obtaining a series of curves for specified values of axial load, the range of possible configurations for a

column length can be covered. The boundary conditions for any particular problem can be fitted to the curves, and the deflected shape of the column for various specified axial loads obtained. From this the load/deflection curve can be obtained. This curve rises initially while the column is in the elastic range but as plasticity develops it rises less and less steeply until eventually a peak is reached, after which it begins to fall. A typical example is shown in Figure 2.4. When several points on such a curve have been obtained the peak load can be obtained reasonably accurately. EICKHOFF[52] gives a more refined technique whereby column lengths, which define a peak point on a load/deflection curve, can be picked directly off a column deflection curve.

This method has several disadvantages. It can only be generally applied to sections symmetrical about the axis of bending, and it cannot take account of initial curvature, or unloading of material strained into the plastic range.

The second method is due to KETTER, KAMINSKY & BEEDLE[32], and is based on work by NEWMARK[33]. At a given stage in the analysis of a column the deflected shape of the column and the loading on it are assumed. Using these assumptions the bending moment and axial load at various points along the column are calculated. The curvature at each of these points follows from the moment/curvature relation. Integrating these curvatures gives a calculated deflected shape. If this is the same as the one assumed then a correct solution has been obtained. If the calculated shape is not the same, modifications are made to the initial assumptions and the process repeated as often as necessary. By obtaining solutions for several deflections a load/deflection curve can be drawn up from which the maximum load can be picked off.

This second method is much more flexible than the first, although the calculations are lengthy To the author's knowledge, only the first method has so far been applied to analyse restrained columns.

2.2. Work leading to the author's analysis

The first attempts at analytical solutions were made after performing the tests on rectangular steel columns described in § 4.1. A moment/curvature chart was prepared assuming ideal elastic-plastic material, and a method similar in principle to the second

method above was used. The analysis was carried out under end moment loading only first. The axial load was then found which increased the deflection of a particular point in the column by a specified amount. This was repeated giving the axial load at steadily increasing deflections until the peak of the load/deflection diagram was reached. By finding the load corresponding to a deflection certain convergence difficulties were avoided.

After analysing several of the tests by hand, the use of the English Electric 'DEUCE' computer was investigated. A computer programme, using autocode facilities, was written to analyse pinned columns of ideal elastic-plastic material. This programme was used to obtain theoretical collapse loads for some of the tests mentioned above.

Considerable difficulties were experienced with analysis of some of the columns, and eventually it was decided to formulate a more general approach capable of dealing with restrained columns. The ideas for this general approach, which is described below, were derived only after the author was familiar with the capabilities of the computer.

2.3. General method of analysis for restrained columns

The system analysed in shown in Figure 2.1. The supports at A and B prevent sway movement of the column ends, while providing elastic rotational end restraints. The column may be initially curved. The column length L* is divided into N equal segments of length λL. The cross-section properties at the division points between these segments are used in the analysis. They may vary from one division point to another.

The loading consists of two moments M_A and M_B and an axial load P which can act at arbitrary eccentricities. M_A and M_B are assumed to be applied to the system first and an analysis for this is carried out. The application of P is then considered, M_A and M_B remaining constant, and values of P determined at various values of column deflection. The line of action of P is assumed to remain the same during loading.

Collapse of the column is assumed to occur by bending in the

---

* All symbols are defined in the text where they first appear, and are in addition collected together in Appendix 1.

plane of Figure 2.1. This bending must take place at right angles to an axis of symmetry. Local and lateral instability are thus neglected.

The assumptions on which the analysis is based are as follows:-

1. Plane sections remain plane after bending
2. Cross-section dimensions are unaffected by loading
3. The stress/strain relation for the column material is known
4. Material strained into the plastic range and subsequently unloaded follows a line on the stress/strain diagram parallel to the initial slope of the diagram.
5. Deflections of the column are small in comparison to its length
6. Deformation due to shearing forces can be neglected

The analysis is based on the second method described in § 2.1 above, although it incorporates a new approach to the determination of the curvature corresponding to a given moment and axial load. Details of this approach are given below, followed by a description of the analysis under end moments only. A description of the analysis under axial load and end moments is then given and finally a short discussion on the convergence of the analytical procedures is made.

Only the principles of the methods are described, full mathematical details being given in Appendix 2.

2.3.1. Determination of curvature

It is necessary in this method of analysis to determine the curvature corresponding to a given axial load P and moment M. Previous authors have usually done this by visual interpolation from charts. A more general approach was developed by the author.

The cross-section is divided into a number of strips parallel to the axis of bending as shown in Figure 2.2a, while the stress/strain curve for the column material is approximated by a series of straight lines as in Figure 2.3. To determine the curvature an iterative procedure is used. A strain distribution (Figure 2.2b) across the section is assumed and the stress at the centre of each strip is picked off the stress/strain curve. The stress in each strip is assumed to be uniform. The loads P_c and M_c corresponding

to the strain distribution are calculated and compared with the values P and M actually proposed on the cross-section. If the differences between the calculated and proposed loads are not within specified limits the strain distribution is modified. By considering the effects of small changes in the strain distribution a set of equations is drawn up from which the required modifications are obtained. The process is repeated until the differences between the calculated and proposed loads are within the specified limits. The value of curvature associated with the strain distribution is then taken as correct.

Unloading of material strained into the plastic range is allowed for by noting the maximum strain to which a particular strip has been subjected and comparing it with the strain currently proposed.

2.3.2. Analysis under end moments M_A and M_B only

For this stage of the analysis assumptions are first made for the moments M_{AB}, M_{BA} on the column length. The bending moments at each division point along the column are calculated and using the procedure described in § 2.3.1. above, the curvatures are obtained. These curvatures are integrated to give calculated deflections at each division point and calculated end rotations $(\theta_A)_c$ and $(\theta_B)_c$, the suffix $(\ )_c$ indicating calculated values. The compatibility of the end rotations must be checked, the necessary conditions for this being:-

$$\left.\begin{aligned}(\theta_A)_c &= (M_A - M_{AB})\,k_A \\ (\theta_B)_c &= (M_B - M_{BA})\,k_B\end{aligned}\right\} \quad \ldots\ldots\ 2.1$$

where k_A, k_B are the rotations/unit moment of the restraining systems at A and B. The L.H. sides of equations 2.1 give the column rotations, while the R.H. sides give the rotations of the restraining systems.

The check is conveniently carried out by calculating quantities γ_A and γ_B, defined by the following equations:-

$$\left.\begin{aligned}\gamma_A &= (\theta_A)_c - (M_A - M_{AB})\,k_A \\ \gamma_B &= (\theta_B)_c - (M_B - M_{BA})\,k_B\end{aligned}\right\} \quad \ldots\ldots\ 2.2$$

From equations 2.1 γ_A and γ_B should be zero. If they are sufficiently small, the values of M_{AB} and M_{BA}, along with the calculated deflections and rotations, are taken as correct. If, on the other hand, γ_A and γ_B are too large, modifications to the assumed values of M_{AB} and M_{BA} must be made. The modifications are obtained from a set of equations which are drawn up by considering the effects of small changes in M_{AB} and M_{BA} on γ_A and γ_B.

The process is repeated with new values of M_{AB} and M_{BA} until γ_A and γ_B are sufficiently small.

2.3.3. Analysis under axial load and end moments

This analysis is carried out at various stages, the deflections of the column increasing between each stage. Some point along the column is chosen as a reference point and solutions found such that the reference point deflection D_R is increased by a specific fraction between successive stages.

At the beginning of the analysis for a particular stage trial assumptions are made for P, M_{AB}, M_{BA}, and for the deflections $(D_o)_a$, $(D_1)_a$, $(D_2)_a$ ..... $(D_N)_a$, at each division point. The bending moment at each division point is calculated. The curvatures are obtained and integrated to give calculated deflections $(D_o)_c$, $(D_1)_c$ ..... $(D_N)_c$, and calculated end rotations $(\theta_A)_c$ and $(\theta_B)_c$.

The comparison between assumed and calculated values is made in two steps a) and b) as follows:-

a) γ_A and γ_B are calculated from equations 2.2 and the difference Δ_R between the assumed and calculated reference point deflection is also calculated, i.e.

$$\Delta_R = (D_R)_c - (D_R)_a \qquad \ldots\ldots\ldots 2.3$$

If a valid solution has been assumed γ_A, γ_B, and Δ_R will be zero. If they are not below certain specified small values, the values of P, M_{AB}, and M_{BA} are modified. The effects of small changes in P, M_{AB}, and M_{BA} on γ_A, γ_B, and Δ_R are calculated, and a set of equations drawn up the solutions to which give the required modifications.

The calculations are then repeated until γ_A, γ_B and Δ_R

a) are within the specified small values. Only then is step b) of the comparison procedure carried out.

b) The assumed and calculated deflections at each division point are compared. If a valid solution has been assumed the values should be the same. If the differences are not below a specified small value the calculated deflections are taken to be nearer the solution.

NEWMARK[33] gives references to mathematic proofs of this for elastic columns. These proofs can be taken to apply to columns in the plastic range provided the degree of plasticity is not affected much by the changes in deflection, since a plastic cross-section can then be considered as elastic with a reduced stiffness.

After substituting the calculated deflections to become new assumed deflections, the calculations are repeated without modifying P, M_{AB}, and M_{BA}.

The calculation of bending moment curvature, and deflections, with subsequent modifications either to P, M_{AB}, and M_{BA}, or to $(D_o)_a$, $(D_1)_a$ ..... $(D_N)_a$, is thus repeated until both checks under a) and b) above are satisfied. The values of P, M_{AB}, M_{BA}, and $(D_o)_a$, $(D_1)_a$ ..... $(D_N)_a$ are then taken to give a correct solution.

The solutions at various stages enable a curve of axial load P versus reference point deflection D_R to be drawn. A typical curve is shown in Figure 2.4. The collapse or failure load P_F is reached when this curve reaches its peak.

2.3.4. Convergence of procedures

The iterative procedures described above may not converge if the assumed values are very different from the true values. Where convergence trouble is experienced the remedy is to cut down the increases in deflection between stages of the analysis. This enables a more accurate estimate of the conditions for the next stage to be made.

With very stocky columns ill conditioning of the equations which give the modification to P, M_{AB}, and M_{BA} can arise. It is probable that a different approach is necessary for such cases.

This is dealt with more fully in Appendix 2, along with other convergence problems.

2.4. Analysis of the special case with bending in symmetrical double curvature

The practical column will always exhibit some imperfection such that the loading on it will never be truly symmetrical. It is, however, of interest to study the symmetrical case, if only to assess how initial imperfections modify the behaviour.

Figure 2.5a shows a typical loading in symmetrical double curvature. In the initial stages of loading the deflections will be the same for both halves of the column, and the analysis is carried out on an equivalent half-column as shown in Figure 2.5b. At some stage in the application of load "unwinding" can take place. This has been demonstrated practially by BAKER and RODERICK[49], and theoretically by BIJLAARD[61]. This "unwinding" is shown in Figure 2.5c. It can be considered as a superimposed deflection as shown in Figure 2.5d.

The condition for "unwinding" to begin is that the critical load associated with the superimposed deflection is equal to the actual load on the column. To calculate the critical load the values of instantaneous stiffness at each division point must be calculated. The calculation of instantaneous stiffness is described first below followed by details of the calculation of critical load.

2.4.1. Calculation of instantaneous stiffness

If "unwinding" begins under constant axial load the only change which occurs at a division point is an increase or decrease in bending moment. If the cross-section at a particular division point is plastic the stiffness will depend on whether the moment is increasing or decreasing. Where the moment increases the stiffness is obtained from information obtained in the curvature calculation. Where the moment decreases some unloading of fibres strained into the plastic range occurs and a close approximation to the stiffness is given by the original elastic stiffness.

If, however, "unwinding" begins during a slight increase of axial load, it is possible for the unloading due to reduction in moment to be inhibited and the stiffness at all division points

must be calculated assuming the plastic zones to remain active.

These two criteria for determining stiffness are similar in principle to those used in determining the reduced modulus load and the tangent modulus load for centrally loaded straight columns. SHANLEY[42] has shown that lateral movement for such columns will begin at the tangent modulus load, the actual collapse loads lying between the tangent modulus loads and reduced modulus loads. It may therefore be concluded that the actual collapse loads of columns bent in symmetrical double curvature will lie between the "unwinding" loads calculated from the two criteria above.

The first criterion mentioned above will be referred to as the von Karman criterion and the second as the Shanley criterion.

2.4.2. Calculation of critical load

The calculation for the critical load is very similar to that described in § 2.3.3. for axial load and end moment loading. The deflected mode of the column is assumed taking the reference point deflection as an arbitrary value. The critical load is estimated along with end moments compatible with the expected end rotations. The bending moment at each division point is calculated and the curvatures calculated using the appropriate instantaneous stiffnesses. Integration of the curvatures gives calculated deflections and end rotations. The comparison and modification procedures then used are exactly the same as those described in § 2.3.3. above. The procedure is repeated until the calculated deflections are reasonably close to the assumed deflections, and the calculated end rotations are compatible with the assumed end moments.

In the elastic range the elastic critical load P_{CR} will be obtained. When plasticity develops in the column the critical load calculated will be less than the elastic critical load and will be termed the reduced critical load P'_{CR}.

2.4.3. Summary of overall analysis for columns bent in symmetrical double curvature

An analysis for the equivalent half-column shown in Figure 2.5b is carried out as described in § 2.3 above. After each stage the reduced critical load of the column is calculated. When the reduced critical load is below the actual the point of "unwinding" has been passed. By plotting a load/deflection curve the point where the

reduced critical load is equal to the actual load on the column can be estimated giving the "unwinding" load.

The reduced critical loads can be obtained using either the von Karman or the Shanley criterion to obtain the instantaneous stiffnesses. The resulting "unwinding" loads will thus be referred to as the von Karman or Shanley "unwinding" loads as appropriate.

2.4.4. Further consideration of reduced critical load

The reduced critical load P'_{CR} can be calculated for any column at any stage of loading. At the peak of the load/deflection curve (Figure 2.4) the column is in neutral equilibrium and thus P'_{CR} must be exactly equal to the load P on the column. Beyond the peak the column is in ~~the~~ unstable equilibrium and P'_{CR} must fall below the load P.

The calculation for P'_{CR} has been included in the computer analysis for the general case and provides a convenient criterion for terminating the analysis, i.e. when $P'_{CR} < P$. In addition the mode of deflection associated with P'_{CR} has proved useful in forecasting the response of the column to increases in axial load.

2.5 Computer programme details

The analysis has been programmed for the English Electric 'DEUCE' computer. Two programmes have been prepared, one for the general case of analysis as outlined in §§ 2.3, and the other for the special case bent in symmetrical double curvature as outlined in §§ 2.4. For the latter case the von Karman load is calculated. The programmes are very similar and are written in the basic machine code using fixed point arithmetic procedures, thus taking full advantage of the speed of the computer.

The programmes occupy $7/16$ of the 8192 word magnetic drum store, while the data can occupy up to $5/16$ of the store. This caters for dividing the column into up to 29 segments, giving 30 division points. At each division point the cross-section can be divided into any number of strips up to 15. The stress/strain curve is approximated by up to 10 straight lines, the same curve being taken to apply in tension and compression. The programmes take account of unloading although a simple modification will cause it to be neglected.

To calculate the Shanley loads for the cases of symmetrical double curvature an auxiliary programme has been written to calculate critical loads only. This auxiliary programme is for a Ferranti 'SIRIUS' computer and is written in SIRIUS autocode.

These three programmes will be referred to in the following chapters as the general, special and auxiliary programmes respectively.

Further details of the computer programmes, including written flow diagrams, are given in Appendix 2.

2.5.1. Programme operation

The input data for the 'DEUCE' programmes consists of the following:-

1. Data for stress/strain curve
2. Data for cross sections at each division point
3. Initial eccentricity at each division point
4. Segment length and location of reference division point
5. End moments M_A and M_B, and K_A and K_B, the rotations of the restraining systems per unit moment

The computer will normally carry out automatically the complete analysis of a problem right up to collapse. If convergence trouble is experienced restore control facilities and various "post-mortem" facilitie are available.

The output for each stage gives first of all values of bending moment, curvature, and deflection for each division point along the column, followed by the axial load and end rotations. When the collapse load is being approached a strain history is also punched out, giving the maximum strains to which each cross-section has been subjected. If desired this strain history can be obtained at every stage in the analysis.

The output for the reduced critical load calculations gives first of all values of stiffness and deflection at each division point followed by the reduced critical load, end rotations, and end moments.

The time taken for an analysis with 14 segments lies between 10 and 60 minutes, an average value being 20 minutes.

For the auxiliary programme in SIRIUS autocode the input

consists of:-

1. Segment length and location of reference division point
2. Instantaneous stiffness values at each division point

The instantaneous stiffness values form part of the output obtained from the special 'DEUCE' programme which determines the von Karman "unwinding" load.

The output from the auxiliary programme consists of the reduced critical load, deflection of each division point and the end moments.

CHAPTER 3

3. Checking validity of analysis

In the first section of this chapter results from rigorous theory developed by HORNE[30] for the rectangular cross-section of ideal elastic-plastic material are used to check the author's methods of calculating and integrating curvature.

In the second section analytical solutions for the collapse loads of restrained columns given by CHWALLA[45] and BAKER, HORNE, & HEYMAN[46] are compared with the solutions obtained by the author's analysis.

In the third section experimental and theoretical collapse loads for restrained columns given by BAKER, HORNE, & HEYMAN[46], and BIJLAARD, FISHER, & WINTER[62], are compared with the loads obtained from the author's analysis.

Finally, comparisons made with work by CHWALLA[19, 20] and CLARK[43] on pinned columns are described and general conclusions are drawn.

3.1. Accuracy of numerical procedures

The possible errors in the numerical procedures for calculating and integrating curvature are discussed separately below, along with the effects of these errors on the overall analysis. The rectangular cross-section of ideal elastic-plastic material is considered. To obtain rigorous analytical solutions theory presented by HORNE[30] is used. In the following the results from the author's numerical procedures will be referred to as calculated values while those obtained from Horne's theory will be referred to as true values.

3.1.1. Accuracy in calculating curvature

Errors can arise from approximating the stress/strain curve as a series of straight lines, and from dividing the cross-section into strips. Since the stress/strain curve for ideal elastic-plastic material (Figure 3.1) is made up of straight lines, only errors due to division into strips are considered here. The number of strips considered is 15 this being the usual value used in the computer programme. A typical comparison between the true stress diagram and that due to division into strips is shown in Figure 3.2.

The error involved in calculating the curvature corresponding

to a given axial load and bending moment varies considerably depending on the degree of plasticity present. Where the cross-section is elastic the calculated value of curvature always exceeds the true value by ·45%. When, however, the curvature is in the region of five times the yield curvature the calculated values can differ from the true values by as much as 20%. The calculated values can be less than or greater than the true values with a tendency to be greater.

A more serious fault in the numerical procedure is that when the true curvature exceeds 7·5 times the yield curvature, it is possible that no solution will be obtained. This is because at least two strips in the cross-section must retain some stiffness in order that the equations mentioned in § 2.3.1. above will yield solutions. Higher curvatures can be dealt with by dividing the cross-section into more strips.

The effects of the errors on the overall analysis will now be assessed. The basic analytical procedure is to find assumed loads and deflections which give bending moments and curvatures, which when integrated give deflections close to the ones assumed.

In the elastic range the loads on the column will tend to be underestimated by about ·5%, since the curvatures due to a particular moment are overestimated.

In the plastic range the effects on the overall analysis are more difficult to assess, but some idea can be gained from the following reasoning. Assume in a particular case, where the curvature values are high, that the true values for load and deflection have been assumed. In calculating the curvature errors up to say 20% will be present. The integration process will thus yield values of deflection which will be too large or too small. The modification procedures will then introduce alterations to the loading to reduce the errors. The magnitude of these alterations will depend on how sensitive the curvature is to changes in axial load and bending moment. Figure 3.3 shows the interaction between axial load, bending moment, and curvature for the rectangular cross-section of ideal elastic-plastic material. It will be seen that where the curvature values are high small changes in either axial load or moment induce large changes in the curvature. Thus in the particular problem considered only very small modifications to the loading will be

necessary to bring the calculated deflections close to the assumed ones. The calculated loads will therefore be very close to the true loads. The curvature diagram which yields these correct calculated deflections may be in error but not to any great extent since any errors must be compensating, i.e. if a large error exists at one division point errors in an opposite sense must be present at other division points.

It may be concluded that errors in the numerical procedure for calculating curvature will not seriously affect the overall analysis. The consequences of not being able to deal with very high curvatures are dealt with after discussing the accuracy of the integration procedures.

3.1.2. Accuracy of integration procedure

The method used is due to NEWMARK[33]. It involves dividing the column length into a number of equal segments. The curvatures at each division point are first obtained and then integrated twice to give deflections. The integration process requires the computation of "concentrated angle changes" at each division point. These are calculated assuming the curvature diagram to follow a parabolic curve through the two adjacent division points.

To check the method, curvature and deflection diagrams have been prepared for several column deflection curves, using the equations given by HORNE[30]. These true diagrams have been obtained for an axial load of 0·6 P_p, where P_p is the load to cause the yield stress to be reached over the whole cross-section, and various values of maximum curvature. Details of the column cross-section and some of the curve properties are given in Figures 3·4 (a) and (b). The curvature and deflection diagrams, along with plots of plastic zones, are given in Figure 3·5(a) through (e).

Integration of the true curvature diagrams was carried out dividing the half-wave-length into 10 segments, this being typical of the computer programme. The values of calculated deflection obtained are shown on each deflection diagram for comparison with the true values.

It will be seen that as plasticity develops the curvature diagram takes on a localised peak. This is the reason for the calculated deflections being seriously in error for $\phi_o/\phi_y = 5·0$

and ϕ_o/ϕ_y = 10.0. For values of ϕ_o/ϕ_y = 2·50 or lower the errors are of the order of 0·1%. The calculated deflections tend generally to be larger than the true deflections although this need not always be the case.

The effects of these errors on the overall analysis can be assessed by finding the axial loads, which when combined with the true deflections, will give calculated deflections close to the true deflections. This has been done for the cases where ϕ_o/ϕ_y = 5·0 and ϕ_o/ϕ_y = 10·0, giving P = 0·5985 P_p and 0·5983 P_p respectively. These values compare very favourably with the true value of 0·6 P_p. The values for calculated maximum curvature fall to ϕ_o/ϕ_y = 4·5 and ϕ_o/ϕ_y = 6·7 respectively, showing considerable discrepancies from the true values.

Thus it can be concluded that the errors in the integration procedure will lead to negligible error in calculating loads for a given deflection; but the values of curvature obtained can show considerable error. This error is unlikely to exceed 10%, where the curvature is less than five times the yield curvature, and will be negligible where the curvature is less than 2·5 times the yield curvature.

3.1.3. Plastic hinges in columns

Horne's theory shows that plastic hinges can form in columns of ideal elastic-plastic material, implying the presence of infinite curvature. Since the curvature calculation will not function above ϕ_o/ϕ_y = 7·5, plastic hinge action cannot be dealt with.

This is not a serious practical limitation since the curvature calculation will deal with very high curvatures when the stress/strain curve follows the smooth "rounded knee" curve typical of metals. If the strain hardening of mild steel is taken into account again very high curvatures can be dealt with.

3.2. Comparison with analytical solutions for end-restrained columns

3.2.1. Comparison with work of CHWALLA[45]

Chwalla has given details of rectangular restrained columns which will fail at an average axial stress of 1500 Kg/cm^2. The stress/strain curve for the column material is shown in Figure 3·6, along with the points chosen to represent it in the author's analysis. Two columns were selected for analysis from Figures 2 and 4 of

Reference 45. The cross-section was divided into 15 strips and the column into 14 segments. The analysis was carried out with the general 'DEUCE' programme both neglecting and considering unloading. Stress/deflection curves for the cases neglecting unloading are shown in Figure 3.7, from which it will be seen that the average axial stresses at collapse obtained from the author's analysis are very close to 1500 kg/cm^2.

The analysis taking account of unloading indicated that it did occur in limited zones towards the ends of the columns, raising the collapse loads by less than 1%.

3.2.2. Comparison with work of BAKER, HORNE, and HEYMAN[46]

The results chosen from this work are shown in Figure 14.19(a) of Reference 46, which gives collapse loads for a range of rectangular section columns of ideal elastic-plastic material, bent in symmetrical single curvature. A copy of this figure is shown in Figure 3.8 with collapse loads obtained by the author's analysis plotted on it. The analysis was carried out dividing the cross-section into 15 strips and the column into 14 segments, while the stress/strain curve was taken as two straight lines (Figure 3.1). Unloading was not considered.

It will be seen from Figure 3.8 that agreement is excellent.

3.3. Analysis of tests on restrained columns

3.3.1. Tests described by BAKER, HORNE, and HEYMAN[46]

These tests are a selection from those carried out by BAKER and RODERICK[47, 48, 49]. Abstracts of the main data are given in Tables 13.1 and 13.2 of Reference 46, along with some theoretical results obtained using the rigorous theory due to HORNE[30]. The restraints were provided by beams welded to the columns, which were of mild steel, and moment loading was applied first by loading these restraining beams. This usually induced a considerable axial load in the column. Further axial load was then applied through a stub column projecting above the beams, leaving the beam loads constant. The axial load was increased until collapse occurred. The experimental collapse loads for the rectangular section columns are plotted against beam load in Figure 3.9. The theoretical collapse loads obtained from Horne's rigorous theory are also shown.

Initially it was thought that the author's analysis could not be applied to these tests since the line of action of the axial load varied throughout the tests, and also the beam depths were large in comparison to the column length. It was however found possible to calculate modified restraint stiffnesses which took account of these factors. A further discrepancy between test and analysis is that the author's analysis assumes the moment loading to be applied under zero axial load. It is considered that the effect of this will not be great.

The column material was mild steel and thus could be considered as ideal elastic-plastic. Specific analysis was not carried out, the collapse loads being obtained by interpolation from the results for columns of ideal elastic-plastic material, presented in Chapter 5. These results were obtained including the effects of unloading. Curves of theoretical collapse load against beam load are shown in Figure 3.9.

For the columns bent in single curvature the agreement between theory and experiment is good, while the two loads calculated from Horne's rigorous theory are very close to the author's curves.

For the columns bent in double curvature the agreement between theory and experiment is also good, but there is considerable disagreement between the loads calculated by Horne's theory and the author's analysis. Horne's theoretical results have been obtained neglecting unloading apart from a single analysis. This single result is in good agreement with that obtained from the author's analysis. The discrepancies in the other cases are almost certainly due to the neglect of unloading.

3.3.2. Tests carried out by BIJLAARD, FISHER and WINTER[62]

Tests were carried out on $1\frac{1}{2}$" square mild steel bars, and on 4 I 9·5 lb mild steel beam sections. Both annealed and unannealed specimens were prepared. Typical stress/strain curves were presented in Figure 12 of Reference 62 a copy of which is given as the author's Figure 3.10 (a). Figure 3.10(b) shows the curves which were used in the computer analysis. The restraint was provided by spring systems while the axial load was applied at specified initial eccentricities.

For the computer analysis the square bar cross section was divided into 15 strips. The I section was bent about the minor axis and the cross section was again divided into 15 strips, 3 taking up the web of the section, and the other 12 taking up the

projecting flanges. In both cases the columns were divided into 14 segments. The general 'DEUCE' programme was used, taking account of unloading. The column was assumed to be uniform in cross-section thus neglecting the rigid end block assemblies. The effect of this on the results would be small, particularly since plasticity did not develop at the ends of the columns to any serious extent. The computer analysis revealed that strain hardening should have occurred in tests 3AI, 14UI, 9AS, and 19US, i.e. in all the tests with large eccentricities. Except for the test 3AI, the effect on the collapse load was negligible.

The comparison between theory and experiment is presented in Figure 3.11. It will be seen that the author's analysis tends to overestimate the carrying capacity slightly, while the approximate analysis of Bijlaard et al. tends to underestimate. The agreement is however very good.

3.4. Comparisons with work on pinned columns

The analysis developed in chapter 2 is specifically for restrained columns. A similar, somewhat simpler, analysis can be developed for pinned columns, and it was thought initially that a separate computer programme would have to be written for this. It was, however, found possible to use the restrained column programme for pinned columns by setting the restraint stiffnesses to very low values.

CHWALLA[19, 20] has presented results for eccentrically loaded pinned columns of various cross-sections. Four rectangular section columns and four Tee section columns from this work have been analysed using the general 'DEUCE' programme. The columns were divided into 14 segments. The rectangular section was divided into 15 strips and the Tee section into 14 strips, two taking up the flange and 12 taking up the stem. In all cases the collapse loads agreed to within 1% of the loads given by Chwalla.

CLARK[43] has presented experimental results for eccentrically loaded pinned aluminium columns of rectangular and rectangular tubular cross-section. For analysis again using the general 'DEUCE' programme the columns were divided into 14 segments and the rectangular cross-section was divided into 15 strips. The tubular section was also divided into 15 strips, 6 taking up the walls parallel to the

axis of bending and the other 9 taking up the walls at right angles. Some of the tests were carried out under central loading and no attempt was made to analyse these. The theoretical collapse loads obtained were all within 3% of the experimental loads.

For one test Clark presented a load/deflection curve and load/strain curves for the centre of the column. The author's analysis for this test gave curves which practically coincided with those given by Clark.

3.5 Conclusions

The numerical procedures of the author's analysis give accurate results except where curvature values are very high. In particular the procedures will not deal with fully plastic hinges.

The analysis gives results in very good agreement with previous analytical studies. The analysis of several sets of tests gives theoretical collapse loads in good agreement with the actual test loads. Both steel and aluminium columns of various types of cross-section have been analysed.

For restrained columns the effects of unloading on the collapse loads are very slight for cases bent in single curvature but can be significant for cases bent in double curvature. The author's analysis taking account of unloading agrees well with a rigorous analysis by Horne.

4. Experimental tests by the author

Three sets of tests are described, the first on pinned rectangular mild steel columns, the second on pinned rectangular aluminium columns, and the third on restrained rectangular aluminium columns. Analysis has been carried out for each set of tests. The tests, results of analysis, and discussion for each set are presented under separate headings below.

The manufacture of the columns, details of test rigs, and details of experimental procedure are dealt with briefly, since a full account of this is given in Appendix 3.

4.1. Tests on pinned rectangular steel columns

4.1.1. Experimental details

66 $\frac{1}{4}$" x $\frac{1}{2}$" mild steel columns of various lengths were tested under loadings designated as cases (a), (b), and (d), shown in Figure 4.1. The moments were applied about the minor axis through a pulley and lever system. The axial load was applied through knife-edges, the actual load being obtained from a lever system. Moment loading was added first and left constant as the axial load was applied in increments until collapse.

The yield stress for all the specimens was found to be close to 19 T/in^2, and using this value P_p and M_p for each column length were calculated. Dividing the experimental collapse loads P_F by P_p and the experimental end moment M_A by M_p gave values for the non-dimensional plots of results shown in Fig. 4.2.

4.1.2. Analysis of tests

Theoretical collapse loads have been obtained by interpolation from the results for columns of ideal elastic-plastic material presented in Chapter 5. As mentioned in Chapter 2 some of these tests had been analysed by an early autocode programme. No significant differences between the results were found.

For the analysis the yield stress was taken as 19 T/in^2 and E as 13,400 T/in^2.

For the case (d) loading in symmetrical double curvature the Shanley loads have been taken. The differences between the Shanley

and von Karman loads are at the most 3%. For some of the case (d) loadings, the theoretical collapse loads were not governed by "unwinding", but by the formation of plastic hinges at the ends of the column. End plastic hinges can also form for case (b) loading, although none of the tests were governed by this criterion.

Some analysis for case (a) loading taking account of an upper yield stress of 1·35 times the lower yield stress was carried out. For reasons given in Appendix 2 analysis with upper yield was difficult and no attempt was made to cover the full experimental range.

The theoretical collapse loads are presented non-dimensionally as interaction curves on Figure 4.2 giving a direct comparison with the experimental collapse loads. The results including the effects of upper yield are shown by a dashed line.

4.1.3. Discussion

It will be seen that the experimental collapse loads are generally above the theoretical collapse loads more especially for the case (b) and (d) loadings. The following factors could lead to higher values.

(a) Upper yield

Beam tests carried out to determine the lower yield stress indicated a value of upper yield about 1·35 x the lower yield stress. The results of analysis taking account of upper yield show that it has a considerable effect on the collapse load.

(b) Rigid end pieces

The axial and end moment loading arrangements resulted in a considerable length at the ends of the columns being effectively rigid. This affects the case (a) loading very little but cases (b) and (d) would be seriously affected especially for the shorter column lengths.

(c) Friction in the loading system

At collapse rotation is taking place in the various knife-edge seats and pivots of the loading system thus mobilising some frictional restraint. This is not considered to be of much importance for case (a) and (b) loadings but case (d) loading could be seriously affected.

In the author's opinion these factors are sufficient to explain the discrepancies between the theoretical and experimental results.

4.2. Tests on pinned rectangular aluminium columns

4.2.1. Experimental details

The columns were manufactured from ¼" thick HE30 WP alloy plate. A typical stress/strain curve for the material is shown in Figure 4.3. Columns of ¼" x ½" section were made up in various lengths.

The test rig for applying axial load consisted of two loading heads which were inserted in an "Olsen" 200,000 lb capacity testing machine. Rotational freedom was provided by ball bearings. Special end fittings allowed the column to be accurately adjusted in position with respect to the loading heads. Small levers were attached to these fittings and end moments applied through them. The centres of rotation of the loading heads were arranged to be at the points where the column emerged from the end fittings. The columns were thus pinned and of uniform cross-section. The effective lengths of the columns tested were 7·24", 5·12" and 3·62".

Tests were carried out for the three cases of loading shown in Figure 4.1. End moments were applied to the column first under a small axial loading. The axial load was then applied initially in increments, reading the deflection after each increment. Since the "Olsen" is a strain-controlled machine it was convenient to carry out the final loading to collapse under continuous slow straining. Simultaneous load and deflection readings were taken "on the run". As soon as the axial load began to drop off the test was stopped.

The collapse loads for the tests are presented in Figure 4.4. Load/deflection plots for some of the tests are presented in Figures 4.5 - 4.7.

4.2.2. Analysis of the tests

The stress strain curve for the material was approximated as shown in Figure 4.3, and the cross-section was divided into 15 equal strips. The analysis for columns under case (a) and (b) loadings was carried out with the general 'DEUCE' programme, the column length

being divided into 14 segments. For the columns under case (d) loadings the von Karman "unwinding" loads were obtained using the special 'DEUCE' programme, dividing the half-column into 14 segments

The Shanley loads for the case (d) loadings were subsequently assessed by a method due to BIJLAARD[61], who showed that for pinned columns "unwinding" would begin when the end slopes of the column became parallel to the thrust lines. The method is only applicable to initially straight columns where no unloading has taken place. These conditions were fulfilled by the tests. To apply the method information from the analysis for the von Karman load was used. The end slope of the column at each stage in the analysis formed part of the normal computer output. The slope of the thrust line at any stage was given by the effective end eccentricity of the load, i.e. M_A/P divided by the half-length of the column. These two slopes were plotted and the point at which they became equal was determined. The axial load corresponding to this point was taken as the Shanley load.

As a check the Shanley load for one particular column was also obtained by the same method as that used in the special 'DEUCE' programme, using the auxiliary 'SIRIUS' programme to calculate the reduced critical loads according to the Shanley criterion. Essentially the same load was obtained as by the method above.

To assess the effects of initial eccentricity on the case (d) loading, one particular column was analysed for various degrees of initial eccentricity. The general programme was used and the column was divided into 28 segments, giving the same segment length as that used for the half column analysis under case (d) loading alone.

The theoretical collapse loads are presented in Figure 4.4 as interaction curves between failure load P_F and end moment M_A, giving a direct comparison with the experimental collapse loads. To complete these curves several additional theoretical collapse loads were obtained along with the tangent modulus and reduced modulus loads for the centrally loaded cases.

Theoretical load/deflection curves to compare with the experimental plots are given in Figures 4.5 - 4.7. In Figure 4.7

the results for the case (d) loading with various degrees of eccentricity are given.

4.2.3. Discussion

It will be seen from Figure 4.4. that the experimental collapse loads are underestimated by about 5 - 10%. A study of the load/deflection curves for the case (a) and (b) loadings (Figures 4.5 and 4.6) shows that the theoretical and experimental curves agree well in the early stages of loading, i.e. when the column is still in the elastic range. At later stages the experimental curves rise above the theoretical.

This divergence can be explained by the strain rate sensitivity of the material. The stress/strain curves were obtained by applying a given load to the specimen and reading the strain after the creep had settled down. Fairly long time intervals were allowed for this, so that the curves are probably very close to the curve for zero strain rate.

In Figure 4.5 there are several points on the curves marked "creep". At these points the moving head of the testing machine was brought to a halt and the drop-off in load was noted after a short time. The presence of this drop-off indicates that the material is strain-rate sensitive, and it is probable that if the readings had been taken after allowing the creep to settle down completely, values much nearer the theoretical would have been obtained. An alternative procedure would have been to obtain the stress/strain curve under a continuous straining rate comparable with that applied in the column tests.

For the case (d) loadings in symmetrical double curvature the differences between the Shanley loads and the von Karman loads are sometimes considerable. Theoretically the central deflection for these tests should remain zero until the Shanley load is reached. Above the Shanley load "unwinding" should begin and the peak or collapse load should lie between the Shanley and von Karman loads. It will be seen from Figure 4.7 that the central deflection increases right from the start of loading for that particular test. All the case (d) loading tests exhibited this behaviour.

The initial eccentricity required to cause the experimental central deflection to vary as shown in Figure 4.7 is of the order

of 0·001". This is as small as can be expected of the test rig. Thus while the tests provide a reasonable check on the theoretical collapse loads, they do not confirm the exact behaviour at failure of a truly symmetrical case.

The results of the analysis including the effect of eccentricity of loading do however provide some evidence on this point. It will be seen that the presence of an initial eccentricity of 0·001", equivalent to $^{L}/5{,}000$, gives a collapse load below the Shanley load. Reducing the eccentricity to 0·000013", equivalent to $^{L}/400{,}000$, gives a collapse load practically midway between the Shanley and von Karman loads.

For this very small eccentricity, it will be noted that significant "unwinding" does not begin until the Shanley load is exceeded. A study of the strain history for this analysis revealed that unloading begins to take place at this point also. This unloading causes the stiffness of certain sections of the column to revert to the original elastic value, and thus the reduced critical load of the column lies above the Shanley load. So the column is still stable in the initial stages of "unwinding". The collapse load is reached when the unloading is insufficient to offset the developing plasticity elsewhere, causing the reduced critical load to fall below the load on the column.

The behaviour revealed in this analysis thus confirms that columns bent in symmetrical double curvature behave in a similar manner to centrally loaded columns.

A more practical point arises from the fact that the normal out-of-straightness to be expected is of the order of $^{L}/1{,}000$ to $^{L}/400$, considerably more than the values treated in Figure 4.7. The presence of such an out-of-straightness will undoubtedly reduce the collapse load to a value well below the Shanley load. It is therefore unwise to consider the ideally straight column in any design procedure for pinned columns.

4.3. Tests on restrained rectangular aluminium columns

4.3.1. Experimental details

The columns were similar to those used for the pinned tests.

The same loading heads and end fittings were used as for the pinned tests. Restraint was provided by steel beams which were

attached to the end fittings. The ends of the beams remote from the column were held in adjustable supports, which were clamped to the testing machine table. Application of end moment to the system was simulated by raising or lowering the beam supports. Strain gauges on the beams enabled the end moments on the column to be assessed at any stage during a test. The restraint stiffness was varied by altering the span of the beams.

The beams were made stronger than the columns so that they remained elastic at all stages in the loading. Thus the restraint stiffness remained constant during a test.

Equal restraint stiffnesses were supplied at the top and bottom ends of the columns, while for tests on columns of the same length the restraint stiffness was held constant. The actual value of restraint stiffness was derived from a non-dimensional restraint factor Q which is defined as follows:-

$$Q = \text{Restraint stiffness} \div 3EI/L \quad \ldots\ldots\ldots\ldots 4.1$$

where the restraint stiffness is in units of moment/radian and $3EI/L$ is derived from the column properties. For each column length a restraint factor was chosen and the appropriate value of restraint stiffness worked out. The spans of the restraining beams were then adjusted to give this value of restraint stiffness.

Initially in calculating the beam span to give a specific value of restraint stiffness the joints in the end fittings were assumed to be rigid. On this basis the restraint stiffness for the tests on the 7·24" long columns was calculated corresponding to the chosen restraint factor of 5·0. After some of these tests had been analysed serious discrepancies between theory and experiment were found, which were traced in part to rotations in the end fitting joints. The rotations in the joints were then assessed and the actual restraint factor for the 7·24" long columns was found to be 4·25.

For the tests on the 5·12" and 3·62" long columns the restraint factor was chosen as 2·0, and the beam spans adjusted accordingly, taking the joint rotation into account. A small error in calculation resulted in a restraint factor of 1·96 being used for the tests on the 5·12" long columns.

In carrying out the tests the end moment loading was applied first. Values of initial moments on the column length were chosen

and applied by raising or lowering the beam supports. A small axial load was necessary at this stage. Three different patterns of moment were applied designated as cases (a), (b), and (d), as shown in Figure 4·8. The axial load was then applied in the same way as for the tests on pinned columns. Simultaneous readings of load, deflection and beam moments were taken during the slow continuous straining to collapse.

The collapse loads for the tests are presented in Figure 4.9. Typical load/deflection and end moment/deflection plots are given in Figures 4.10 - 4.13. For the case (d) loadings in symmetrical double curvature load/end moment plots are drawn.

4.3.2. Analysis of tests

The stress/strain curve shown in Figure 4.3 was used, while the cross-section was divided into 15 equal strips. The columns under case (a) and (b) loading were analysed by the general 'DEUCE' programme, dividing the column length into 14 segments. For the columns under case (d) loading the von Karman "unwinding" loads were obtained from the special 'DEUCE' programme, the half-column length being divided into 14 segments. It was found for cases with high initial end moments M_{AB} and M_{BA} that "unwinding" would not necessarily occur. The collapse load in such cases was taken as that of the half-column (Figure 2.5b).

An attempt was made to obtain the Shanley loads for the columns under case (d) loading from a criterion given by BIJLAARD[61]. This criterion applies only if the column is initially straight and the degree of unloading is small. For most of the tests large zones of unloaded material developed, so that this approach had to be abandoned.

The Shanley loads were finally obtained by the same method as that used in the special 'DEUCE' programme, using the auxiliary SIRIUS programme to calculate the reduced critical loads according to the Shanley criterion.

The 'DEUCE' programmes require values of M_A and M_B, the external moments initially applied to the system (Figure 2.1). In the tests the effects of applied external moments were provided by moving the beam supports. Thus values of M_A and M_B had to be worked out which would give the same effect as that caused by the

movement of the beam supports. To do this values of column moments M_{AB} and M_{BA} under zero axial load were obtained by extrapolation from the experimental values under small axial loads. Values of M_A and M_B were then estimated which would give theoretical values of M_{AB} and M_{BA} under zero axial load reasonably close to the extrapolated values. In the elastic range this was quite simple but for high values of M_{AB} and M_{BA} which induced plasticity in the column some trial and error calculations were necessary.

As mentioned in § 4.3.1. above, a few of the tests on the 7·24" long columns were analysed as soon as they were completed taking a theoretical value of 5.0 for the restraint factor. These tests were re-analysed under the modified value of 4·25. For the tests on the 5·12" and 3·62" columns the restraint factors were taken as 1·96 and 2·0 respectively.

For one case (d) loading an additional analysis was carried out considering the presence of an eccentricity of 0·001". For this analysis the column was divided into 28 segments, giving the same segment length as in the half-column analysis.

The theoretical collapse loads are presented as interaction curves in Figure 4.9, giving a direct comparison with the experimental collapse loads. Both the Shanley and von Karman loads for the case (d) loadings are shown, along with the zones where "unwinding" is reckoned not to occur.

Load/deflection and moment/deflection curves for typical case (a) and (b) tests are given in Figures 4.10 and 4.11, while curves for cases (d) loading are given in Figures 4.12 and 4.13. The case in Figure 4.12 also shows the theoretical result considering eccentricity.

4.3.3. Discussion

i) Case (a) and (b) loadings

A study of Figure 4.9 shows that for the 7·24" columns the author's analysis overestimates the collapse loads, for the 5·12" columns the collapse loads are forecast almost exactly, and for the 3·62" columns the collapse loads are slightly under-estimated. Taking the strain-rate effect mentioned in § 4.2.3. into account an under-estimate of the collapse loads would be expected for all the tests. That this is not the case is considered to be due to variation in the restraint factor from the assumed theoretical values.

A check was made on the restraint factor calculations after the analysis had been completed, and the rotations in the joints of the end fittings were assessed by a more accurate method. No errors were found in the calculations but the rotations in the joints were found to be very much greater than those initially obtained. A serious experimental error must have been made in the initial assessment. It was calculated that the restraint factors Q for the tests were 3·57, 1·73, and 1·75, against the values of 4·25, 1·96, and 2·0, used in the analysis. After making a study of the results for columns of ideal elastic-plastic material given in Chapter 5 it was realised that these large variations in restraint factor would not affect the collapse loads in the same proportion. The tests were therefore not re-analysed. It is estimated that theoretical collapse loads obtained using the lower restraint factor values would lie about 5% lower than those given in Figure 4.9.

For the tests on the 7·24" columns it had not been realised that the joint rotations would be significant and no particular care was taken in tightening up the joints. It is probable therefore that the restraint was reduced still further on this account, i.e. below the value of 3·57. A study of the typical end moment/deflection curve in Figure 4·10 shows that the restraining moments did not develop to the extent forecast by the author's analysis. At collapse the theoretical and experimental moments differ by about 50 lb in. It is considered that this would more than offset the strain-rate effect, so that the fact that the experimental collapse load lies below the theoretical is not unexpected.

For the tests on the 5·12" columns the joints in the end fittings were tightened up very carefully and it is probable that the calculated restraint factor of 1·73 was applicable to the tests. The differences between theory and experiment should thus be due to the restraint factor being taken as 1·96 for the analysis, and to the strain rate effect. A study of the typical end moment/deflection curves in Figure 4.11 shows that at collapse the theoretical and experimental moments differ by 20 lb/in. The experimental axial loads initially lie below the theoretical curve and as collapse is reached they become almost coincident. In this case it can be concluded that the strain-rate effect is just balancing the effect

of the incorrect restraint factor.

The 3·62" columns exhibit the same behaviour with the experimental axial loads rising slightly above the theoretical curve at collapse. This could be due to the much higher strains (up to 5%) which were developed in these tests.

Despite these discrepancies the analysis gives a good representation of the general behaviour of these columns. It can be concluded that the discrepancies are due to experimental faults, rather than inaccuracy in the analysis.

ii) Case (d) loading

Reference to Figure 4.9 shows that the collapse loads for the tests under case (d) loading follow the same trends as for the case (a) and (b) loadings. These trends can also be attributed to the influence of strain-rate sensitivity and to the errors in the theoretical restraint factors.

With regard to detailed behaviour the question of "unwinding" is of most interest. According to the analysis the cases portrayed in Figures 4.12 and 4.13 should have collapsed without "unwinding", The reduced critical load according to the Shanley criterion is shown in 4.12 and it will be seen that it does not fall below the actual column load, indicating that the column will always be stable against "unwinding". For the case shown in Figure 4.13 the reduced critical load is always above 5,000 lb and has not been plotted.

Thus for both these cases the experimental moments M_{AB} and M_{BA} should have followed the theoretical curve obtained from the half-column analysis, and the central deflection should have remained zero up to and through collapse. It will be seen from Figures 4.12 and 4.13 that initially the experimental values followed this behaviour. At collapse, however, the central deflection was increasing rapidly, and one or other of the column moments had almost stopped decreasing.

It was suspected that the reason for these discrepancies was the presence of initial eccentricity and this was the reason for carrying out the analysis of the case shown in Figure 4.12, where an eccentricity of loading of 0·001" is considered. The curves on Figure 4·12 show that the central deflection and column moments for

this analysis vary in the same manner as in the experimental test although the experimental deviations from symmetrical behaviour are much greater. An important point emerges in that the theoretical quarter point deflections are both increasing at collapse. This is inconsistent with "unwinding" which implies that one quarter point deflection should increase and the other decrease (Figure 2.5c). Thus the increments in deflection at collapse can be considered as made up of two waves, one a symmetrical "unwinding" wave and the other an anti-symmetric wave tending to promote the S shape of the column. In this particular case the anti-symmetric wave is predominant suggesting that "unwinding" is not the failure criterion.

A further point is that the presence of the 0·001" deflection has a very small effect on the collapse load reducing it from 3,310 lb to 3,300 lb. This indicates that despite the presence of some "unwinding" the collapse load is still largely controlled by the collapse load of the half-column.

It can therefore be concluded that in some cases "unwinding" will not govern collapse of columns bent in symmetrical double curvature. BIJLAARD[61] has stated that "unwinding" will always govern collapse of such columns, but this statement is based on the assumption that unloading is negligible. The author's analysis has shown that unloading can be extensive and it is this feature of behaviour that leads to the possibility that "unwinding" may not occur. Some carefully controlled experiments are required to finally clarify this question.

4.4. General Conclusions

The agreement between the results from the author's tests and from the author's analysis is not as good as that obtained in Chapter 3 where tests by other authors were considered. It has been shown that the discrepancies can be attributed either to faults in the author's experimental procedure or to defects in the test rigs.

It is considered, therefore, that the combined evidence from Chapter 3 and this chapter confirms the general validity of the author's analysis, and of the assumptions on which it is based.

CHAPTER 5

5. Analysis of columns of ideal elastic-plastic material

The computer programmes were written with a view to analysing the behaviour of columns over a wide range of conditions. This has been done for the rectangular column of ideal elastic-plastic material (Figure 3.1), some 220 columns under specific conditions having been analysed. In the course of this work some 30,000 output cards were obtained, each containing 8 numbers, and it is plain that only a fraction of the total output can be presented here.

The variables considered are discussed first followed by the presentation of the results. The behaviour of pinned and restrained columns is discussed under separate headings and the theoretical collapse loads are compared with the working loads according to B.S.449 - 1959.

Finally the major conclusions are stated.

5.1. Variables considered

5.1.1. Slenderness

This variable is govered by the parameter P_P/P_E, where P_P is the load to cause yield over the whole column cross-section, and P_E is the Euler load of the column. The parameter is dependent on the slenderness ratio L/r of the column, the yield stress fy, and the modulus of elasticity E of the column material. Analysis has been carried out for P_P/P_E = 0·5, 1·0, 2·0 and 4·0. For steel with a yield stress of 16 T/in^2 and modulus of elasticity of 13,000 T/in^2 this is equivalent to L/r values of 63·3, 89·5, 126·6 and 179·1.

5.1.2. Restraint stiffness

Equal restraint stiffnesses were taken at the top and bottom of the column and it was assumed that they remained constant and active up to and through collapse. The values were controlled by the restraint factor Q which is defined as:-

$$Q = \text{Restraint stiffness} \div \frac{3EI}{L} \quad \ldots\ldots\ldots\ldots 5.1$$

where $\frac{3EI}{L}$ refers to the column length and is in fact the rotational stiffness of the pinned column against end moments. Thus if a framed building is being considered Q can be taken as roughly

equivalent to the beam to column stiffness ratio.

Analysis has been carried out for Q = 0, 0·5, 1·0, 2·0, 5·0 and 100·0. Q = 0 gives a pin-ended condition and Q = 100·0 may be taken to give a fixed-end condition.

5.1.3. Moment loading

Four different moment loading patterns were considered designated as cases (a), (b), (c), and (d), as shown in Figure 5.1. For Q = 0, i.e. pinned columns, only cases (a), (b) and (d) were considered. For each value of Q an upper limit to the value of M_A was set. In all cases the moment loading was applied first and then left constant as the axial load was applied.

5.1.4. Initial curvature

The effect of this has been studied for pinned columns only. The curvature was taken as the half-wave of a cosine curve with a maximum ordinate c_m defined by:-

$$c_m = \cdot 32\, D_y \sqrt{P_P/P_E} \qquad \ldots\ldots\ldots 5.2$$

where Dy is the central deflection of the column when both end moments are equal to My, the moment to cause first yield in the absence of axial load. For fy = 16 T/in^2 and E = 13,000 T/in^2 this gives a value of c_m = L/394. The parameters used in the Perry-Robertson formula in B.S. 449 - 1959 imply a c_m value equal to L/576 for a rectangular cross-section. Thus this analysis is more conservative than B.S. 449.

5.2. Calculation and presentation of results

The analysis was carried out taking a rectangular cross-section column 2" deep and 0·75" wide, divided into 15 equal strips. The column material had an E value of 5,000 T/in^2 with a yield stress f_y of 20 T/in^2. These dimensions and material properties were selected to take full advantage of the accuracy of the fixed point arithmetic procedures of the computer programmes.

The column was assumed to be of uniform cross-section. The columns under case (a), (b), and (c) loadings were analysed with the general 'DEUCE' programme. Generally the column length was divided into 14 segments, although in some cases 22 segments were used. For the columns under case (d) loading (in symmetrical double curvature) the special 'DEUCE' programme was used, the half-column

length being divided into 14 segments. This gave the von Karman "unwinding" loads, and the Shanley loads were subsequently calculated making use of the auxiliary 'SIRIUS' programme. For the initially curved columns under case (d) loading the general version of the 'DEUCE' programme was used, dividing the column into 14 segments.

The results are expressed in a non-dimensional form, axial load being expressed as a fraction of P_p, moment as a fraction of M_p, deflection as a fraction of D_y, and curvature as a fraction of ϕ_y. Thus the results can be applied generally to columns of ideal elastic-plastic material.

Separate sections below deal with the presentation of results for pinned and restrained columns.

5.2.1. Presentation of pinned column results

To give some idea of the general behaviour of the pinned columns, a plot is given in Figure 5.2 of the plastic zones at collapse, i.e. at the point defined by the peak of the load/deflection diagram. For the case (d) loadings on initially straight columns, the plastic zones at the Shanley "unwinding" loads are shown.

Figure 5.3 gives the collapse loads plotted as sets of interaction curves between P_F/P_p and M_A/M_p, each set dealing with one value of the slenderness parameter P_p/P_E. The curves for case (a), (b), and (d) loadings are shown as full lines while those for the same loadings including the effects of initial curvature are shown as dashed lines. For the case (d) loadings the Shanley "unwinding" loads are given. The differences between the Shanley and von Karman loads are in fact too small to be visible in Figure 5.3.

Two additional lines are drawn on each diagram. One gives combinations of axial load and end moment which will give a plastic hinge at end A of the column. This gives the maximum possible load. The other line expresses the design condition given in B.S. 449 - 1959 for sections under combined bending and thrust, i.e.:-

$$\frac{f_c}{P_c} + \frac{f_{bc}}{P_{bc}} = 1 \qquad \text{.....5.3}$$

where f_c = calculated average axial compressive stress

p_c = allowable compressive stress under axial load alone

f_{bc} = maximum compressive stress due to bending

p_{bc} = allowable compressive stress due to bending

Values of p_c were taken from Table 17 of B.S.449 - 1959, for steel to B.S.15. The L/r values for entering Table 17 corresponding to P_P/P_E = 0·5, 1·0, 2·0 and 4·0 were calculated taking f_y = 16 T/in^2 and E = 13,000 T/in^2 and are given in § 5.1.1. above. The value of p_{bc} was taken as 10·5 T/in^2.

The maximum moment allowed in the absence of axial load is thus:-

$$(M)_{max.} = \frac{10{\cdot}5}{16} M_y \qquad \ldots\ldots\ldots 5.4$$

For a rectangular section $M_p = 1{\cdot}5\ M_y$ so that the maximum moment, which is always applied at end A of the column, is governed by:-

$$\left(\frac{M_A}{M_P}\right)_{max.} = \frac{10{\cdot}5}{16} \times \frac{1}{1{\cdot}5} = {\cdot}4375 \qquad \ldots\ldots\ldots 5.5$$

The maximum average axial stress allowed in the absence of moment is p_c so that the maximum axial load is governed by:-

$$\left(\frac{P}{P_P}\right)_{max.} = \frac{p_c}{16} \qquad \ldots\ldots\ldots 5.6$$

Plotting the points given by equations 5.5 and 5.6 and joining them gives a line which satisfies equation 5.3.

5.2.2. Presentation of restrained column results

To give some idea of the general behaviour of restrained columns, an analysis for each of the four loading cases is presented in detail in Figures 5.4 - 7. A load/deflection diagram along with bending moment, deflection, curvature and plastic zone diagrams at various stages in the loading are shown for each analysis.

For a large number of columns under case (d) loading the collapse load of the half-column was reached without "unwinding" being indicated. In an attempt to clarify this behaviour an analysis was carried out for a particular case with $M_B = -0{\cdot}9\ M_A$, thus introducing a slight initial lack of symmetry. A comparison between this case and the corresponding case with $M_B = -M_A$ is shown in Figure 5.8.

The collapse loads are plotted in two ways. In Figure 5.9 they are plotted as sets of interaction curves between P_F/P_P and

M_A/M_P, each set dealing with particular values of Q and P_P/P_E. In Figures 5.10 - 13 they are plotted again as sets of interaction curves, this time between P_F/P_P and $(M_{AB})_{P=0}/M_P$. $(M_{AB})_{P=0}$ denotes the value of M_{AB} on the column after application of the external end moments M_A and M_B, i.e. before any axial load is applied. Each Figure covers the results for a particular value of P_P/P_E and contains four sets of interaction curves which deal separately with the loading cases (a), (b), (c) and (d). For the case (d) loadings the Shanley loads are given. It was found that the von Karman loads were usually only very slightly above the Shanley loads. Where "unwinding" was reckoned not to occur, the collapse loads for the half-column were taken.

For comparison the curves for collapse loads of pinned columns, i.e. Q = 0, and the line expressing the B.S.449 design condition for maximum working load are also given in Figures 5.10 - 13. The B.S.449 condition was obtained in the same way as for the pinned columns, taking the slenderness ratio as 0·7 times the pinned value. In this case $(M_{AL})_{P=0}$ is taken as the value of moment to be used when calculating f_{bc} the maximum compressive stress due to bending.

As mentioned in § 2.3.4. the computer programmes would not deal with some cases of loading. To complete the interaction curves extrapolation and interpolation have been carried out. Where the curves have been obtained in this way they are designated by dashed lines.

5.3. Discussion of pinned column results

5.3.1. General behaviour

For columns under case (a) loading Figure 5.2. shows that at collapse the plastic zones do not penetrate deeply into the cross-section, and are well spread out along the column length. This indicates that the deflections at collapse are not excessive. Load/deflection diagrams have been plotted for all the pinned column results and generally the maximum deflections at collapse for case (a) loadings are of the order of two to three times the deflection under moments alone.

For columns under case (b) and (d) loadings the same conclusion applies generally, but for the lower P_P/P_E values, i.e.

less slender columns, plastic hinges begin to form at the ends. For the higher values of P_P/P_E under case (d) loading, the collapse load is governed by the Euler load.

Initial curvature has very little effect on the general behaviour of the case (a) and (b) loadings, except for the cases under no end moments at all. It has a considerable effect on the case (d) loadings because in such cases the initially curved column begins to "unwind" immediately the axial load is applied, while the initially straight column does not begin to "unwind" until very near the collapse load.

A basic conclusion is that the behaviour may be governed completely by elastic theory, completely by plastic theory, or by a complex interaction of the two.

5.3.2. Collapse loads

A comparison between the sets of interaction curves in Figure 5.3 confirms the well known sensitivity of the collapse loads to the effects of slenderness. For $P_P/P_E = 0{\cdot}5$, however, the loads are beginning to be bounded by the condition for a fully plastic hinge at the end of the column. Reductions in the P_P/P_E value below $0{\cdot}5$ cannot therefore gain much in carrying capacity.

For each set of curves the variation in moment loading pattern has a significant effect on the collapse loads. The effects are roughly similar for $P_P/P_E = 2{\cdot}0$ and $P_P/P_E = 4{\cdot}0$. Earlier work by the author with 'DEUCE' autocode programmes indicates that the effects of moment loading pattern for values of P_P/P_E up to $15{\cdot}0$ are very similar to the effects at $P_P/P_E = 4{\cdot}0$. As P_P/P_E falls below $0{\cdot}5$ the variation in moment loading pattern will have less significant effects as all load cases will tend to be governed by the plastic hinge criterion.

The effects of initial curvature are significant where the end moments are small and for case (d) loading in symmetrical double curvature. Otherwise the effects are small in comparison with the effects of slenderness and moment loading pattern. It is for this reason that initial curvature was not considered in the analysis of restrained columns.

5.4 Discussion of restrained column results

5.4.1. General behaviour

The four typical examples for each case of moment loading, which are presented in Figures 5.4 - 7, are discussed in turn below.

Figure 5.4 portrays the example chosen from the results for columns under case (a) loading. It will be seen that the column moments M_{AB} and M_{BA}, initially quite large under moment loading only, reduce as axial load is applied, and eventually reverse and restrain the column. The bending moments at points near the ends of the column initially increase and then decrease causing the unloading shown. At the centre of the column the bending moment continues

to increase and plasticity penetrates well into the cross-section, giving a zone of very high curvature. The peak of the load deflection curve is not reached until plasticity begins to develop at the ends of the column under the increasing restraining moments.

A study of the results for other columns under case (a) loading has revealed several variations from this typical behaviour. The first is that while the column moments M_{AB} and M_{BA} always become less as axial load is applied, they need not reverse before collapse is reached. It follows that the development of plasticity at the ends of the column is not essential to collapse. The second is that the amount of unloading depends to some extent on the magnitude of the end moment loading and the P_P/P_E value. For the lower end moments M_A and M_B and high P_P/P_E values the unloading zones are much smaller. The third variation is that for higher P_P/P_E values the central curvatures do not rise to such high values.

For several columns under case (a) loading difficulty was experienced because the values of curvature at the centre of the column rose above the limiting value discussed in § 3.1.1., indicating that possibly plastic hinges should be forming. A rough check using the rigorous equations given by HORNE[30] showed that central plastic hinges would develop for only very few of the columns analysed.

Figure 5.5 portrays the example chosen from the results for columns under case (b) loading. It will be seen that the column moment M_{AB} alters in the same way as for the case (a) example, but since M_{BA} is already a restraining moment under moment loading only, its value increases as axial load is applied. The location of the point of maximum moment is initially at end A, but after a certain stage it begins to move towards the centre of the column. Shortly after the point of maximum moment passes a given cross-section the moment on that cross-section begins to decrease and unloading starts. At end B plasticity begins to develop early in the loading and penetrates almost to the same depth as at the point of maximum moment in the column length.

A study of the results for other columns under case (b) loading reveals that generally the column moment M_{AB} does not reverse before collapse is reached. The amount of plasticity and unloading varies in the same way as for the case (a) loading.

Figure 5.6 portrays the case (c) example. The behaviour is essentially the same as for the case (b) example, with a tendency for more pronounced plastic zones to develop at end B.

Figure 5.7 portrays the example chosen from the results for columns under case (d) loading. The behaviour of the half-column is similar to that of the case (b) example, except that plasticity does not develop at the lower end of the half-column, i.e. the centre of the full column.

The reduced critical loads P'_{CR} associated with the single curvature "unwinding" mode of deflection are shown, the Shanley criterion having been used. It will be seen that the reduced critical load drops below the actual load on the column slightly before the peak of the load/deflection curve for the half-column. Thus this column should collapse by "unwinding". For this example the reduced critical loads of the half-column have also been calculated. These loads are equivalent to the reduced critical loads associated with the double curvature mode of deflection for the whole column. It will be seen that the reduced critical load in the double curvature mode can be less than in the single curvature mode.

For many case (d) loadings the reduced critical load associated with "unwinding" did not drop below the load on the half-column, even after the peak of the load/deflection curve was reached, indicating that "unwinding" would not occur. For some cases, on the other hand, "unwinding" begins while the column is in the elastic range.

Figure 5.8 gives some of the results for a case where $M_B = -0{\cdot}9M_A$, i.e. very close to a case (d) loading. For the corresponding case where $M_B = -M_A$ it was reckoned that "unwinding" would not occur and the collapse load was taken as the collapse load of the half-column. It will be seen that the collapse load for the case where $M_B = -0{\cdot}9\ M_A$ is only very slightly below that for the symmetrical case. A study of the plastic zone diagrams shows that the overall behaviour of the two cases is very similar. It is considered that this example confirms that "unwinding" need not govern the collapse of a column bent in symmetrical double curvature.

5.4.2. Discussion of collapse loads of restrained columns

Figure 5.9 confirms the sensitivity of the collapse loads to the effects of slenderness. In contrast to the pinned column behaviour the collapse loads do not become bounded by an end plastic hinge criterion for low values of P_P/P_E. As P_P/P_E tends to zero, i.e. as the column becomes more and more stocky, the collapse loads tend to P_P regardless of the moment loading. This is because the plasticity in stocky columns allows the restraining systems to carry all the moment loading, without producing a significant column deflection.

The variation in collapse load due to moment loading pattern is not as great as that due to slenderness. It is of interest to note that for a given value of M_A/M_P the case (a) loading is always the most critical, and the case (d) loading the least critical. Generally the collapse loads for the case (b) loading lie roughly midway between those for case (a) and (d) loadings.

The effect of variation in the magnitude of end restraint on the collapse loads is most clearly seen from Figures 5.10 -13. A variation in restraint factor Q from 0·5 to 100·0 generally produces as much change in the collapse load as a variation in P_P/P_E from 0·5 to 4·0. Thus the magnitude of the restraint must be considered as a major factor in determining the collapse loads of restrained columns.

It should be noted that for cases (b), (c) and (d) loadings, end moments M_A and M_B can be applied such that full plastic hinges are developed at end A, or at ends A and B for case (d) loadings. The start of axial loading causes these hinges to disappear because part of the cross-section unloads under the decreasing column moment M_{AB}. As explained in Chapter 3 the analysis will not deal with plastic hinges. It was, however, generally possible to complete an analysis with a value of $(M_{AB})_{P=0}$ reasonably close to M_P, thus entailing the minimum of extrapolation on the interaction diagrams.

5.5. Comparison with B.S.449 - 1959

5.5.1. Pinned column results

The load factors implied in B.S.449 can be obtained by dividing the loads at collapse according to the author's analysis by the working loads according to B.S.449. The load factor appropriate to a given point on an interaction curve can be found

by drawing a line from the origin of the interaction diagrame to that point. The load factor is then given by:-

$$L.F. = \frac{\text{Distance from origin to point on interaction curve}}{\text{Distance from origin to where line cuts the working load line}}$$

The maximum and minimum load factors for various loading patterns have been found by trial and error and are shown in Table 5.1 below.

Table 5.1 - Load factors for pinned columns

$\frac{P_F}{P_E}$	Minimum L.F. Case (a) Initially curved	Minimum L.F. Case (a) Initially Straight	Maximum L.F. Case (b) Initially curved	Maximum L.F. Case (d) Initially curved
0·5	1·95	2·15	2·80	3·00
1·0	1·85	2·0	2·65	3·10
2·0	1·80	1·95	2·70	3·25
4·0	1·80	1·90	2·60	3·50

The load factor implied in the Perry-Robertson formula, on which the permissible stresses in B.S.449 are based, is 2.0, so that the minimum values of 1·8, though unconservative, are not alarming. It is probable, however, that with cross-sections with lower shape factors, e.g. I sections bent about the major axis, the minimum load factors could fall to 1·5.

The maximum load factors indicate that the B.S.449 design can be conservative. If the case (d) loading is rejected as being unlikely to arise in design, the maximum value of 2·8 does not appear excessive.

It can be concluded that the design of pinned columns according to B.S.449 is reasonably satisfactory. Unfortunately the pinned column under known end moment loading is extremely rare in practice.

5.5.2. Restrained column results

The working loads according to B.S.449 have been obtained assuming an effective length of 0·7L. This is only justified if adequate restraint is provided. It is considered unlikely that a designer would assume adequate restraint unless the beam to column

stiffness ratio was at least equal to 1·0. The maximum and minimum load factors have therefore been obtained for Q = 1·0 and Q = 5·0. The load factors can be assessed by the same method as was used for pinned columns provided $(M_{AB})_{P=0}$ for the collapse loading is less than M_y, the yield moment. When this is so the external moment loading is directly proportional to $(M_{AB})_{P=0}$. The collapse loads at the minimum load factor were found to fulfil this condition and the maximum load factors were assessed for an upper limit of $(M_{AB})_{P=0} = M_y$ corresponding to the collapse loading. The results are presented in Table 5.2 below.

Table 5.2 - Load factors for restrained columns

$\frac{P_P}{P_E}$	Q	Minimum L.F. Case (a) Loading	Maximum L.F. Case (d) Loading
0·5	1·0	2·25	3·50
1·0	1·0	2·30	3·60
2·0	1·0	2·05	3·60
4·0	1·0	1·80	3·60
0·5	5·0	2·25	3·70
1·0	5·0	2·55	3·85
2·0	5·0	2·55	4·05
4·0	5·0	2·30	4·50

The load factors for cases where $(M_{AB})_{P=0} > M_y$ for the collapse loading must be obtained by a trial and error procedure. This has been done for a few cases and the maximum values are somewhat higher than those given in Table 5.2 above.

For the restrained column case (a) loading is probably less common that case (b), (c), and (d) loadings. It can thus be concluded that the B.S.449 procedure will generally be conservative, although it is possible for unconservative cases to occur.

The large range over which the load factor may vary indicates that the design of restrained columns according to B.S.449 is unsatisfactory.

5.6. Conclusions

It has been shown that the behaviour of columns up to collapse

is generally governed by a complex interaction between elastic and plastic theory, although some particular cases can be governed entirely by either elastic or plastic theory.

The major factors influencing the collapse loads of pinned columns were found to be slenderness, and the magnitude and arrangement of moment loading.

The major factors influencing the collapse loads of restrained columns were found to be slenderness, magnitude and arrangement of moment loading, and magnitude of end restraint.

For both pinned and restrained columns it was found that case (d) loading in symmetrical double curvature is always less critical than case (a) loading in symmetrical double curvature.

The design criteria suggested in B.S.449 - 1959 for members under combined bending and thrust are found to be reasonably satisfactory for pinned columns. For restrained columns, however, the B.S.449 criteria can lead to very conservative results and are considered unsatisfactory.

CHAPTER 6

6. Conclusions

A summary is given first of the major conclusions, followed by suggestions for future work in this field.

6.1. Major conclusions

An analysis for restrained columns held against sway and bent about one axis of symmetry has been developed and programmed for an electronic computer. Results obtained using this analysis have been compared with results of analysis and tests by other authors. Tests carried out by the author on pinned steel columns, pinned aluminium columns, and restrained aluminium columns, have also been analysed. The general level of agreement between theory and experiment is very good and it is concluded that the analysis can be relied on to give a good estimate of the collapse load of a given column, as well as forecasting its behaviour during loading.

The analysis has been used to analyse restrained rectangular columns of ideal elastic-plastic material over a wide range of conditions. It is concluded that the axial load-carrying capacity of pinned columns is influenced mainly by slenderness, along with the magnitude and pattern of end moment loading. The influence of initial curvature is not found to be significant except where the moments coming on to the column ends are small. The axial load-carrying capacity of restrained columns is found to be influenced by slenderness, magnitude and pattern of end moment loading, and the degree of end restraint available. For a given value of end restraint and a given value of out-of-balance external moments it is found that the most critical loading condition is always where the moments produce symmetrical single curvature. The influence of initial curvature was not investigated for restrained columns.

A comparison has been made of the collapse loads obtained for columns of ideal elastic-plastic material with working loads obtained using the criteria given in B.S.449 for members under combined bending and thrust. It is concluded that these criteria are satisfactory when applied to pinned columns. For restrained columns, however, the ratio of collapse load to working load varies over a wide range and it is concluded that B.S,449 is unsatisfactory for such columns.

6.2. Suggestions for future research

The major point here is to what extent this work could be used in developing design methods. It was concluded in Chapter 5 that column behaviour may be completely controlled by either elastic or plastic theory and more usually by a complex interaction of the two. It seems unlikely therefore that design methods based entirely on elastic or plastic theory will be satisfactory.

In the author's opinion a design method could be developed based on interaction diagrams such as those shown in Figure 5.9. For a given trial section the values of P_P/P_E, Q, M_A/M_P, and M_B/M_P could be calculated, M_A and M_B being given by the out-of-balance fixed end moments acting at the column ends. The value of P_F/P_P could then be read off an appropriate diagram. The value of P/P_P corresponding to the factored design load would then be compared with P_F/P_P. A considerable range of interaction diagrams would have to be prepared but in the author's opinion the amount of computer time required for this would not be excessive.

A difficulty which would have to be resolved in such a design approach lies in the assessment of Q when plasticity develops in the restraining members. It is probable that conservative assumptions can be developed for this.

For designing compression members in trusses the out-of-balance fixed end moment M_A and M_B will generally be very small, and in such cases the effect of initial curvature will be of primary importance. The interaction diagrams could be prepared taking account of a standard initial curvature and so would take account of this.

The existing computer programmes will only deal with columns bent about one axis, but it seems essential that a design method capable of dealing with biaxial loading be developed. As mentioned below the analytical method used in this thesis can be extended to consider biaxial bending. Thus interaction diagrams could be prepared for this case also. It is possible that a very large range of diagrams would be necessary to give adequate coverage to the practical range of columns and loadings, thus making the design method too cumbersome. The author considers, however, that the approach is still worth investigating.

Specific suggestions for future research are given below.

6.2.1. Suggestions for analytical work

The existing computer programmes can be used to derive design interaction diagrams for various types of columns, e.g. steel I-sections bent about either axis. The effect of variable cross-section along the column can also be studied. Since single curvature bending is found to be more critical for uniform columns, it may prove advantageous to add material to the mid-length of the column.

Amendments could be made to the existing programmes, considerably increasing their scope. Variation in end restraint stiffness during loading could be included, thus taking account of the development of plasticity in restraining members. Different sequences of loading could also be studied, e.g. axial load applied first and left constant as moment loading is applied.

The analytical method can be extended to deal with bending about both axes. Torsional effects could also be included, provided warping resistance and the Wagner effect were neglected, and the assumption made that the torsional rigidity is unaffected by plasticity in the longitudinal direction. The method would then be capable of dealing with the important case of the I section bent about the major axis, provided initial curvature about the minor axis was present.

Details concerning the extension of the method are given in an Appendix to the programme specification.*

6.2.2. Suggestions for experimental work

As suggested in Chapter 4 some carefully controlled experiments on restrained columns bent in symmetrical double curvature would confirm whether or not "unwinding" always governs collapse of such columns. A parallel series of tests on equivalent half-columns (Figure 2.5b) would provide the half-column collapse loads for comparison.

Other experimental work would be determined by the cases considered in analysis.

It should be noted that the analytical approach developed in

---

* See footnote on Page 67

the thesis effectively carries out an "experiment" on a mathematical model. Thus it should not be necessary to carry out large numbers of tests.

REFERENCES

1. B.S.449, 1959. "The Use of Structural Steel in Building." British Standards Institution.

2. EULER, L. "Sur la Force des Collonnes." Academie Royale des Science et Belles Lettres de Berlin, Mem. Vol. 13 (1759), p. 252 English translation by J.A. van den Broek, Amer. J. Physics, Vol. 15 (1947), p. 309.

3. SCHEFFLER, H. The original reference to this work has not been traced. According to STEPHENSON[12] details are given in "Columns' by E.H. Salmon, Henry Frowde and Hodder and Stoughton, London, 1921, p. 129.

4. AYRTON, W.E. and PERRY, J. "On Struts." Engineer, Vol. 62, (1886), p. 464.

5. ROBERTSON, A. "The Strength of Struts." Selected Engineering Paper No. 28, Institution of Civil Engineers, 1928.

6. YOUNG, D.H. "The Rational Design of Steel Columns." Trans. A.S.C.E., Vol. 101, (1936), pp. 422 - 500.

7. STEPHENSON, H.K., and CLONINGER, K. "Stress Analysis and Design of Steel Columns." Bulletin No. 129, (1953) Engr. Expt. Sta., College Station, Texas, U.S.A.

8. BAKER, J.F., "An Investigation of the Stress Distribution in a Number of Three-Storey Steel Building Frames." Final Report Steel Structures Research Committee, H.M.S.O., 1936, p. 436.

9. BAKER, J.F. and WILLIAMS, E.L. "The Behaviour of a Pillar forming Part of a Continuous Member in a Building Frame." Final Report, Steel Structures Research Committee, H.M.S.O., 1936, p. 436.

10. BAKER, J.F. and WILLIAMS, E.L. "A Study of the Critical Loading Conditions in Building Frames." Final Report, Steel Structures Research Committee, H.M.S.O., 1936, p. 471.

11. BAKER, J.F. and WILLIAMS, E.L. "The Design of Stanchions in Building Frames." Final Report, Steel Structures Research Committee, H.M.S.O., 1936, p. 511.

12. STEPHENSON, H.K. "Stress Analysis and Design of Steel Columns: A General Solution to the Compression Member Problem." Proceedings, Thirty-Fourth Annual Meeting of the Highway Research Board (January 1955), Reprint 52, Texas Engineering Experiment Station, College Station, Texas, U.S A.

13. WOOD, R.H., LAWTON, W.T. and GOODWIN, E., "Rapid Design of Multi-Storey Rigid Jointed Steel Frames: Systematic Improvements in Stanchion Design." Note A58, July 1957, Building Research Station, Garston Watford, Herts.

14. ENGESSER, F. "Uber die Knickfestigkeit gerader Stäbe." Zeitung der deutscher Architekt und Ingenieur Verein, Hannover, Vol. 35 (1889), p. 455.

15. JASINSKI, F. Schweizerische Bauzeitung, Vol. 25, 1895, p. 172.

16. ENGESSER, F. "Uber Knickfragen." Schweizerische Bauzeitung, Vol. 26, 1895, p. 24.

17. von KARMAN, T. "Die Knickfestigkeit gerader Stäbe." Physikalische Zeitschrift." Vol. 9 (1908), p. 136. (This is a summary of Reference 18.)

18. von KARMAN, T. "Untersuchungen uber Knickfestigkeit." Mitteilungen uber Forschungsarbeiten auf den Gebiete des Ingenieurswesens, Heft 81 (1910).

19. CHWALLA, E. "Theorie des aussermittig gedrückten Stäbes aus Baustahl." Stahlbau, Vol. 7, (1934), pp. 161-165, 173-176, 180-184.

20. CHWALLA, E. "Der Einfluss der Querschnittsform auf das Tragvermögen ausser mittig gedruckter Stahlstäbe." Stahlbau, Vol. 8 (1935), pp. 193-197, 204-207.

21. CHWALLA, E. "Aussermittig gedrückte Baustahlstäbe mit elastisch eingespannten Enden und verschieden grossen Angriffshebeln." Stahlbau, Vol. 10 (1937), pp. 57-60. (This is the second part of a two part paper.)

22. JEZEK, K. "Die Tragfähigkeit des excentrisch beanspruchten und des querbelasteten Druckstabes aus einen ideal plastischen material." Sitzungsberichte der Akademie der Wissenschaften in Wien, Abteilung IIa, Vol. 143, (1934).

23. JEZEK, K. "Die Tragfähigkeit des gleichmassig quer belasteten Druckstabes aus einem ideal plastischen material." Stahlbau, Vol. 8 (1935), p. 33.

24. JEZEK, K. "Näherungsberechnung der Tragfahigkeit excentrisch gedrückter Stahlstäbe." Stahlbau, Vol. 8 (1935), p. 89.

25. JEZEK, K. "Die Tragfahigkeit axial gedruckter und auf Biegung beanspruchter Stahlstäbe." Stahlbau, Vol. 9 (1936), pp. 12-14, 22-24, 39-40.

26. ROS, M. "Die Bemessung zentrisch und excentrisch gedrückter Stäbe auf Knickung." Report of 2nd International Congress of Bridge and Structural Engineers, Vienna, 1928.

27. WESTERGAARD, H.M. and OSGOOD, W.R. "Strength of Steel Columns." Trans. ASME, Vol. 49 - 50 (1928), Part I, APM50-9.

28. HARTMANN, F. "Der einseitige (excentrischen) Druck bei Stäben aus Baustahl." Zeitschrift der Osterreichischen Ingenieur und Architekten Verein, Vol. 85 (1933).

29. KOLLBRUNNER, C.F. "Zentrisch und excentrisch Druck von an beiden Enden gelenkig gelagerten Rechteck stäben aus Avional M und Baustahl." Stahlbau, Vol. 11 (1938), p. 25.

30. HORNE, M.R. "The Elastic-Plastic Theory of Compression Members." Journal of the Mechanics and Physics of Solids, Vol. 4 (1956), p. 104.

31. ELLIS, J.S. "Plastic Behaviour of Compression Members." Journal of the Mechanics and Physics of Solids, Vol. 6 (1958), p. 282.

32. KETTER, R.L., KAMINSKY, E.L. and BEEDLE, L.S. "Plastic Deformation of Wide-Flange Beam Columns." Trans. A.S.C.E. Vol. 120 (1955), p. 1028.

33. NEWMARK, N.M. "Numerical procedures for Computing Deflections, Moments and Buckling Loads." Trans. A.S.C.E., Vol. 108 (1943) p. 1161.

34. GALAMBOS, T.V. and KETTER, R.L. "Columns under Combined Bending and Thrust." Proc. A.S.C.E., Vol. 84, EM2 (1959), p. 1.

35. MASON, R.E., FISHER, G.P. and WINTER, G. "Eccentrically Loaded, Hinged Steel Columns." Proc. ASCE, Vol. 84 (1958), EM4.

36. JOHNSTON, B.G. and CHENEY, L. "Steel Columns of Rolled Wide-Flange Section." Progress Report No. 2, American Institute of Steel Construction, November 1942.

37. KETTER, R.L., BEEDLE, L.S. and JOHNSTON, B.G. "Column Strength under Combined Bending and Thrust." Research Supplement, The Welding Journal, Vol. 31 (1952), p. 607.

38. MASSONET, C. and CAMPUS, F. "Recherches sur le Flambement de Colonnes en Acier A37, a Profil en Double Te, Sollicitees obliquement." I.R.S.I.A., Bulletin No. 17, April 1956.

39. "Second Progress Report of the Special Committee on Steel Columns." Trans. A.S.C.E., Vol. 95 (1931).

40. GALAMBOS, T.V. "Inelastic Lateral Torsional Buckling of Wide-Flange Beam-Columns." Ph.D. Dissertation, Lehigh University, 1959.

41. KETTER, R.L. "Further Studies on the Strength of Beam-Columns." Proc. A.S.C.E., Vol 87, ST8 (1961).

42. SHANLEY, F.R. "Inelastic Column Theory." J. Aero. Sci., Vol. 14, No. 5 (1947), p. 261.

43. CLARKE, J.W. "Eccentrically Loaded Aluminium Columns." Trans. A.S.C.E., Vol. 120, (1955) p. 1116.

44. AUSTIN, W.J. "Strength and Design of Metal Beam-Columns." Proc. A.S.C.E., Vol. 87, ST4 (1961).

45. CHWALLA, E. "Aussermittig gedrückter Baustahlstäbe mit elastisch eingespannten Enden und verschieden grossen Angriffshebeln." Stahlbau, Vol. 10 (1937), pp. 49-52. (This is the first part of a two part paper.)

46. BAKER, J.F., HORNE, M.R. and HEYMAN, J. "The Steel Skeleton," Vol. II, Cambridge University Press (1942), Chapters 13, 14 and 15.

47. BAKER, J.F. and RODERICK, J.W. "The Behaviour of Stanchions Bent in Single Curvature." Trans. Inst. Weld., Vol. 5 (1942).

48. BAKER, J.F. and RODERICK, J.W. "Further Tests on Stanchions." Weld Res., Vol. 2 (1948).

49. BAKER, J.F. and RODERICK, J.W. "The Behaviour of Stanchions Bent in Double Curvature." Weld. Res., Vol. 2 (1948).

50. RODERICK, J.W. and HORNE, M.R. "The Behaviour of a Ductile Stanchion Length when Loaded to Collapse." B.W.R.A., Report No. FE1/11, 1948.

51. BAKER, J.F., HORNE, M.R. and RODERICK, J.W. "The Behaviour of Continuous Stanchions," Proc. Roy. Soc. A., Vol. 198 (1949).

52. EICKHOFF, K.G. "The Plastic Behaviour of Columns and Beams." Ph.D. Thesis, Cambridge University, 1955.

53. RODERICK, J.W. "The Behaviour of Stanchions Bent in Single Curvature." B.W.R.A., Report No. FE1-5/24.

54. RODERICK, J.W. "Tests on Stanchions Bent in Single Curvature about both Principal Axes." B.W.R.A., Report No. FE1/36, 1953.

55. HEYMAN, J. "Tests on I-Section Stanchions Bent about the Major Axis." British Welding Journal, August 1957.

56. HORNE, M.R. "The Stanchion Problem in Frame Structures Designed according to Ultimate Carrying Capacity." Proc. I.C.E., Vol. 5, Part III, 1956, p. 105.

57. CAMPUS, F. and MASSONET, C. Correspondence on Ref. 56, Proc. I.C.E., Vol. 5, Part III, 1956, p. 558.

58. HORNE, M.R. "Multi-Storey Frames." Symposium on the Plastic Theory of Structures, Session II, British Welding Journal, August 1956.

59. HORNE, M.R. "The Design of I-Section Stanchions with Plastic Hinges at One or Both Ends." B.W.R.A., Report No. FE1/50, 1956.

60. HORNE, M.R., GILROY, J.M., NEILE, S. and WILSON, G. "Further Tests of I-Section Stanchions Bent about the Major Axis." British Welding Journal, June 1956.

61. BIJLAARD, P.P. "Buckling of Columns with Equal and Unequal End Eccentricities and Equal and Unequal Rotational End Restraints." Proceedings, Second U.S. National Congress of Applied Mechanics, Ann Arbor, Michegan, 1954.

62. BIJLAARD, P.P., FISHER, G.P. and WINTER, G. "Eccentrically loaded, end-restrained columns." Trans. A.S.C.E., Vol. 120, 1955, p. 1070.

63. OJALVO, M. "Restrained Columns." Proc. A.S.C.E., Vol. 86, EM5, 1960.

64. "Commentary on Plastic Design in Steel-Compression Members." Proc. A.S.C.E., Vol 86, EM1 (1960).

65. BLEICH, F. "Buckling Strength of Metal Structures." McGraw-Hill Book Company, 1952, p. 51.

66. "Guide to Design Criteria for Metal Compression Members." Column Research Council, Engineering Foundation, U.S.A. 1960, pp. 81-83.

67. EICKHOFF, K.G. Correspondence on Ref. 56, Proc. I.C.E., Vol. 5, Part III, 1956, p. 564.

APPENDIX A1

A1. Notation

e = Strain

f = Stress

f_y = Yield stress

E = Modulus of Elasticity

ϕ = Curvature

ϕ_y = Curvature at first yield under moment loading only

I = Second moment of area

r = Radius of gyration

L = Column length

N = Number of segments into which column length is divided

L = Segment length

$C_o, C_1, \ldots\ldots C_x, \ldots\ldots C_N$ = Initial deflections at each division point

$d_1, d_2, \ldots\ldots dx, \ldots\ldots d_{N-1}$ = Deflections due to loading

$D_o, D_1, \ldots\ldots\ldots D_x, \ldots\ldots D_N$ = Total deflections at each division point

$e_o, e_1, \ldots\ldots e_x, \ldots\ldots e_N$ = Axial strains at the column axis for each division point cross-section

$\phi_o, \phi_1, \ldots\ldots \phi_x \ldots\ldots \phi_N$ = Curvatures of column axis at each division point cross-section

$\Delta_o, \Delta_1, \ldots\ldots \Delta_x \ldots \Delta_N$ = Differences between assumed and calculated deflections at each division point

R = Number of reference division point

D_R = Deflection of reference division point

Δ_R = Difference between assumed and calculated deflection at reference division point

θ_A, θ_B = End rotations of column due to loading

k_A, k_B = Rotations of end restraining systems/unit moment

γ_A, γ_B = Differences between calculated end rotations of columns and rotations of end restraining systems

Q = Restraint factor

D_y = Central deflection of column under equal terminal moments equal to M_y

Notation for loading

P = Axial load

P_F = Failure or collapse load

P_E = Euler load ($= \pi^2 EI/L^2$)

P_{CR} = Elastic critical load

P'_{CR} = Reduced critical load

F_P = Load to cause yield stress in compression over whole cross-section

M = Bending moment

$M_o, M_1, \ldots M_x, \ldots M_N$ = Bending moments at each division point

M_A = External moment applied at top of column

M_B = External moment applied at bottom of column

M_{AB} = Moment on the column length at the top

M_{BA} = Moment on the column length at the bottom

$(M_{AB})_P = 0$ = Moment on the column length at the top after applying M_A and M_B and before application of P

M_y = Moment to produce first yield in the absence of axial load

M_P = Full plastic moment in the absence of axial load

Notation for a typical division point cross-section x

$a_o, a_1, \ldots a_r, \ldots a_q$ = Areas of cross-section strips

$y_o, y_1, \ldots y_r, \ldots y_q$ = Distances of centres of gravity of strips from the column axis

e_r = Strain at the centre of gravity of strip r

f_r = Stress at the centre of gravity of strip r

$(e_m)_r$ = Maximum strain to which strip r has been subjected

$(f_m)_r$ = Stress corresponding to $(e_m)_r$

$(Et)_r$ = Tangent modulus appropriate to strip r

α = Difference between calculated and required value of P_x

β = Difference between calculated and required value of M_x

$X_x = \frac{\partial \alpha}{\partial e_x}$

$Y_x = \frac{\partial \beta}{\partial e_x} = \frac{\partial \alpha}{\partial \phi_x}$

$Z_x = \frac{\partial \beta}{\partial \phi_x}$

Suffixes

a - Signifies a value assumed at the start of an iteration cycle

c - Signifies a value calculated at the end of an iteration cycle

η - Signifies a modification to an assumed value before starting another iteraction cycle

Notation for stress/strain curve

f_o', f'_1, ... f'_s ..... f'_u = Stresses at points chosen to define stress/strain curve

e'_o, e'_1 , ...e'_s ..... e'_u = Strains at points chosen to define stress/strain curve

$(E_t)'_o$, $(E_t)'_1$, ... $(E_t)'_s$ ..... $(E_t)'_u$ = Tangent modulus for each of the straight line portions of the stress/strain curve.

APPENDIX A2

A2. Mathematical details of restrained column analysis

The calculation of curvature at a division point is described first, a written flow diagram for the procedure being included. The calculation of the effects of slight changes in axial load and bending moment on the curvature is then described, followed by a brief reference to the integration procedure.

Descriptions of the analysis under end moment loading only, the analysis under end moment loading and axial load, and the analysis for the reduced critical load, follow under separate headings. Written flow diagrams for each analysis are given.

The convergence of the various iterative procedures is discussed and the methods developed for obtaining initial estimates to quantities are described.

Finally, a written flow diagram giving the main outline of the computer programme for the general case is given, with details of the values stored after each of the major steps in the analysis.

More details of the computer programmes can be obtained in the programme specifications.*

A2.1 Calculation of curvature at a typical division point cross-section x

It is required to calculate the curvature corresponding to given values of axial load and bending moment, which will be denoted by P_x and M_x. Preliminary estimates of axial strain e_x at the column axis and curvature ϕ_x of the column axis will be available.

Referring to Figure 2.2b the strain e_r** at the centre of

---

* The specifications for the 'DEUCE' programmes are held by the Civil Engineering Department, Glasgow University, Glasgow W.2, while the specification for the 'SIRIUS' programme is held by the Cement and Concrete Association, Wexham Springs, Stoke Poges, Slough, Bucks.

** Strictly speaking the strip strains should be denoted by e_{xo}, e_{x1}, ... e_{xr}, ... e_{xq}. To avoid confusion the x suffix has been omitted where convenient.

gravity of any cross-section strip r, distant y_r from the column axis, is given by:-

$$e_r = e_x + \phi_x y_r \qquad \text{A2.1}$$

The value of stress f_r corresponding to this strain is obtained from the stress/strain curve (Figure 2.3) by an interpolation procedure, along with the appropriate value of tangent modulus $(Et)_r$, which is required later. If unloading is to be considered then a maximum value of strain $(e_m)_r$ to which the strip has been subjected will be available. If e_r is less than $(e_m)_r$ as shown in Figure A2.1 then:-

$$\left.\begin{aligned} f_r &= (f_m)_r - \{(e_m)_r - e_r\}(E_t)'_0 \\ \text{and} \quad (E_t)_r &= (E_t)'_0 \end{aligned}\right\} \qquad \text{A2.2}$$

The area of strip r is denoted by a_r and thus the axial force in the strip is given by $a_r f_r$. The total calculated axial force $(P_x)_c$ is given by:-

$$(P_x)_c = \sum_{r=0}^{q} a_r f_r \qquad \text{A2.3}$$

Similarly the total calculated bending moment $(M_x)_c$ about the column axis is given by:-

$$(M_x)_c = \sum_{r=0}^{q} a_r f_r y_r \qquad \text{A2.4}$$

If these calculated values $(P_x)_c$ and $(M_x)_c$ are reasonably close to the required values P_x and M_x, the correct values for e_x and ϕ_x have been assumed. If they are not sufficiently close, modification to e_x and ϕ_x must be made and new values of $(P_x)_c$ and $(M_x)_c$ obtained.

To evaluate the modifications it is convenient first to calculate the following quantities:-

$$\left.\begin{aligned} \alpha &= (P_x)_c - P_x \\ \beta &= (M_x)_c - M_x \end{aligned}\right\} \qquad \text{A2.5}$$

α and β should be zero and the modifications to e_x and ϕ_x should be such as to reduce them to zero. Denoting the modifications

by $(e_x)_\eta$ and $(\phi_x)_\eta$, the following governing equations hold:-

$$\left.\begin{aligned} \frac{\partial \alpha_x}{\partial e_x}(e_x)_\eta + \frac{\partial \alpha}{\partial \phi_x}(\phi_x)_\eta &= -\alpha \\ \frac{\partial \beta}{\partial e_x}(e_x)_\eta + \frac{\partial \beta}{\partial \phi_x}(\phi_x)_\eta &= -\beta \end{aligned}\right\} \quad \text{A2.6}$$

The partial derivatives in equations A2.6 are obtained by differentiating equations A2.5, noting that P_x and M_x are constants, i.e.:-

$$\left.\begin{aligned} \frac{\partial \alpha}{\partial e_x} &= \frac{\partial (P_x)_c}{\partial e_x} \quad ; \quad \frac{\partial \alpha}{\partial \phi_x} = \frac{\partial (P_x)_c}{\partial \phi_x} \\ \frac{\partial \beta}{\partial e_x} &= \frac{\partial (M_x)_c}{\partial e_x} \quad ; \quad \frac{\partial \beta}{\partial \phi_x} = \frac{\partial (M_x)_c}{\partial \phi_x} \end{aligned}\right\} \quad \text{A2.7}$$

The partial derivatives on the R.H. sides of equations A2.7 are calculated by considering the effects of slight changes in e_x and ϕ_x, denoted by δe_x and $\delta \phi_x$, as shown in Figure A2.2.

δe_x produces changes in strain equal to δe_x over the whole cross-section (Figure A2.2a). The stress change at any strip r equals $\delta e_x (E_t)_r$, and thus the total change $\delta (P_x)_c$ in calculated axial force is given by:-

$$\delta (P_x)_c = \sum_{r=0}^{q} \delta e_x (E_t)_r a_r$$

i.e.
$$\frac{\partial (P_x)_c}{\partial e_x} = \sum_{r=0}^{q} (E_t)_r a_r \quad \text{A2.8}$$

Similarly
$$\frac{\partial (M_x)_c}{\partial e_x} = \sum_{r=0}^{q} (E_t)_r a_r y_r \quad \text{A2.9}$$

$\delta \phi_x$ produces a change in strain at the centre of gravity of any strip r equal to $\delta \phi_x y_r$ (Figure A2.2b), with a corresponding stress change given by $\delta \phi_x y_r (E_t)_r$. Thus in this case the total change $\delta (P_x)_c$ in calculated axial force is given by:-

$$\delta (P_x)_c = \sum_{r=0}^{q} \delta \phi_x (E_t)_r a_r y_r$$

i.e.
$$\frac{\partial (P_x)_c}{\partial \phi_x} = \sum_{r=0}^{q} (E_t)_r a_r y_r \quad \text{A2.10}$$

Similarly
$$\frac{\partial (M_x)_c}{\partial \phi_x} = \sum_{r=0}^{q} (E_t)_r a_r y_r^2 \quad \text{A2.11}$$

For convenience the following abbreviating symbols are used:-

$$X_x = \frac{\partial (P_x)_c}{\partial e_x} = \frac{\partial \alpha}{\partial e_x} = \sum_{r=0}^{q} (E_t)_r a_r$$

$$Y_x = \frac{\partial (M_x)_c}{\partial e_x} = \frac{\partial (P_x)_c}{\partial \phi_x} = \frac{\partial \beta}{\partial e_x} = \frac{\partial \alpha}{\partial \phi_x} = \sum_{r=0}^{q} (E_t)_r a_r y_r$$

$$Z_x = \frac{\partial (M_x)_c}{\partial \phi_x} = \frac{\partial \beta}{\partial \phi_x} = \sum_{r=0}^{q} (E_t)_r a_r y_r^2 \qquad \text{A2.12}$$

Since the values of $(E_t)_r$ are known for each strip the values of X_x, Y_x and Z_x can be found thus giving the coefficients for the L.H. sides of equations A2.6. Solving these equations leads to values for $(e_x)_\eta$ and $(\phi_x)_\eta$ as follows:-

$$(e_x)_\eta = \frac{\beta Y_x - \alpha Z_x}{X_x Z_x - Y_x^2}$$

$$(\phi_x)_\eta = \frac{\alpha Y_x - \beta Z_x}{X_x Z_x - Y_x^2} \qquad \text{A2.13}$$

The modified values of e_x and ϕ_x, denoted by e'_x and ϕ'_x are given by:-

$$e'_x = e_x + (e_x)_\eta$$

$$\phi'_x = \phi_x + (\phi_x)_\eta \qquad \text{A2.14}$$

Using these modified values new calculated values of $(P_x)_c$ and $(M_x)_c$ are obtained. If they are still not reasonably close to the required values the modification procedure must be carried out again. The procedure is repeated as often as necessary. The problem of convergence is discussed later (§ A2.7).

Sign Convention

Strip areas a_0, a_1, ... are taken as positive, along with compressive stress and strain. Since the axial force P is a product of stress x area, compressive force is positive.

Other quantities are conveniently defined by referring to Figure 2.1. M is defined as positive when it produces concavity towards the left. Positive curvature is taken as the result of applying positive M. It is found that for consistency y must be taken as positive to the left of the column axis and negative to the right.

It is of interest to note that the column axis can be chosen arbitrarily and that the calculation is exactly the same for cross-sections in tension.

Flow diagram for computer programme

The flow diagram is shown in Figure A2.3. It should be noted that values of $(P_x)_c$, $(M_x)_c$, e_x, ϕ_x, X_x, Y_x, Z_x and $X_x Z_x - Y_x^2$ are stored away after each calculation is complete. These values provide an initial trial for the next calculation and the values of X, Y_x, Z_x, and $X_x Z_x - Y_x^2$ are used elsewhere in the programme.

In calculating the stress at any cross-section strip the programme was arranged to take account of unloading, a strain history being kept for all the strips in each division point cross-section. The programme could not deal with strips which yielded first in one direction and then in the other.

A2.2. Effects of slight changes in axial load and bending moment

In assessing the effects of slight changes in the assumed loading on the column it is necessary to assess the effects of slight changes in axial load and bending moment on the curvature. Denoting such changes at any cross-section x by dP_x and dM_x, and the consequent changes in e_x and ϕ_x by de_x and $d\phi_x$, the following governing equations hold:-

$$\left.\begin{aligned} \frac{\partial P_x}{\partial e_x}\, de_x + \frac{\partial P_x}{\partial \phi_x}\, d\phi_x &= dP_x \\ \frac{\partial M_x}{\partial e_x}\, de_x + \frac{\partial M_x}{\partial \phi_x}\, d\phi_x &= dM_x \end{aligned}\right\} \qquad \text{A2.15}$$

The values of X_x, Y_x, and Z_x, are stored with the results of the last curvature calculation and give partial derivatives as follows:-

$$X_x = \frac{\partial (P_x)_c}{\partial e_x} \; ; \; Y_x = \frac{\partial (M_x)_c}{\partial e_x} = \frac{\partial (P_x)_c}{\partial \phi_x} \; ; \; Z_x = \frac{\partial (M_x)_c}{\partial \phi_x}$$

When $(P_x)_c = P_x$ and $(M_x)_c = M_x$, it follows that:-

$$X_x = \frac{\partial P_x}{\partial e_x} \; ; \; Y_x = \frac{\partial M_x}{\partial e_x} = \frac{\partial P_x}{\partial \phi_x} \; ; \; Z_x = \frac{\partial M_x}{\partial \phi_x}$$

Substituting in equations A2.15 and solving for $d\phi_x$ gives:-

$$d\phi_x = \frac{dM_x X_x - dP_x Y_x}{X_x Z_x - Y_x^2} \qquad \text{A2.16}$$

A2.3. Integration Procedure

The method is exactly the same as that given by NEWMARK in reference 33, pp. 1168-1170, under the heading of "Simplified procedure for smooth angle change curves", to which reference should be made for full details. The procedure gives values of d_1, d_2, .. d_{N-1}, which must be added to the initial deflections c_1, c_2, ... c_{N-1}, to give calculated deflections D_1, D_2, ... D_{N-1}. The end deflections D_o and D_N are given directly by C_o and C_N.

The end rotations are calculated from formulae as follows:-

$$\left.\begin{aligned}(\Theta_A)_c &= \frac{d_1}{\lambda L} + \frac{\lambda L}{24}\left(7\phi_o + 6\phi_1 - \phi_2\right)\\ (\Theta_B)_c &= \frac{d_{N-1}}{\lambda L} + \frac{\lambda L}{24}\left(7\phi_N + 6\phi_{N-1} - \phi_{N-2}\right)\end{aligned}\right\} \quad \text{A2.17}$$

It should be noted that these rotations are due to loading only.

The sign convention used is conveniently defined by reference to Figure 2.1. The deflections and end rotations shown there are taken as positive. End A of the column is conventionally regarded as the top of the column, and division point numbering always starts from there.

This method of integration is elegant and has been shown to be very accurate in the elastic range. It can easily be extended to deal with rigid end gusset lengths, but it becomes cumbersome when dealing with unequal segments, or with a step-wise variation in cross-section along the column.

A2.4. Analysis under end moments only

It is required to find a solution under applied moments M_A and M_B (Figure 2.1). It is assumed that when $M_A = M_B = 0$, $M_{AB} = M_{BA} = 0$.

At the start of the analysis initial estimates for M_{AB} and M_{BA} must be made. The procedure for this is given later. Assuming that estimates are available, the bending moment at any division point cross-section x is given by:-

$$M_x = M_{AB} + \frac{(M_{BA} - M_{AB})\,x}{N} \quad \text{A2.18}$$

Using the procedure given in A2.1, the curvature corresponding to this bending moment is found, and when the curvatures at all

division points have been found, the integration procedure given in A2.3 is used to give calculated deflections and end rotations. To check whether valid assumptions for M_{AB} and M_{BA} have been made, the end rotations must be checked for compatibility. The conditions for this are:-

$$\left.\begin{aligned}(\theta_A)_c &= (M_A - M_{AB})\,k_A \\ (\theta_B)_c &= (M_B - M_{BA})\,k_B\end{aligned}\right\} \qquad \text{A2.19}$$

It is convenient to carry out the check by calculating the following quantities:-

$$\left.\begin{aligned}\gamma_A &= (\theta_A)_c - (M_A - M_{AB})\,k_A \\ \gamma_B &= (\theta_B)_c - (M_B - M_{BA})\,k_B\end{aligned}\right\} \qquad \text{A2.20}$$

From equations A2.19, γ_A and γ_B should be zero for compatibility to be satisfied. If they are not sufficiently small modifications to M_{AB} and M_{BA} must be made such that on recalculation γ_A and γ_B are equal to or at least closer to zero.

Denoting the necessary modifications by $(M_{AB})_\eta$ and $(M_{BA})_\eta$ the following governing equations hold:-

$$\left.\begin{aligned}\frac{\partial \gamma_A}{\partial M_{AB}}(M_{AB})_\eta + \frac{\partial \gamma_A}{\partial M_{BA}}(M_{BA})_\eta &= -\gamma_A \\ \frac{\partial \gamma_B}{\partial M_{AB}}(M_{AB})_\eta + \frac{\partial \gamma_B}{\partial M_{BA}}(M_{BA})_\eta &= -\gamma_B\end{aligned}\right\} \qquad \text{A2.21}$$

From equations A2.20 by partial differntiation the following are obtained:-

$$\left.\begin{aligned}\frac{\partial \gamma_A}{\partial M_{AB}} &= \frac{\partial (\theta_A)_c}{\partial M_{AB}} + k_A \quad ; \quad \frac{\partial \gamma_A}{\partial M_{BA}} = \frac{\partial (\theta_A)_c}{\partial M_{BA}} \\ \frac{\partial \gamma_B}{\partial M_{AB}} &= \frac{\partial (\theta_B)_c}{\partial M_{AB}} \quad ; \quad \frac{\partial \gamma_B}{\partial M_{BA}} = \frac{\partial (\theta_B)_c}{\partial M_{BA}} + k_B\end{aligned}\right\} \qquad \text{A2.22}$$

The partial derivatives on the R.H. sides of equations A2.22 are obtained by considering the effects of changes in M_{AB} and M_{BA} on $(\theta_A)_C$ and $(\theta_B)_C$. For convenience unit changes are considered.

Effect of unit change in M_{AB}

The change in bending moment at a typical division point cross-section x is given by:-

$$(dM_x)_{dM_{AB}=1} = 1 - \frac{x}{N} \qquad \text{A2.23}$$

From equation A2.16, the corresponding change in curvature is:-

$$(d\phi_x)_{dM_{AB}=1} = \frac{\left(1 - \frac{x}{N}\right) X_x}{X_x Z_x - Y_x^2} \qquad \text{A2.24}$$

Values of X_X and $X_X Z_X - Y_X^2$ are available from the results of the curvature calculations, and thus the changes in curvature at each division point are calculated.

The logical procedure now would be to add these changes in curvature to the values just integrated and integrate again. The differences between the calculated end rotations thus obtained and those previously obtained would give the partial derivatives $\frac{\partial(\theta_A)_c}{\partial M_{AB}}$ and $\frac{\partial(\theta_B)_c}{\partial M_{AB}}$ directly.

The procedure actually used, which gives the same result, is to integrate the changes in curvature only, using an integration procedure which does not add in the initial deflections C_o, C_1,... C_N. The calculated end rotations from this integration, denoted by $d\theta_A$ and $d\theta_B$, give the required partial derivatives directly, i.e.:

$$\left.\begin{aligned}(d\theta_A)_{dM_{AB}=1} &= \frac{\partial(\theta_A)_c}{\partial M_{AB}} \\ (d\theta_B)_{dM_{AB}=1} &= \frac{\partial(\theta_B)_c}{\partial M_{AB}}\end{aligned}\right\} \qquad \text{A2.25}$$

Effect of unit change in M_{BA}

The change in bending moment at a typical division point cross-section x is given by:-

$$(dM_x)_{dM_{BA}=1} = \frac{x}{N} \qquad \text{A2.26}$$

and from equation A2.16 the corresponding change in curvature is:-

$$(d\phi_x)_{dM_{BA}=1} = \frac{\frac{x}{N} X_x}{X_x Z_x - Y_x^2} \qquad \text{A2.27}$$

Integration of these changes in curvature as for unit M_{AB} leads to calculated end rotations which give the required partial derivatives directly, i.e.:-

$$\left.\begin{aligned}(d\theta_A)_{dM_{BA}=1} &= \frac{\partial(\theta_A)_c}{\partial M_{BA}} \\ (d\theta_B)_{dM_{BA}=1} &= \frac{\partial(\theta_B)_c}{\partial M_{BA}}\end{aligned}\right\} \quad \text{A2.28}$$

The coefficients of equations A2.21 can now be set up and solutions for $(M_{AB})_\eta$ and $(M_{BA})_\eta$ obtained. Denoting the modified values of M_{AB} and M_{BA} by M'_{AB} and M'_{BA}, they are given by:-

$$\left.\begin{aligned}M'_{AB} &= M_{AB} + (M_{AB})_\eta \\ M'_{BA} &= M_{BA} + (M_{BA})_\eta\end{aligned}\right\} \quad \text{A2.29}$$

Using these modified values new calculated deflections and end rotations are obtained and the compatibility checked once again. Modifications to M_{AB} and M_{BA} are carried out as often as necessary.

Flow diagram for computer programme

This is given in Figure A2.4. A start is made by calculating γ_A and γ_B corresponding to $M_{AB} = M_{BA} = 0$. A facility is provided to read values of M_{AB} and M_{BA} manually. The reasons for this are given in § A2.7, while details of the data to be stored after a solution has been obtained are given in § A2.8.

A2.5 Analysis under end moment loading and axial load

It is required to find the axial load P which when combined with end moments M_A and M_B will produce a specified deflection D_R at a specified division point called the reference point. To start the analysis initial estimates for P, M_{AB}, M_{BA}, and for the divisiom point deflections $(D_o)_a$, $(D_1)_a$, ...$(D_x)_a$.....$(D_N)_a$ must be made. The procedure for obtaining these is outlined in § A2.7.

Assuming that estimates are available the bending moment at each division point cross-section is given by:-

$$M_x = M_{AB} + \frac{(M_{BA} - M_{AB})x}{N} + P(D_x)_a \quad \text{A2.30}$$

The axial load acting on each division point cross-section is taken as equal to P since the column deflections are assumed to be small. The curvatures at each division point are calculated and integrated to give calculated deflections $(D_o)_c$, $(D_1)_c$,..... $(D_X)_c$.....$(D_R)_c$ .....D_N, and calculated end rotations $(\theta_A)_c$ and $(\theta_B)_c$. These calculated values must now be checked for compatibility.

The compatibility of the end rotations and of the reference point deflection is checked by calculating the following quantities:-

$$\left.\begin{aligned} \gamma_A &= (\theta_A)_c - (M_A - M_{AB})\,k_A \\ \gamma_B &= (\theta_B)_c - (M_B - M_{BA})\,k_B \\ \Delta_R &= (D_R)_c - (D_R)_a \end{aligned}\right\} \qquad \text{A2.31}$$

γ_A, γ_B, and Δ_R should be zero. If they are not sufficiently small, modifications to P, M_{AB} and M_{BA} are made and new calculated deflections and end rotations obtained. Denoting the modifications by P_η , $(M_{AB})_\eta$, and $(M_{BA})_\eta$ the following governing equations hold:-

$$\left.\begin{aligned} \frac{\partial \gamma_A}{\partial P} P_\eta + \frac{\partial \gamma_A}{\partial M_{AB}} (M_{AB})_\eta + \frac{\partial \gamma_A}{\partial M_{BA}} (M_{BA})_\eta &= -\gamma_A \\ \frac{\partial \gamma_B}{\partial P} P_\eta + \frac{\partial \gamma_B}{\partial M_{AB}} (M_{AB})_\eta + \frac{\partial \gamma_B}{\partial M_{BA}} (M_{BA})_\eta &= -\gamma_B \\ \frac{\partial \Delta_R}{\partial P} P_\eta + \frac{\partial \Delta_R}{\partial M_{AB}} (M_{AB})_\eta + \frac{\partial \Delta_R}{\partial M_{BA}} (M_{BA})_\eta &= -\Delta_R \end{aligned}\right\} \qquad \text{A2.32}$$

The partial derivatives which form the coefficients of equations A2.32 are obtained by differentiating equations A2.31, giving:-

$$\frac{\partial \gamma_A}{\partial P} = \frac{\partial (\theta_A)_c}{\partial P} \; ; \; \frac{\partial \gamma_A}{\partial M_{AB}} = \frac{\partial (\theta_A)_c}{\partial M_{AB}} + k_A \; ; \; \frac{\partial \gamma_A}{\partial M_{BA}} = \frac{\partial (\theta_A)_c}{\partial M_{BA}} \qquad \text{A2.33}$$

$$\left.\begin{aligned} \frac{\partial \gamma_B}{\partial P} &= \frac{\partial (\theta_B)_c}{\partial P} \; ; \; \frac{\partial \gamma_B}{\partial M_{AB}} = \frac{\partial (\theta_B)_c}{\partial M_{AB}} \; ; \; \frac{\partial \gamma_B}{\partial M_{BA}} = \frac{\partial (\theta_B)_c}{\partial M_{BA}} + k_B \\ \frac{\partial \Delta_R}{\partial P} &= \frac{\partial (D_R)_c}{\partial P} \; ; \; \frac{\partial \Delta_R}{\partial M_{AB}} = \frac{\partial (D_R)_c}{\partial M_{AB}} \; ; \; \frac{\partial \Delta_R}{\partial M_{BA}} = \frac{\partial (D_R)_c}{\partial M_{BA}} \end{aligned}\right\} \quad \text{A2.33}$$

The partial derivatives on the R.H. sides of equations A2.33 are found by considering the effects of unit changes in P, M_{AB} and M_{BA}.

A unit change in P produces a change in bending moment dM_x at division point cross-section x equal to $(D_x)_a$. Referring to equation A2.16, the consequent change in curvature is given by:-

$$(d\phi_x)_{dP=1} = \frac{(D_x)_a X_x - Y_x}{X_x Z_x - Y_x^2} \qquad \text{A2.34}$$

Integrating these curvatures gives values of end rotation $d\theta_A$, $d\theta_B$, and reference deflection dD_R, which give the following partial derivatives directly, i.e.

$$(d\theta_A)_{dP=1} = \frac{\partial (\theta_A)_c}{\partial P} \; ; \; (d\theta_B)_{dP=1} = \frac{\partial (\theta_B)_c}{\partial P} \; ; \; (dD_R)_{dP=1} = \frac{\partial (D_R)_c}{\partial P} \qquad \text{A2.35}$$

A unit change in M_{AB} produces a change in curvature at division point cross-section x given by:-

$$(d\phi_x)_{dM_{AB}=1} = \frac{(1 - x/N) X_x}{X_x Z_x - Y_x^2} \qquad \text{A2.36}$$

Integrating these curvatures gives

$$(d\theta_A)_{dM_{AB}=1} = \frac{\partial (\theta_A)_c}{\partial M_{AB}} \; ; \; (d\theta_B)_{dM_{AB}=1} = \frac{\partial (\theta_B)_c}{\partial M_{AB}} \; ; \; (dD_R)_{dM_{AB}=1} = \frac{\partial (D_R)_c}{\partial M_{AB}} \qquad \text{A2.37}$$

A unit change in M_{BA} produces changes in curvature given by:-

$$(d\phi_x)_{dM_{BA}=1} = -\frac{x/N \, X_x}{X_x Z_x - Y_x^2} \qquad \text{A2.38}$$

Integrating these curvatures gives:-

$$(d\theta_A)_{dM_{BA}=1} = \frac{\partial (\theta_A)_c}{\partial M_{BA}} \; ; \; (d\theta_B)_{dM_{BA}=1} = \frac{\partial (\theta_B)_c}{\partial M_{BA}} \; ; \; (dD_R)_{dM_{BA}=1} = \frac{\partial (D_R)_c}{\partial M_{BA}} \qquad \text{A2.39}$$

The coefficients for the L.H. sides of equations A2.32 are now formed and solutions for the modifications P_η , $(M_{AB})_\eta$, and $(M_{BA})_\eta$ obtained. The new values of P, M_{AB}, and M_{BA}, denoted by P', M'_{AB}, and M'_{BA}, are given by:-

$$\left.\begin{aligned} P' &= P + P_\eta \\ M'_{AB} &= M_{AB} + (M_{AB})_\eta \\ M'_{BA} &= M_{BA} + (M_{BA})_\eta \end{aligned}\right\} \qquad \text{A2.40}$$

Calculated deflections and end rotations corresponding to these new values are obtained, and further modifications to P, M_{AB}, and M_{BA} carried out as outlined above, until γ_A, γ_B, and Δ_R are sufficiently small.

At this point the calculated deflections at division points other than the reference point are compared with the assumed deflections. If they are not sufficiently close, the calculated deflections are taken as new assumed deflections, and new calculated deflections and end rotations are obtained once again. The changes in assumed deflections can result in values of γ_A, γ_B, and Δ_R which are not sufficiently small and thus further modifications to P, M_{AB}, and M_{BA} may be necessary.

The procedure is repeated until γ_A, γ_B, and Δ_R are sufficiently small and the calculated deflections sufficiently close to the assumed deflections. A valid solution has then been obtained.

The flow diagram for the computer programme is shown in Figure A2.5.

A2.6. Calculation of reduced critical load

It is required to calculate the critical load of an initially straight column with the same end restraints as the actual column, but possessing reduced stiffnesses at division points where plasticity is present. Where no plasticity is present the procedure gives the elastic critical load.

The first step is to determine the stiffnesses at each division point. The change in curvature at division point x due to a unit change in M_x (i.e. the stiffness) is obtained by reference

to equation A2.16 and is given by:-

$$(d\phi_x)_{dM_x=1} = \frac{X_x}{X_x Z_x - Y_x^2} \qquad \text{A2.41}$$

For convenience, $\frac{X_x}{X_x Z_x - Y_x^2}$ will be denoted by $\frac{1}{(EI)'_x}$

The stiffness obtained from equation A2.41 only applies if the cross-section is subjected to a moment which is in the same direction as the existing one. If the moment reverses, unloading of fibres stressed into the plastic range occurs. In such cases the stiffness can be taken as the original elastic stiffness which is denoted by $\frac{1}{(EI)_x}$

The mode of deflection associated with the critical load must now be assumed, and for convenience the magnitude of the reference point deflection is taken as unity (Figure A2.6). Values of P'_{CR}, $(M_{AB})_{CR}$, and $(M_{BA})_{CR}$ must also be assumed, the values of $(M_{AB})_{CR}$ and $(M_{BA})_{CR}$ being dependent on the magnitude of the deflections. The procedure for obtaining initial estimates is covered in §A2.7.

Denoting the assumed deflections by $(D_o)_a$, $(D_1)_a$, ... $(D_X)_a$, ... $(D_N)_a$ and dropping the suffix $(\ )_{CR}$, the bending moment at division point cross-section is given by:-

$$M_x = M_{AB} + \frac{(M_{BA} - M_{AB})x}{N} + P'(D_x)_a \qquad \text{A2.42}$$

The curvature due to this moment is given by:-

$$\phi_x = \frac{M_x}{(EI)'_x}, \left(\text{or } \frac{M_x}{(EI)_x} \text{ if appropriate} \right) \qquad \text{A2.43}$$

Integrating these curvatures gives calculated deflections $(D_o)_c$, $(D_1)_c$,..... $(D_X)_c$, ... $(D_N)_c$, and calculated end rotations $(\theta_A)_c$ and $(\theta_A)_c$. These values must now be checked for compatibility.

Referring to Figure A2.6b, the conditions for compatibility of end rotation and reference point deflection are:-

$$\left.\begin{aligned} (\theta_A)_c &= -M_{AB} k_A \\ (\theta_B)_c &= -M_{BA} k_B \\ (D_R)_c &= 1 \end{aligned}\right\} \qquad \text{A2.44}$$

These are conveniently checked by calculating the following quantities which should be zero if compatibility is satisfied:-

$$\left.\begin{aligned} \gamma_A &= (\theta_A)_c + M_{AB}\, k_A \\ \gamma_B &= (\theta_B)_c + M_{BA}\, k_B \\ \Delta_R &= (D_R)_c - 1 \end{aligned}\right\} \qquad \text{A2.45}$$

If γ_A, γ_B, and Δ_R are not sufficiently close to zero then modifications to P', M_{AB}, M_{BA} are made and new calculated deflections and end rotations obtained. Denoting the necessary modifications by P'_η , $(M_{AB})_\eta$, and $(M_{BA})_\eta$ the following governing equations hold:-

$$\left.\begin{aligned} \frac{\partial \gamma_A}{\partial P'} P'_\eta + \frac{\partial \gamma_A}{\partial M_{AB}} (M_{AB})_\eta + \frac{\partial \gamma_A}{\partial M_{BA}} (M_{BA})_\eta &= -\gamma_A \\ \frac{\partial \gamma_B}{\partial P'} P'_\eta + \frac{\partial \gamma_B}{\partial M_{AB}} (M_{AB})_\eta + \frac{\partial \gamma_B}{\partial M_{BA}} (M_{BA})_\eta &= -\gamma_B \\ \frac{\partial \Delta_R}{\partial P'} P'_\eta + \frac{\partial \Delta_R}{\partial M_{AB}} (M_{AB})_\eta + \frac{\partial \Delta_R}{\partial M_{BA}} (M_{BA})_\eta &= -\Delta_R \end{aligned}\right\} \qquad \text{A2.46}$$

To obtain the partial derivatives which form the coefficients of equations A2.46, equations A2.45 are differentiated giving:-

$$\left.\begin{aligned} \frac{\partial \gamma_A}{\partial P'} &= \frac{\partial (\theta_A)_c}{\partial P'} ; \quad \frac{\partial \gamma_A}{\partial M_{AB}} = \frac{\partial (\theta_A)_c}{\partial M_{AB}} + k_A ; \quad \frac{\partial \gamma_A}{\partial M_{BA}} = \frac{\partial (\theta_A)_c}{\partial M_{BA}} \\ \frac{\partial \gamma_B}{\partial P'} &= \frac{\partial (\theta_B)_c}{\partial P'} ; \quad \frac{\partial \gamma_B}{\partial M_{AB}} = \frac{\partial (\theta_B)_c}{\partial M_{AB}} ; \quad \frac{\partial \gamma_B}{\partial M_{BA}} = \frac{\partial (\theta_B)_c}{\partial M_{BA}} + k_B \\ \frac{\partial \Delta_R}{\partial P'} &= \frac{\partial (D_R)_c}{\partial P'} ; \quad \frac{\partial \Delta_R}{\partial M_{AB}} = \frac{\partial (D_R)_c}{\partial M_{AB}} ; \quad \frac{\partial \Delta_R}{\partial M_{BA}} = \frac{\partial (D_R)_c}{\partial M_{BA}} \end{aligned}\right\} \qquad \text{A2.47}$$

The partial derivatives on the R.H. sides of equations A2.47 are

obtained by considering the effects of unit changes in P', M_{AB}, and M_{BA}.

A unit change in P' produces a change in bending moment at cross-section x equal to $(D_x)_a$. Thus the change in curvature is given by:-

$$(d\phi_x)_{dP'=1} = \frac{(D_x)_a}{(EI)'_x} \; , \left(\text{or } \frac{(D_x)_a}{(EI)_x} \right) \qquad \text{A2.48}$$

Integrating these changes in curvature gives values of calculated end rotation $d\theta_A$, $d\theta_B$, and of reference deflection dD_R which give the following partial derivatives directly, i.e.:-

$$(d\theta_A)_{dP'=1} = \frac{\partial(\theta_A)_c}{\partial P'} \; ; (d\theta_B)_{dP'=1} = \frac{\partial(\theta_B)_c}{\partial P'} \; ; (dD_R)_{dP'=1} = \frac{\partial(D_R)_c}{\partial P'} \qquad \text{A2.49}$$

A unit change in M_{AB} produces a change in bending moment at division point cross-section x given by:-

$$(dM_x)_{dM_{AB}=1} = 1 - \frac{x}{N} \qquad \text{A2.50}$$

leading to a change in curvature given by:-

$$(d\phi_x)_{dM_{AB}=1} = \left(1 - \frac{x}{N}\right)\frac{1}{(EI)'_x} \; , \left[\text{or } \left(1 - \frac{x}{N}\right)\frac{1}{(EI)_x} \right] \qquad \text{A2.51}$$

Integrating these changes in curvature gives partial derivatives as follows:-

$$(d\theta_A)_{dM_{AB}=1} = \frac{\partial(\theta_A)_c}{\partial M_{AB}} \; ; (d\theta_B)_{dM_{AB}=1} = \frac{\partial(\theta_B)_c}{\partial M_{AB}} \; ; (d\theta_R)_{dM_{AB}=1} = \frac{\partial(D_R)_c}{\partial M_{AB}} \qquad \text{A2.52}$$

A unit change in M_{BA} will produce a change in bending moment at division point cross-section x equal to x/N giving:-

$$(d\phi_x)_{dM_{BA}=1} = \frac{x}{N(EI)'_x} \; , \left(\text{or } \frac{x}{N(EI)_x} \right) \qquad \text{A2.53}$$

Integrating these changes in curvature gives partial derivatives as follows:-

$$(d\theta_A)_{dM_{BA}=1} = \frac{\partial(\theta_A)_c}{\partial M_{BA}} \; ; (d\theta_B)_{dM_{BA}=1} = \frac{\partial(\theta_B)_c}{\partial M_{BA}} \; ; (dD_R)_{dM_{BA}=1} = \frac{\partial(D_R)_c}{\partial M_{BA}} \qquad \text{A2.54}$$

The coefficients of equations A2.47 are now formed and solutions for P'_η , $(M_{AB})_\eta$, $(M_{BA})_\eta$ obtained which are added to P', M_{AB}, and M_{BA}. Calculated deflections and end rotations corresponding to these modified values of P', M_{AB}, and M_{BA} are obtained. γ_A, γ_B, and Δ_R are calculated once more and they should now be insignificant.

The calculated and assumed deflections at other division points are now compared. If they are not sufficiently close the assumed deflections are replaced by the calculated ones and new calculated deflections and end rotations obtained. The changes in the assumed deflections may result in values of γ_A, γ_B, and Δ_R which are not sufficiently small and further modifications to P', M_{AB}, and M_{BA} may be necessary.

When γ_A, γ_B, Δ_R and the differences between assumed and calculated deflections at all division points are sufficiently small a valid solution has been obtained.

The analysis as described above gives the reduced critical load according to the von Karman criterion (§ 2.4.1.). To obtain the load according to the Shanley criterion, the values of stiffness are taken as $\left(\frac{I}{EI}\right)'_x$ regardless of the direction of the moments.

The flow diagram for the analysis for the von Karman reduced critical load, as programmed for 'DEUCE', is given in Figure A2.7. The flow diagrame for the Shanley analysis is similar except that Step 4 is omitted and steps 10 and 11 are carried out immediately after Step 1 and the resulting partial derivatives stored away. This is because these partial derivatives are not affected by modifications to the assumed deflections. The 'DEUCE' programme can be simply amended to calculate the Shanley reduced critical load.

A2.7. Convergence

The convergence of the iterative procedures described above is dependent mainly on the equations involving partial derivatives. In the plastic range these partial derivatives vary as the load varies and thus the equations are strictly applicable only if the first trial calculations give a degree of plasticity close to the true value. The methods for obtaining the estimates for the first trial calculations and some of the convergence difficulties are discussed under separate headings below.

A2.7.1. Curvature calculation

Before starting the analysis proper initial trial values were obtained by calculating and storing X_X, Y_X, Z_X, $X_X Z_X - Y_X^2$, corresponding to $e_X = \phi_X = (P_X)_c = (M_X)_c = 0$. Elsewhere in the analysis the trial values were taken from a previous calculation, either from the previous stage of the analysis, or from the previous iteration within a stage.

Convergence difficulties with the curvature calculation are dependent mainly on the stress/strain curve, examples of which are shown in Figure A2.8. Also shown are the corresponding moment/curvature curves for a rectangular cross-section under constant axial load.

Curve (a) presents no difficulties.

Curve (b) does not usually present any difficulties unless the flat portion of the curve is long when the same troubles arise as with curve (c).

Curve (c) presents a difficulty in that there are upper limits to the values of P_X and M_X which can be carried by the cross-section. As these limits are approached a slight change in P_X or M_X will produce very large changes in e_X and ϕ_X. Because of this equations A2.6 can yield values of $(e_X)_\eta$ and $(\phi_X)_\eta$ which are much too large. The modified values of e_X and ϕ_X are then so far from the true values that convergence is impossible. This problem has been largely overcome in the computer programme by setting limits to $(e_X)_\eta$ and $(\phi_X)_\eta$. It still remains possible, however, for the procedure not to lead to a solution, when P and M are approaching limiting values. If values of P and M exceed the upper limits it is obvious that no solution can be obtained.

Stress/strain curve (d) presents the same difficulties as curve (c) with an added complication in that two values of curvature can correspond to a given moment. Around the peak of the moment/curvature diagram the procedure is as likely to arrive at one value of curvature as the other. For this reason any analytical approach to this type of cross-section will be difficult and no attempt at it has been made.

Curve (e) is characteristic of annealed mild steel. The presence of the drop from upper to lower yield results in values of

X_x, Y_x, and Z_x which are not correct. In addition inaccuracies in the calculation of $(P_x)_c$ and $(M_x)_c$ arise because the cross-section strip in which the drop in stress occurs cannot reasonably be assumed to have a uniform stress. Despite these factors a number of columns of material with an upper yield 35% in excess of the lower yield have been successfully analysed.

Curves (f) and (g) result in moment/curvature curves which again can have two values of curvature corresponding to a given moment.

In the computer programme a limiting number of iterations through the procedure was set and if this was exceeded the computer stopped. It was arranged that certain remedial measures could be taken to continue the analysis. These remedial measures are described in A2.7.3 below.

A2.7.2. Analysis under end moment loading only

The method for obtaining initial trial values of M_{AB} and M_{BA} has already been indicated in §A2.4. If the column behaves elastically under end moment loading only, these initial trial values will prove to be correct.

If, however, the moment loading is such that plasticity is induced in the column, initial trial values are obtained which are too large. If the values are such that the capacity of one or other of the division point cross-sections is exceeded, the curvature calculation will fail. To deal with this a facility for reading initial trial values manually was inserted in the computer programme.

With regard to convergence, difficulties were occasionally experienced when initial trial values of M_{AB} and M_{BA}, inducing a high degree of plasticity, arose. The procedure would diverge until eventually a failure in the curvature calculation occurred. In such cases the manual read facility was used to read lower trial values.

A2.7.3. Analysis under axial load and end moments

Between stages in the analysis the reference point deflection D_R was increased by a specified fraction called the stage fraction. To obtain trial estimates of P, M_{AB}, M_{BA}, and D_o, D_1, ... D_x,.... D_N, appropriate to the increased value of D_R, a complicated procedure based on the results of the previous two stages in the analysis was

used. Further details are not given because the author is now of the opinion that a straightforward extrapolation procedure would be just as accurate. For the first stage after the analysis under end moments only extrapolation is not possible, and a procedure based on the results of the reduced critical load analysis could be used.

If the trial estimates of P, M_{AB}, M_{BA} are not reasonably close to the true values the calculation can diverge. No check on divergence was included in the programme since the process very quickly resulted in ridiculous values of P, M_{AB} and M_{BA}, which led in turn to failures in the curvature calculation. The remedy in such cases was to reduce the stage fraction and start again, recalculating D_R and making new trial estimates. By making the stage fraction small enough the analysis could always be continued, although the calculation time naturally increased.

Where an analysis diverges it is possible in the curvature calculation for values of $(P_X)_c$, $(M_X)_c$, e_x, ϕ_x .... etc. to be stored which are very far from the true values. To avoid convergence trouble after the stage fraction modification, the current values of $(P_X)_c$ ..... etc. are replaced by the values corresponding to the last successfully completed stage in the analysis.

A difficulty can arise with equations A2.21 where stocky columns subjected to loading other than near-symmetrical single curvature are concerned. In the early stages of axial loading on such columns the influence on the curvature of the bending moments due to axial load can be much less than the influence of the axial load itself. It is then possible for a modification in P to produce exactly the same effects on γ_A, γ_B, and Δ_R as a combination of modifications in M_{AB} and M_{BA}. Ill conditioning of equations A2.21 results and ridiculous solutions for P_η , $(M_{AB})_\eta$ and $(M_{BA})_\eta$ are obtained. In this case reducing the stage fraction cannot lead to a solution and thus where this trouble was experienced the analysis had to be abandoned. A method of solution for this type of problem is to find the deflections corresponding to specified axial loads in early stages of loading, switching to finding the loads corresponding to specified deflections at a suitable point. Detailed procedures for this approach have not been formulated.

With regard to the initial estimates for D_o , D_1 .....D_N

it was found that generally the estimates were very close to the true values and no convergence difficulties were experienced on this account.

The initial factor controlling convergence is the stage fraction. This was supplied as part of the initial data for the programme. Where curvature calculations failed, indicating a divergent calculation, manual control was provided to modify the stage fraction and re-enter the estimating section. This manual control could be replaced by an automatic procedure built into the programme

A2.7.4. Reduced critical load analysis

The initial deflections for the first calculation, i.e. after the analysis under moment loading only, were taken as proportional to the deflection from the moment loading analysis, adjusting these deflections such that the reference point deflection was equal to unity. The initial values for P'_{CR}, $(M_{AB})_{CR}$, and $(M_{BA})_{CR}$, were read in as part of the data, although values of zero can be used. For analysis at other stages of loading, the solution appropriate to the previous stage was taken to give initial estimates.

Convergence difficulties arose only with columns where the critical loads associated with the single curvature and double curvature modes were very close to one another. If the previous stage had resulted in a predominantly single curvature mode of deflection, and a double curvature mode was appropriate to the stage being considered, the deflection modification procedure led only very slowly to the solution. In the programme 100 iterations were specified as a limit and occasionally this was not sufficient.

No convergence difficulties arose with the calculations for the Shanley loads for the columns bent in symmetrical double curvature, carried out using the auxiliary SIRIUS autocode programme. A symmetrical sine wave was used as an estimate in this case. The stiffnesses in the upper and lower halves of such columns are symmetrical and thus the single curvature mode of deflection is symmetrical and the double curvature mode is antisymmetrical. The critical load for the single curvature mode was found without difficulty even when the critical load associated with the double curvature mode was the lower of the two. The critical load for the

double curvature mode was found by working with the half-column (Figure 2.5b).

A2.8 Flow diagram for the complete programme

The flow diagram for the general case of analysis is shown in Figure A2.8. The flow diagram for the special case of analysis for columns bent in symmetrical double curvature is similar, the initial data being taken from the half-column. The analysis for reduced critical load in this case is slightly different in that the whole column must be considered.

The data to be stored after each of the major steps in the programme is given below.

Data read in initially and stored

i) Stress/strain diagram detials
ii) Cross-section strip details for each division point cross section
iii) Initial eccentricity at each division point
iv) Values of N, R, λL, and stage fraction
v) Values of K_A and K_B
vi) Values of M_A and M_B
vii) Trial values of P'_{CR}, $(M_{AB})_{CR}$, $(M_{BA})_{CR}$

Data to be stored after analysis under end moment loading only

i) Store deflections D_o, D_1, ... D_N, and moments M_{AB} and M_{BA} (for use in estimating values for first analysis under end moment loading and axial load).

ii) Calculate strains at each cross-section and store in strain history if yield strain e'_o is exceeded (for use in curvature calculations if unloading takes place).

iii) Store $(P_x)_c$, $(M_x)_c$, ... $X_x Z_x - Y_x^2$, for each division point cross-section (for use if curvature calculation fails in first analysis under end moment loading and axial load).

Data to be stored after a reduced critical load analysis

i) Store P'_{CR}, $(M_{AB})_{CR}$ and $(M_{BA})_{CR}$, and deflections at each division point, (for use as estimates for next calculation).

Data to be stored after an analysis under end moment loading and axial load

i) Store D_o, D_1, ... D_N, and P, M_{AB}, M_{BA} from previous

analysis and replace with the values from the analysis just completed (for use in estimating the values for the next analysis).

ii) Store $(P_X)_c$, $(M_X)_c$, ... $X_X Z_X - Y_X^2$, for each division point, (for use if curvature calculation fails in next analysis).

iii) Calculate strains at each cross-section strip and overwrite the value in the strain history if it is exceeded, except where the calculated strain is still below the yield strain e'_o.

APPENDIX 3

A.3 Detailed experimental procedure for column tests

The lay-out of this appendix is as follows:-

A3.1 Tests on pinned steel columns

A3.1.1. Preparation of columns

The cross-section of column chosen for test was $\frac{1}{4}$" x $\frac{1}{2}$", failure being induced by bending about the weak axis. The columns were prepared by machining down from $\frac{5}{16}$" x $\frac{5}{8}$" ordinary M.S. black bar. Tests were carried out without annealing. All specimens were prepared from the same delivery of $\frac{5}{16}$" x $\frac{5}{8}$" bar.

After the columns had been accurately machined, cross arms were welded on at each end in order that moments could be applied during test. The application of axial load was through case-hardened steel saddles which were fitted at each end. Figure A3.1 shows typical details of a test column. Alignment of the steel saddles was checked and adjusted by using a jig. The straightness of the specimens was usually well within 0·005" and the centre section was always aligned with the lines joining the saddle grooves, the ends being adjusted as well as possible.

The presence of the welded cross-arm and steel saddle meant that approximately $\frac{5}{8}$" at each end of the columns was rigid.

Approximately 80 columns were prepared in lengths from 4·25" - 16·25" overall, giving an L/r range of 60 - 250.

A3.1.2. Details of test rig

Details are given in Figures A3.2 - 4, and Plates A3.1 - 4. Axial load is applied through a lever with 10 x magnification acting through an assembly supported by flat springs which allow relatively free movement over a short range. The axial load is balanced by a 5T capacity Ski-Hi hydraulic jack, with which the axial shortening of the column is taken up. This ensures that the assembly remains in a neutral position with respect to the flat springs and the lever load is carried by the column alone.*

---

* This axial loading system was designed by Mr J.G.S. Smith, prior to the author's start on this research.

The moment loading is applied as a couple at each end of the column to avoid affecting the axial load.

No means of eliminating eccentricity of loading about the strong axis of the column is included, it being assumed that the much larger moment of inertia about the strong axis makes the effects of any such eccentricity negligible.

A3.1.3. Test procedure

In all tests the end moments were first applied under a small axial load. This axial load was necessary to hold the specimen against any shear from unequal moments.

The axial load was then increased and deflection readings at the centre of the column taken at each increment of load. Large increments were added at the start of a test and smaller increments as the maximum load was approached.

Creep under constant load occurred with most columns, but this settled down quickly. About two minutes were allowed between load increments when creep was present. Collapse was not usually catastrophic, but consisted of a slow steady creep under constant load, eventually becoming faster. Complete collapse of the columns was avoided by the descent of the loading lever on to a stop. Visual inspection of the specimen during and after test revealed the locations where plastic zones had developed and this was noted down for each test.

A3.1.4. Determination of yield stress

After the series of tests was completed the yield stress of each column was determined by performing beam tests. For the short columns the cross-arms were cut off and extension pieces welded on to give a beam of 12" span. For the longer columns (12·25" and 16·25") no extension pieces were necessary. Two equal loads were applied at the third points of the beam giving a central region under constant bending moment. Load was added until the central deflection was increasing slowly under constant load. The central bending moment then prevailing was equated to the full plastic moment of the section and the yield stress calculated.

The yield stress was found to lie in a range between 18·5 and 19·5 Ton/in^2, and a value of 19 Ton/in^2 was assumed when analysing

the results.

A3.2. Tests on aluminium columns

A3.2.1. Preparation of columns

The columns were cut by bandsaw from the same piece of HE30WP aluminium alloy plate, nominally ¼" thick. They were then machined down to ½" width. The depth of the plate was found to vary between 0·250" and 0·253" and for convenience the columns were grouped in two batches, the first containing columns approximately 0·250" deep, and the second containing columns 0·253" deep. Each set of tests on columns of a particular length was made on columns selected from one or other of these batches. Approximately 60 columns were prepared, in lengths of 4⅞", 6⅜", and 8½".

A3.2.2. Determination of stress/strain curves

Two specimens, prepared from the same piece of plate as the columns, were tested in tension using a Baty extensometer over a 2" gauge length.

After analysing the first series of tests, there was some doubt as to the validity of the stress/strain curve obtained from these two specimens and two further specimens, selected at random from the columns, were tested. For these cases the curves were obtained in two stages, first with Huggenberger gauges (over a 1" gauge length), to determine the initial part of the curve accurately, and then with the Baty extensometer up to about 2% strain.

The loading on the specimens was initially applied in increments corresponding to about 1 Ton/in^2 stress, dropping to lower increments as yielding commenced. After each increment of load, the stress was held constant and the strain read after creep had settled down.

The results from all four tests are given in Figure A3.5 along with the curve used in the computer analysis. The curve in compression was assumed to be the same as in tension.

A3.2.3. Details of test rig

The axial load was applied through two loading heads which were designed for a maximum load of 6,000 lbs. The column ends were clamped into end fittings which were held to the loading heads. Traversing screws enabled the end fittings to be adjusted in position.

Details of the loading headsand end fittings are given in Figure A3.6 and Plate A3.5.

The loading heads were initially constructed on a "gimbal" principle to allow freedom of rotation in any direction. For convenience in this series of tests the apparatus was adapted to give freedom of rotation in one direction only. This is the reason for certain apparently superfluous details. The centre of rotation of the loading heads is at the point where the column emerges from the end fitting. Since the end fittings are $\frac{5}{8}$" deep the effective column lengths were $1\frac{1}{4}$" less than the manufactured lengths. The effective lengths in the tests were 3·62", 5·12", and 7·24".

The loading heads were placed in an "Olsen" 200,000 lb testing machine, the upper head being clamped to the travelling head of the machine and the lower head simply resting on the testing machine table.

Levers were used for applying end moments in the tests on pinned columns as shown in Plate A3.6. For clarity the apparatus is shown set up outside the testing machine. The lever arrangement shown is for case (a) loading (Figure 4.1). The lever arrangements for the other loading cases are shown schematically in Figure A3.7.

The apparatus for the tests on restrained columns is shown in Plate A3.7. The restraining beams used for this series of tests were of mild steel, 0·500" x 0·300". The support assembly at the ends of the beams is shown in Plate A3.8. The ball-bearing through which the beam passes provided a rotational freedom not required in this series of tests. The assembly provided a simple support which was raised or lowered, thus providing the same effect as an external moment applied to the system. The span of the beams could be adjusted to cover a range of restraint conditions. 2" long electrical resistance strain gauges were attached to the top and bottom of the beams to enable the bending moments at any stage to be determined.

A3.2.4. Test procedure for pinned columns

Stub beams were first inserted into the end fittings which were then clamped to the column ends. The lower end fitting was set in the lower loading head and held in place by lightly tightening the traversing screws. The travelling head of the testing machine

carrying the upper loading head was then lowered into position until a small axial load of about 100 lbs was being carried by the column. The traversing screws on the upper loading head were also tightened up lightly.

To align the column dial gauges were set to measure the deflections of the centre and one of the quarter points of the column. A small increment of axial load was applied and the direction of increase of the central deflection indicated the predominant eccentricity and also which way the column ends had to be moved in order to eliminate the eccentricity. One or other of the column ends was traversed to and fro until an increment of load of 1000 lb did not alter the central deflection more than 0·001". At this stage the direction of increase of the quarter point deflection was noted. To eliminate the quarter point deflection the ends of the column were moved by equal and opposite amounts, as near as could be judged, and then one of the ends was readjusted so that the central deflection again did not change more than 0·001" under an increment of 1000 lb load. If the quarter point deflection under the increment of 1000 lb was more than 0·001" further adjustments were carried out. The column was reckoned to be correctly aligned when both the central and quarter point deflections altered less than 0·001" under an increment of axial load of 1000 lb.

In most cases alignment was not a serious problem as careful loosening of the traversing screws enabled the end fittings to be replaced in the loading heads in almost exactly the same position. When alignment was completed, a dial gauge was set to measure the central deflection. For the case (d) loadings in symmetrical double curvature the deflections of one of the quarter points was also measured. Dial gauges reading to 0·001" were used.

The end moment was now added in increments, adjusting the travelling head of the testing machine between increments so that the axial load on the column remained at about 200 lb. This was necessary because the bending of the column effectively shortened the distance between the ends of the column and caused a reduction in axial load. In one case, before this effect was noted, the lower loading head was lifted right off the testing machine table thus upsetting the deflection readings. Also under case (b) and (d) loadings considerable horizontal shears were developed which on

several occasions caused the lower loading head to slide sideways, necessitating a complete restart to the setting up procedure. The 200 lb axial load was generally sufficient to prevent this happening.*

The deflection after applying the moment loading being noted, the axial load was added by manipulating the testing machine controls. Loading was applied initially in increments reading the load and deflection after each increment. When the load was near the maximum considerable dropping off in load (with a slight increase in deflection) occurred when the travelling head of the machine was brought to a halt. For convenience it was decided to carry out the final stages of loading to collapse with the strain control of the machine set to its lowest value. This gave a slow continuous increase in deflection and it was found quite convenient to note load and deflection simultaneously. Immediately the load began to drop off testing was discontinued.

Removal of the tested specimen was carried out by raising the travelling head of the testing machine until the axial load reduced to about 200 lb, removing the end moment loading levers, slackening off the traversing screws, and then raising the travelling head of the machine clear so that the column and end fittings could be lifted out.

A3.2.5. Calibration of restraining beams

Two calibrations had to be carried out on the restraining beams, first to calibrate the strain gauge readings in terms of moment on the beams, and second to find out the effective stiffness of particular spans of the beams.

The strain gauge readings were taken on an 11 channel direct reading strain bridge, produced by Tecquipment Ltd., Alfreton Road, Nottingham, (Code No. C.U.11). The readings on the dials of this instrument had to be adjusted until a line on a cathode ray oscilloscope became horizontal.

To perform the moment calibration the beams were inserted into the end fittings which were then gripped firmly in a vice. Moments were applied by adding weights at a specific distance from the strain

---

* If the author were to carry out more tests the lower loading head would be firmly fixed to the testing machine table.

gauge centre line and the corresponding changes in reading on the Tecquipment bridge recorded. From the mean of several readings the calibration factor was worked out. The centre line of the strain gauges was at a distance of $2\frac{3}{4}$" from the ℄ of the column so that the bending moment at the column end is given by:-

$$M_{col.} = M_{s.g.} \left(\frac{L_b}{L_b - 2{\cdot}75} \right)$$

where $M_{S.G.}$ is the moment at the centre line of the strain gauges and L_b is the span of the beams.

The stiffnesses of the beams were first calculated assuming that the end fittings gave a rigid beam/column joint. After the first series of tests it was realised that considerable deformation was taking place in the end fitting joints.

The stiffnesses were then determined experimentally by gripping the end fittings in a vice such that the beams projected horizontally Loads were applied at various points along the beam and the resulting deflections under the points of application of load measured. Dividing a given deflection by the distance from the column centre line to the load gave the rotation which would occur in a beam of that span subjected to end moment equal to that applied by the load. This procedure did not take account of the rotation in the joint between the column and the end fitting. This was assessed independently by inserting a column into the end fitting and clamping the fitting in a vice such that the column projected horizontally. A load was then added and the deflection under it measured. Knowing the column size and the modulus of elasticity of the column material the deflection assuming a fully encastré condition was calculated. The difference between this and the measured deflection divided by the distance from the load to the end fitting, was taken to give the rotation in the joint. Thus the total effective stiffness was calculated and a chart drawn up giving effective stiffness against beam span.

After the series of tests had been completed the rotation in the column to end fitting joint were reassessed by a more accurate method. A spare column was fitted into the end fitting which was again held such that the column projected horizontally. Mirrors were attached to the column close to where it emerged from

the end fitting and also to the main body of the end fitting. A telescope was arranged to view a scale through these mirrors, and u used to obtain the relative rotation between the column and the end fitting body when a load was applied to the column. The rotation in the short length of column between the point of attachment of the mirror and the end fitting was calculated from a knowledge of the bending moment, modulus of elasticity and moment of inertia of the cross-section. The rotations in the joints measured by this method were of the order of twice those obtained from the method described in the preceding paragraph. In the author's opinion the discrepancy is most probably due to an experimental error being made in the first method.

A3.2.6. Test procedure for restrained aluminium columns

The end fittings were first attached to the columns and the lower end fitting set in the lower loading head. The upper loading head was lowered into position and the traversing screws tightened up lightly under a load of 200 lbs. A rough preliminary alighnment was carried out if necessary at this point. After the zero of the beam strain gauges had been read the support assemblies plus the beams were moved up into position and the ends of the beams inserted into the end fittings. The end fitting joints were tightened up and the support assemblies clamped down to the testing machine table.

The final alignment was carried out as follows. The beam supports were adjusted such that the beam bending moments were zero, i.e. no moment was being applied to the column. This was done by setting the appropriate reading on the Tecquipment bridge and adjusting the beam support until the trace on the oscilloscope was horizontal.* After two or three adjustments of each beam in turn the desired condition was achieved. Attention was now concentrated on one end of the column and a small increment of axial load added. The direction in which the moment altered was noted and the increment of load removed. The end fitting was then traversed in a direction to offset the development of this moment and both beam moments readjusted to zero. The increment in axial load was again added and the alteration of moment noted once more. This

---

* The trace could be clearly seen from up to 10 ft away which considerably facilitated this procedure.

procedure was continued until the moment at that end was unaffected by the addition of axial load. Attention was then transferred to the other end and the same procedure applied there. By dealing with each end in turn as often as necessary alignment was completed. Correct alignment was assumed when an increment of 1000 lb. axial load caused both beam moments to alter less than 1 lb.in. This aligning technique was found to be much superior to that adopted for pinned columns though it took longer to carry out.

The moment loading was simulated by raising or lowering the beam supports as shown in Figure 4.8. The value of $(M_{AB})_{P = 0}$ was decided on prior to each testand the corresponding readings on the Tecquipment strain bridge worked out. The supports were then adjusted until the required value of $(M_{AB})_{P = 0}$ was obtained. This had to be carried out in stages, bringing the axial load up to the nominal value of 200 lb. between stages. Care was taken that the values of moment at any stage did not exceed the required values.

The axial loading was applied in increments in the early part of each test, and readings of axial load, beam strain gauges, and central deflection noted after each increment. At roughly 80% of the maximum load the strain control was set to its lowest value, and readings thereafter taken "on the run". It was found that the deflection then usually increased very slowly and generally did not alter more than 0·001" while the beam strain gauges and axial load were being read.

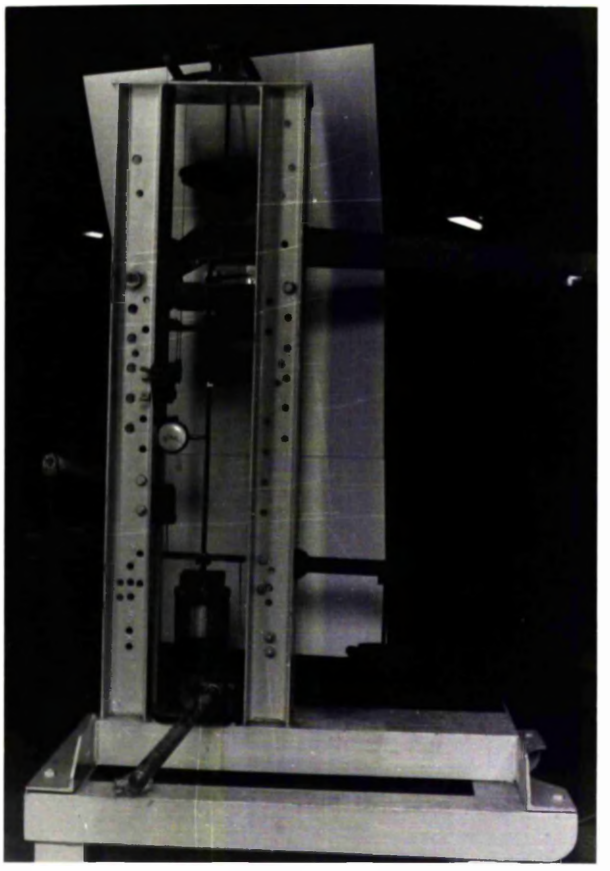

Plate A3.1 Test rig for rectangular steel columns.

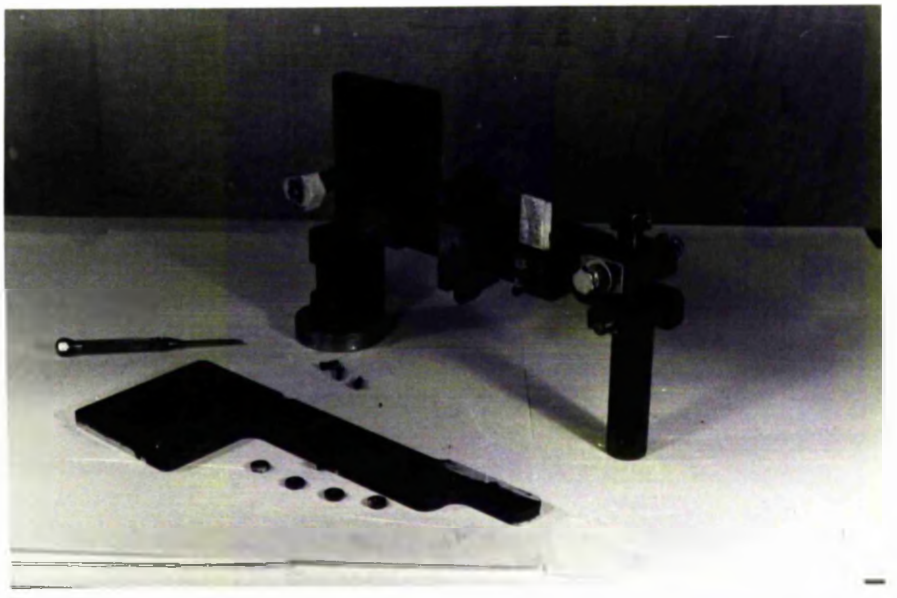

Plate A3.2 Details of axial loading head

Plate A3.3 Application of moment loading.

Plate A3.4 Lever system for applying moment loading.

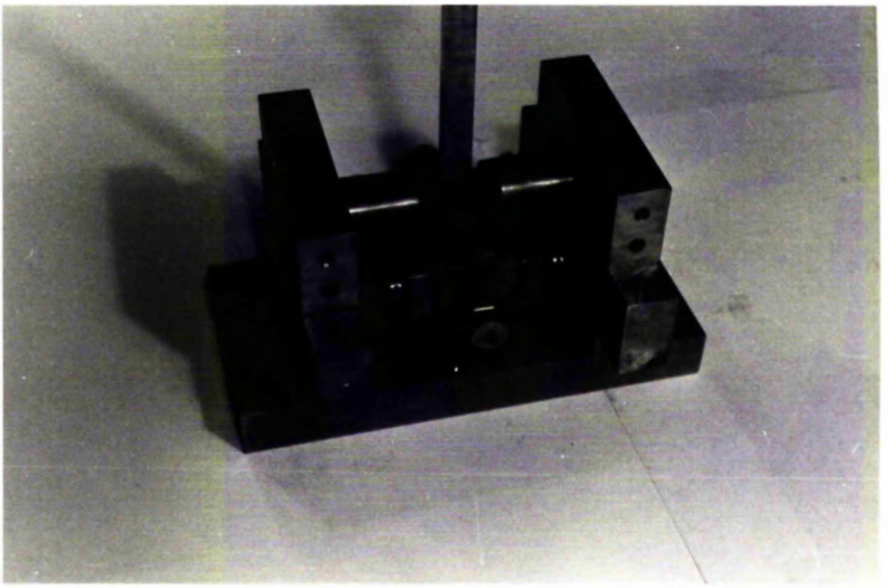

Plate A3.5 Loading head for tests on aluminium alloy columns.

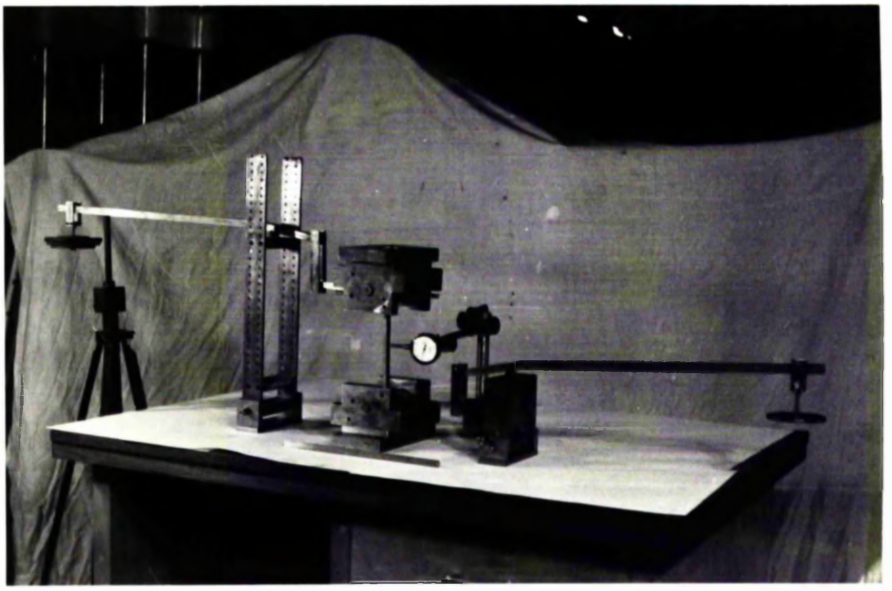

Plate A3.6 Arrangements for tests on pinned aluminium columns, (set up outside testing machine).

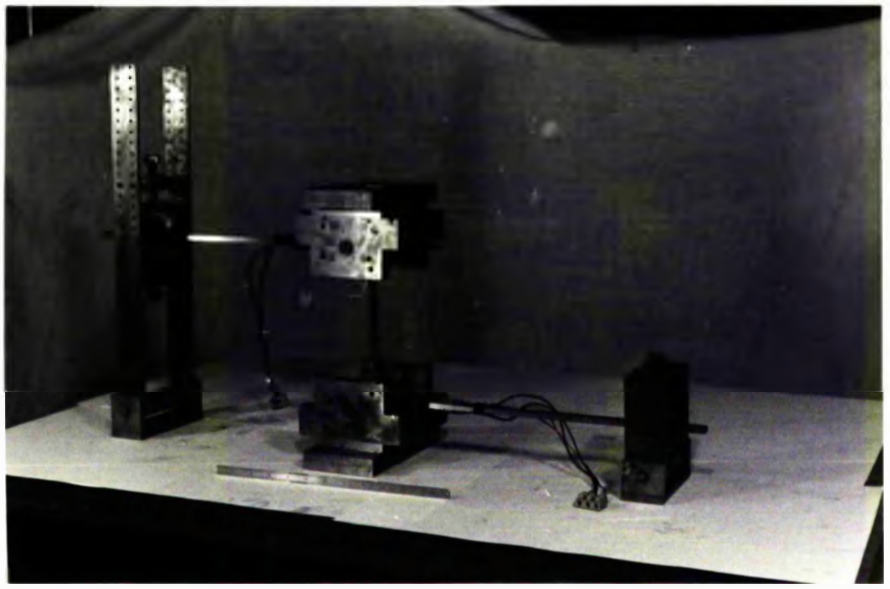

Plate A3.7 Arrangement for tests on restrained aluminium columns

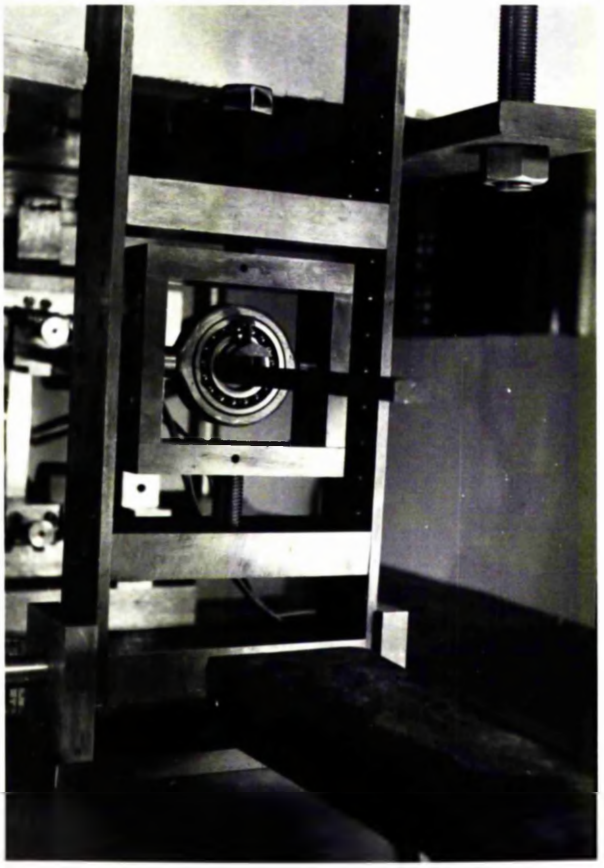

Plate A3.8 Support

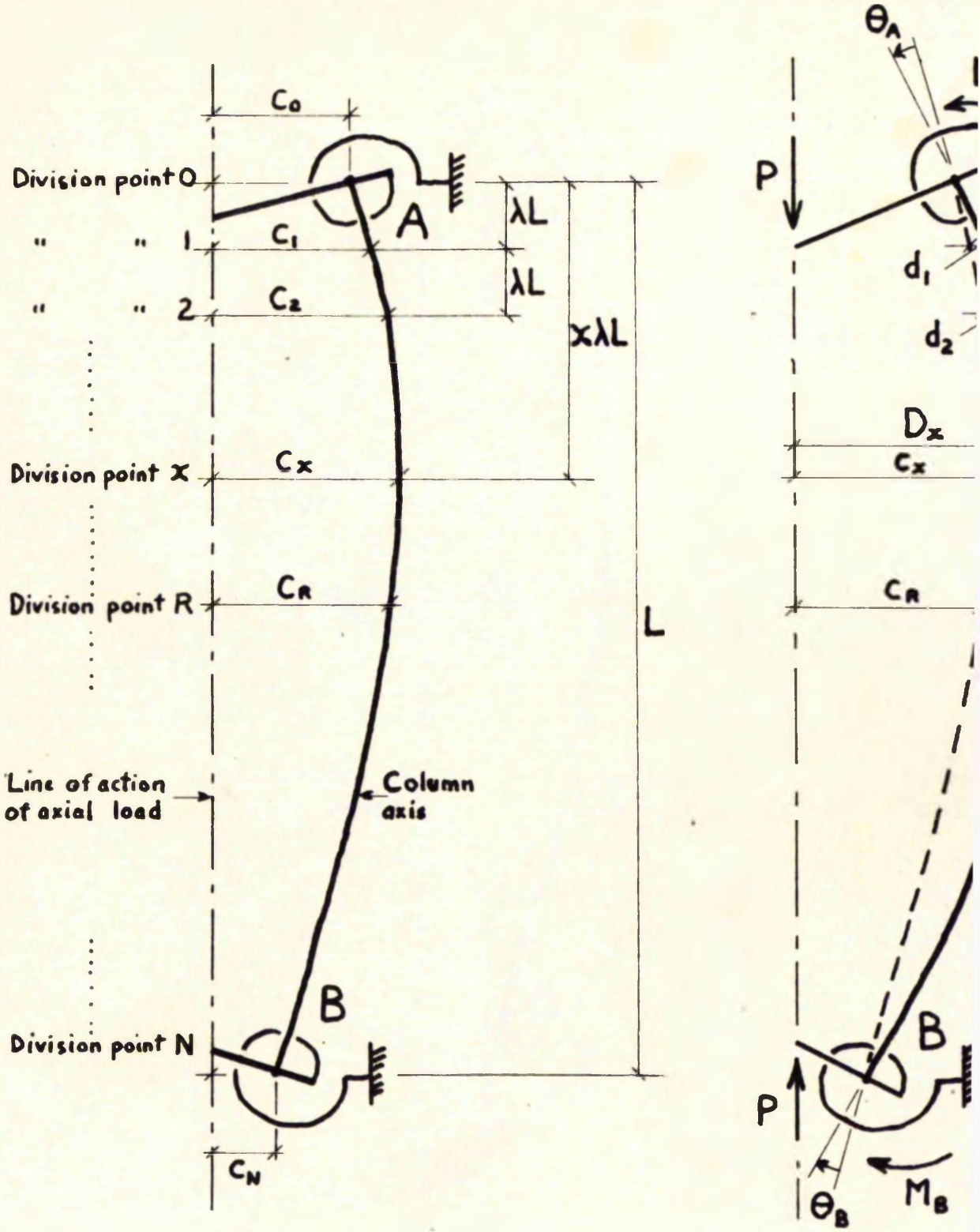

(a) Loaded (b) Loaded

FIG. 2.1. SYSTEM ANALYSED

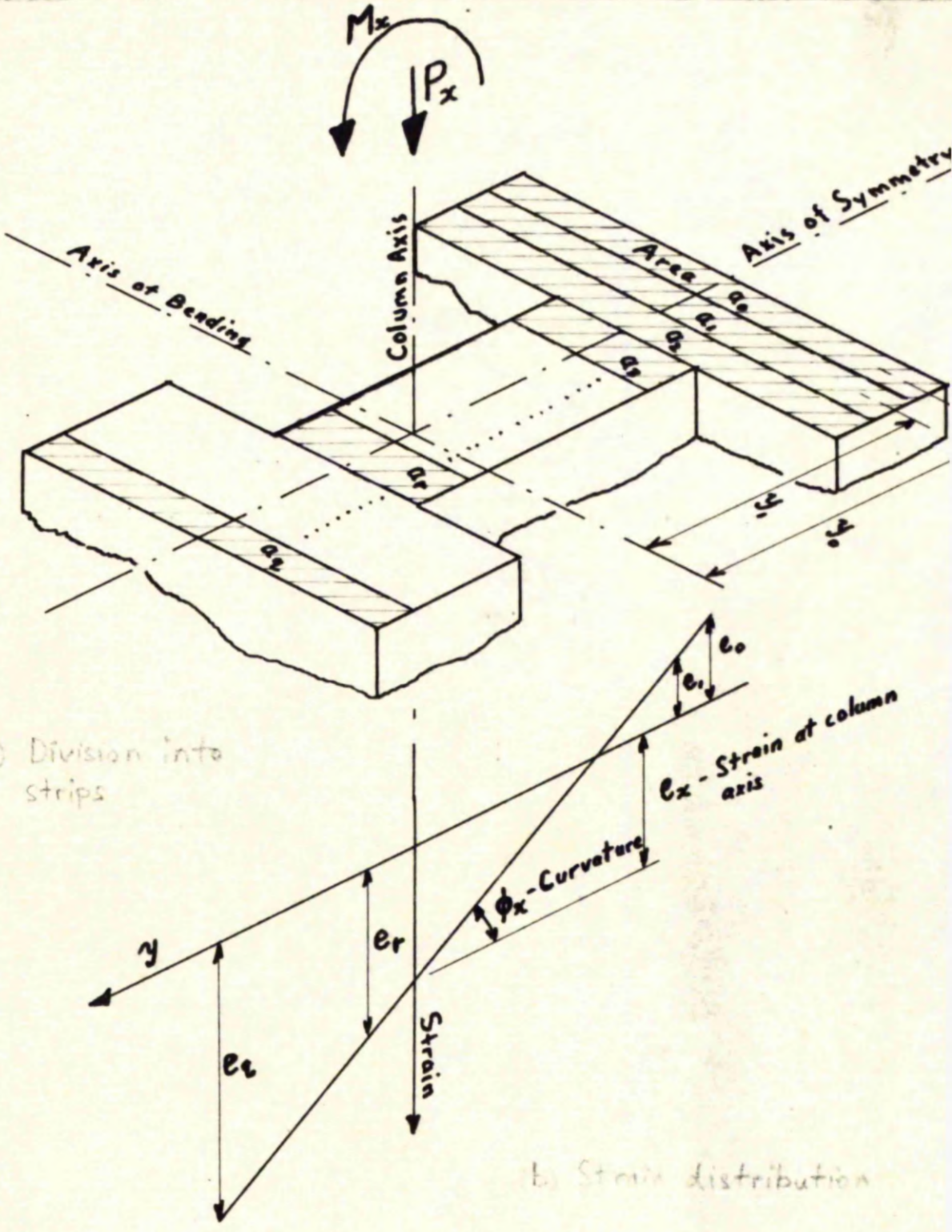

FIG. 2.2. CROSS-SECTION DETAILS

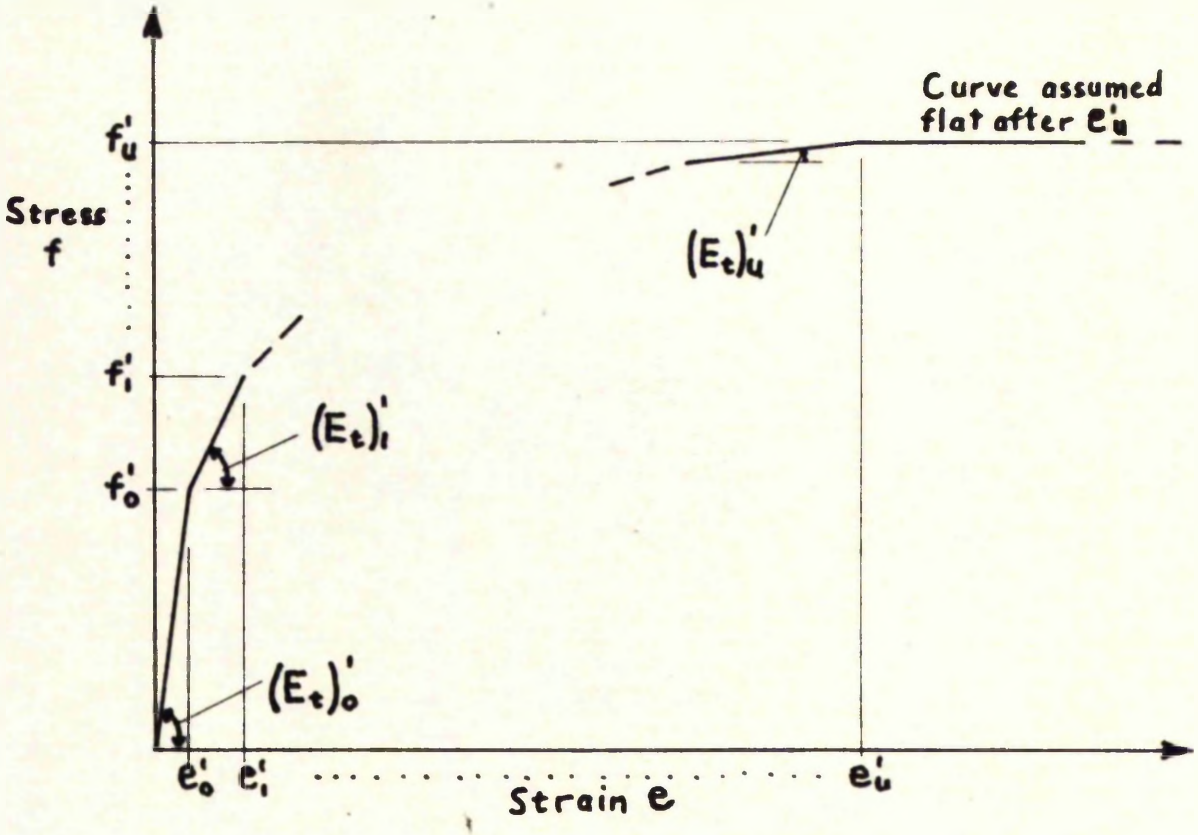

FIG. 2.3. STRESS-STRAIN CURVE.

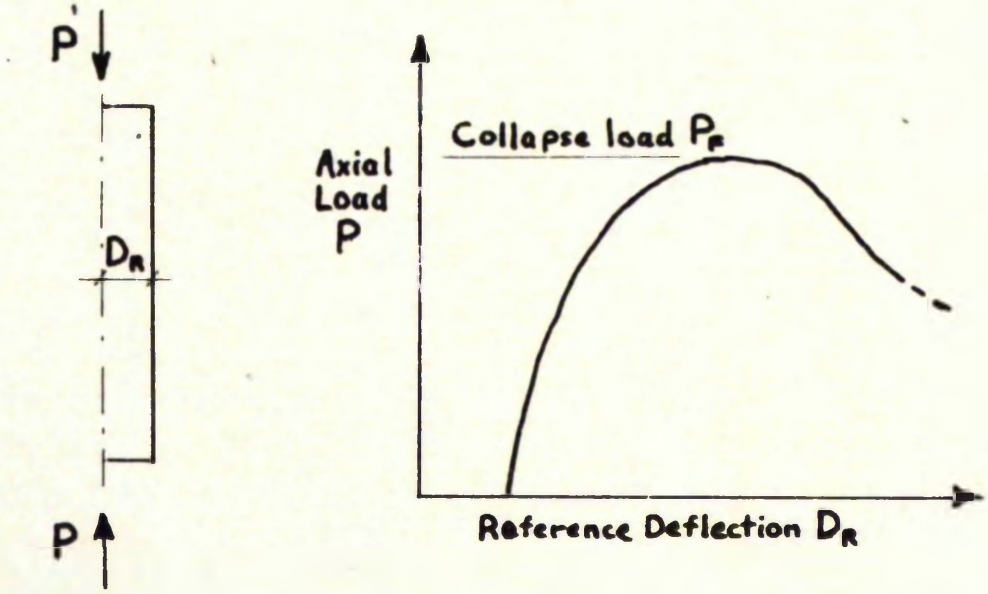

FIG. 2.4. TYPICAL LOAD-DEFLECTION CURVE.

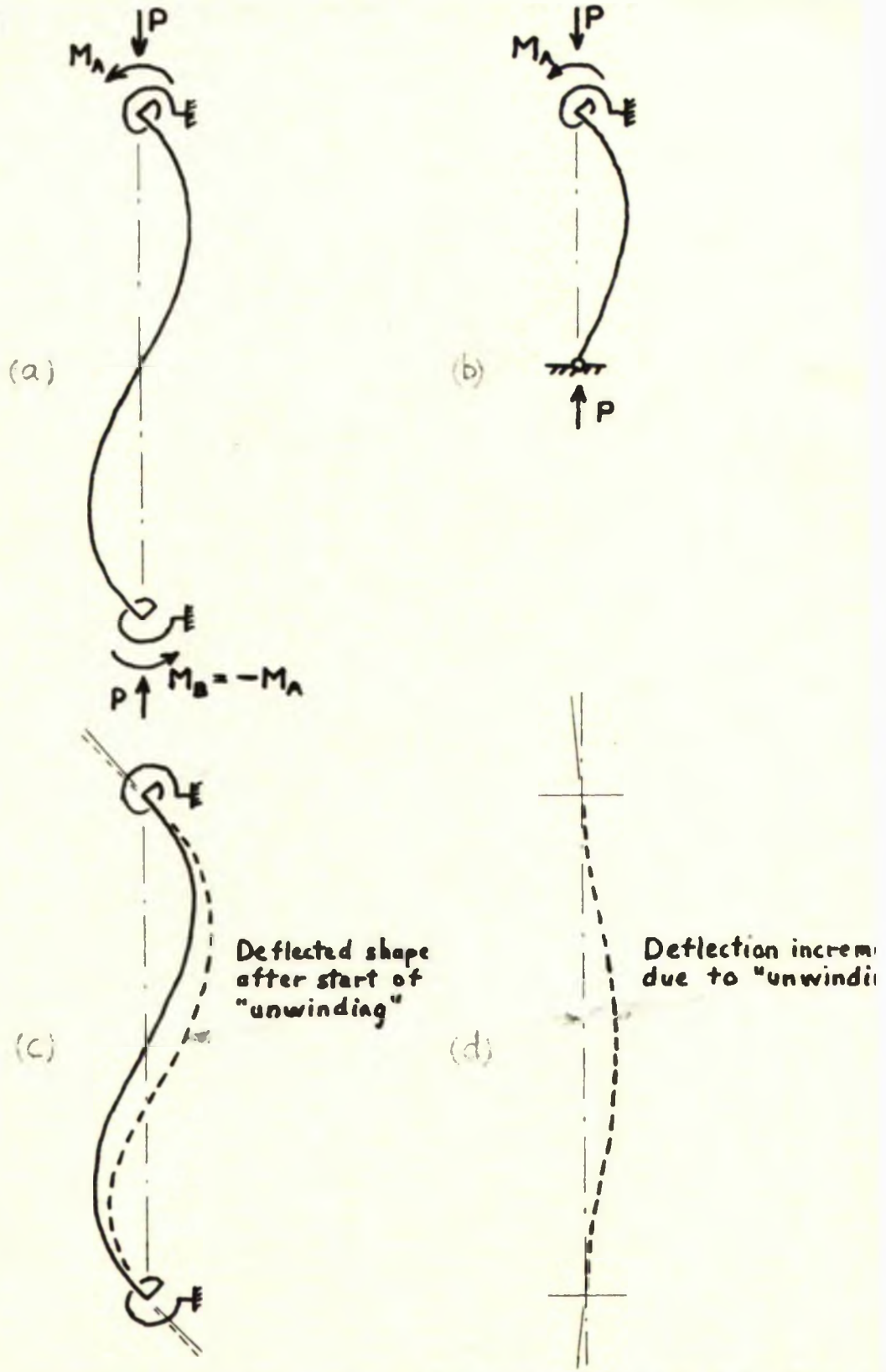

FIG. 2.5. COLUMN BENT IN SYMMETRICAL DOUBLE CURVATURE

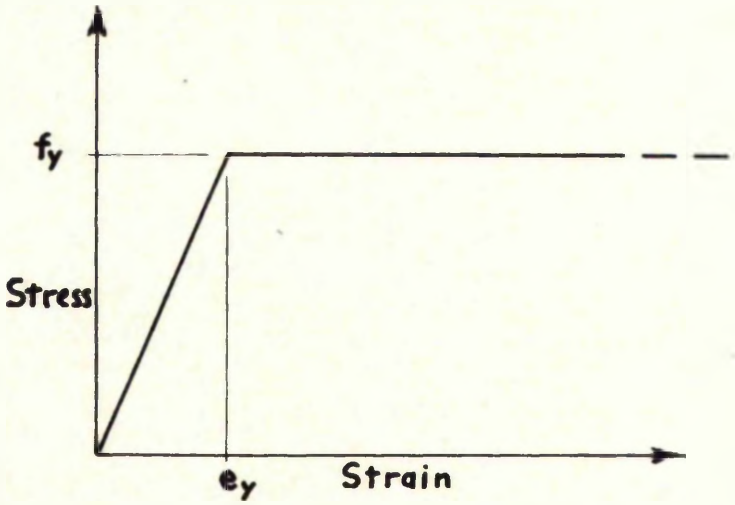

FIG. 3.1: STRESS-STRAIN DIAGRAM FOR IDEAL ELASTIC-PLASTIC MATERIAL.

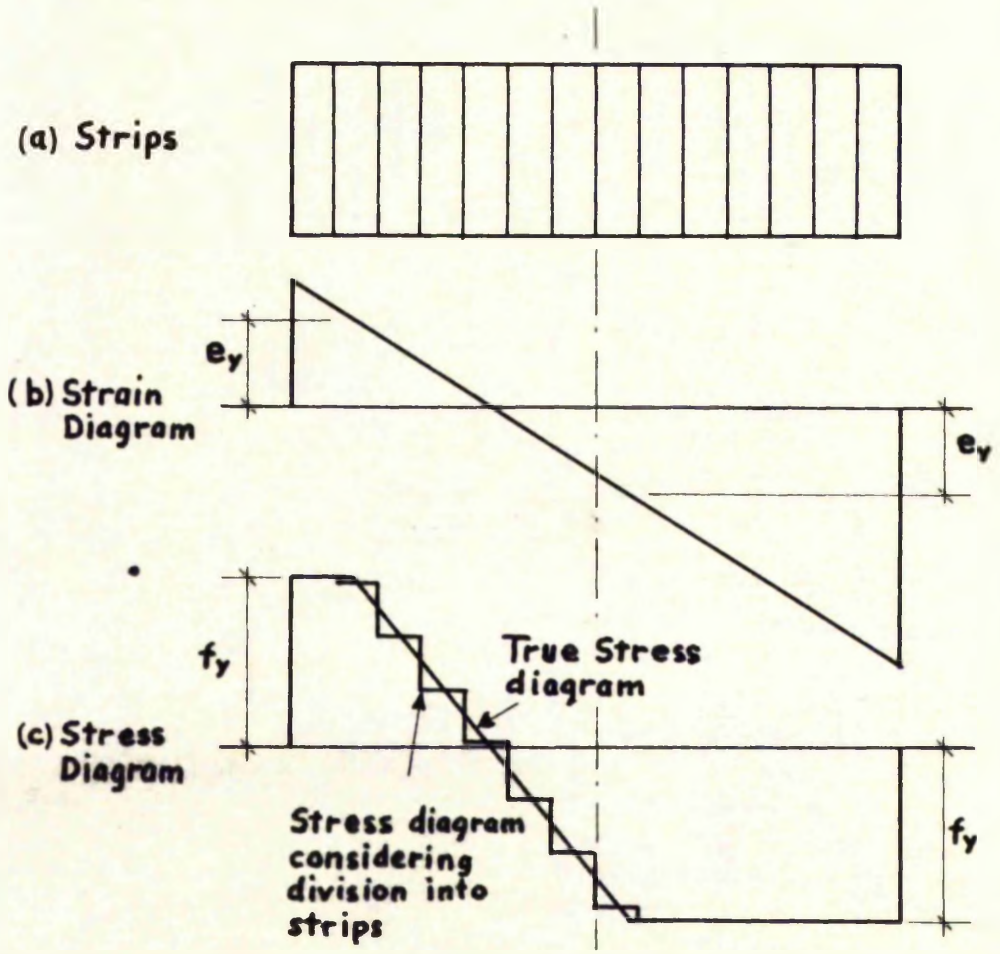

FIG. 3.2. CONSEQUENCES OF DIVISION OF CROSS-SECTION INTO STRIPS.

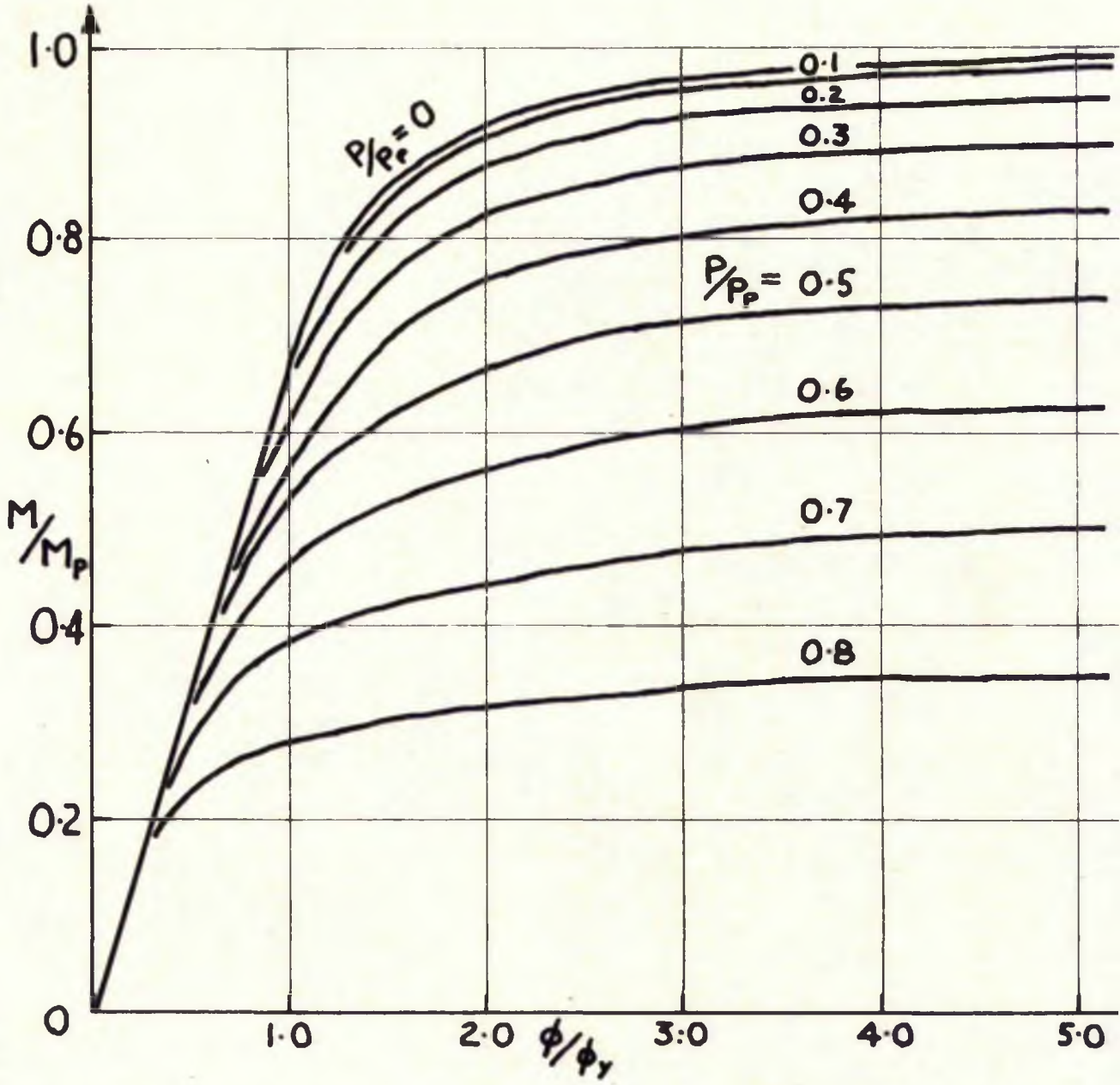

FIG. 3.5. INTERACTION BETWEEN AXIAL LOAD, BENDING MOMENT, AND CURVATURE FOR THE RECTANGULAR CROSS-SECTION OF IDEAL ELASTIC-PLASTIC MATERIAL.

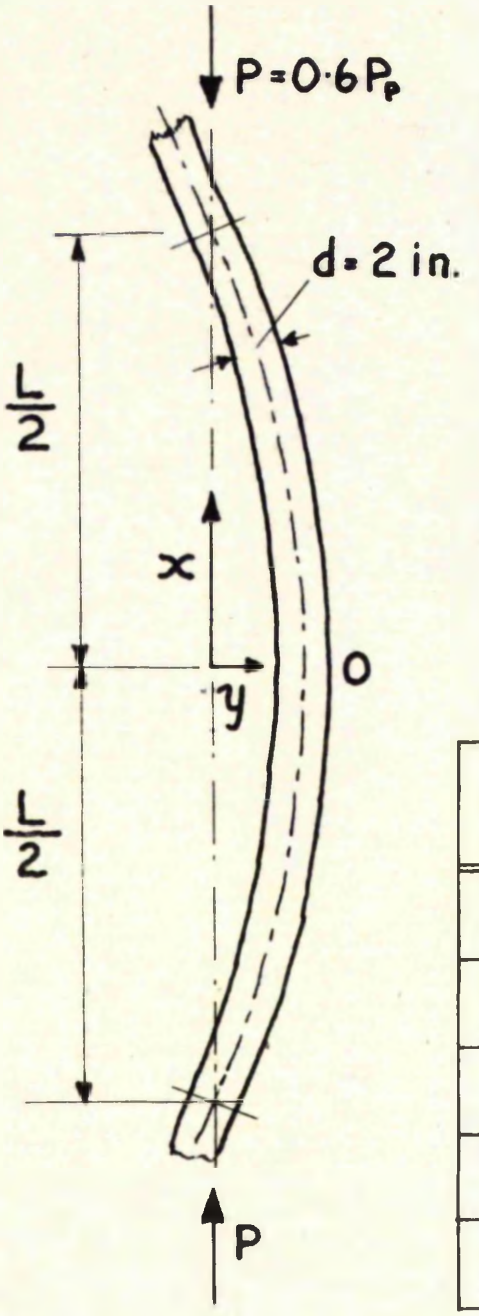

(a) System analysed

Material Properties

$E = 5000\ T/in^2$

$f_y = 20\ T/in^2$

giving $\phi_y = \cdot 004\ in^{-1}$

$\frac{\phi_o}{\phi_y}$	ϕ_o-in.$^{-1}$	y_o-in.	L - in.
0·4	·0016	·222	37·02
2·5	·0100	·489	26·78
5·0	·0200	·523	23·52
10·0	·0400	·531	21·46
∞	∞	·533	19·34

(b) Wavelength details calculated from rigorous equations

FIG. 3.4. COLUMN DEFLECTION CURVE DETAILS.

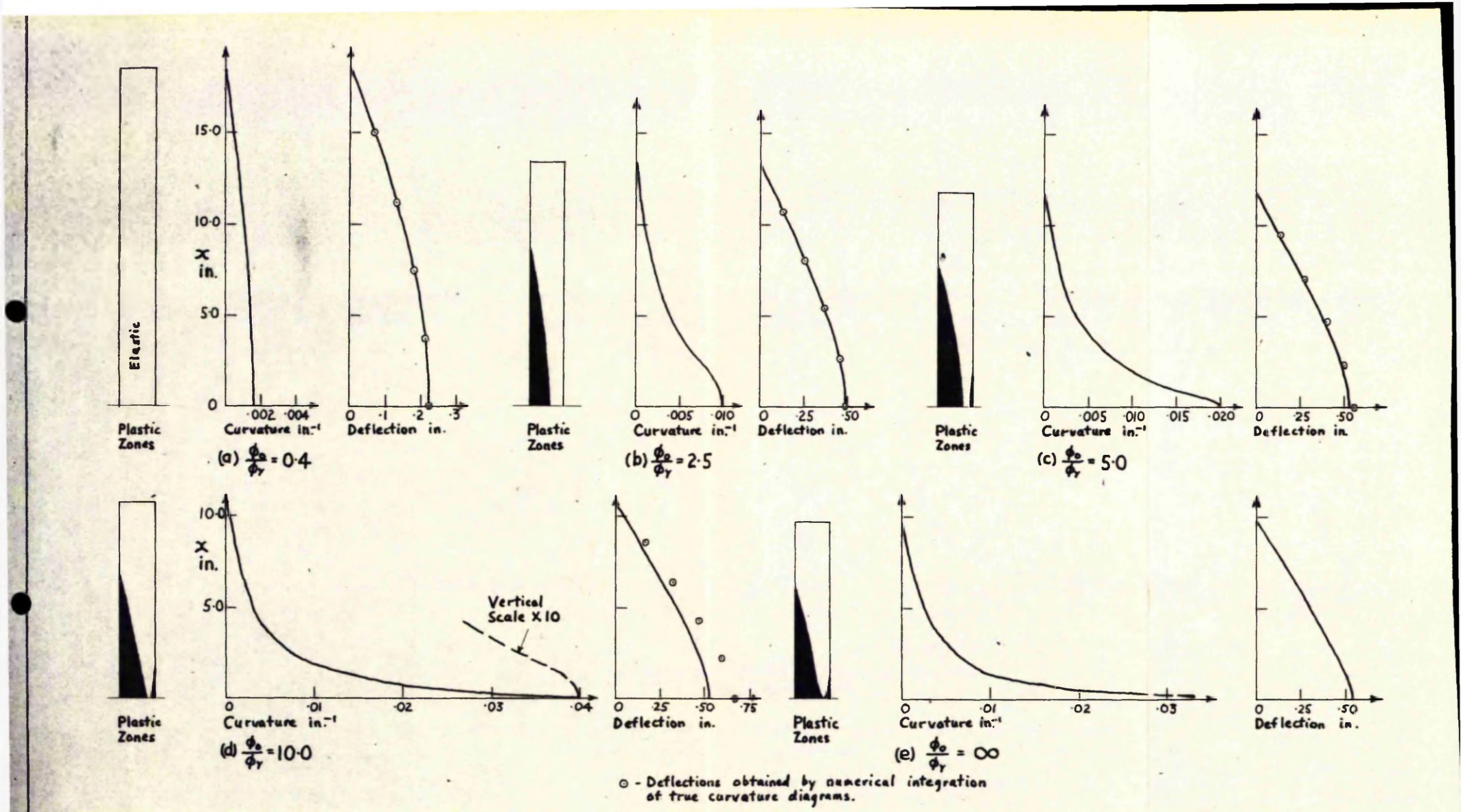

o - Deflections obtained by numerical integration of true curvature diagrams.

FIG 3.5. CURVATURE AND DEFLECTION DIAGRAMS FOR QUARTER-WAVES OF COLUMN-DEFLECTION CURVES.

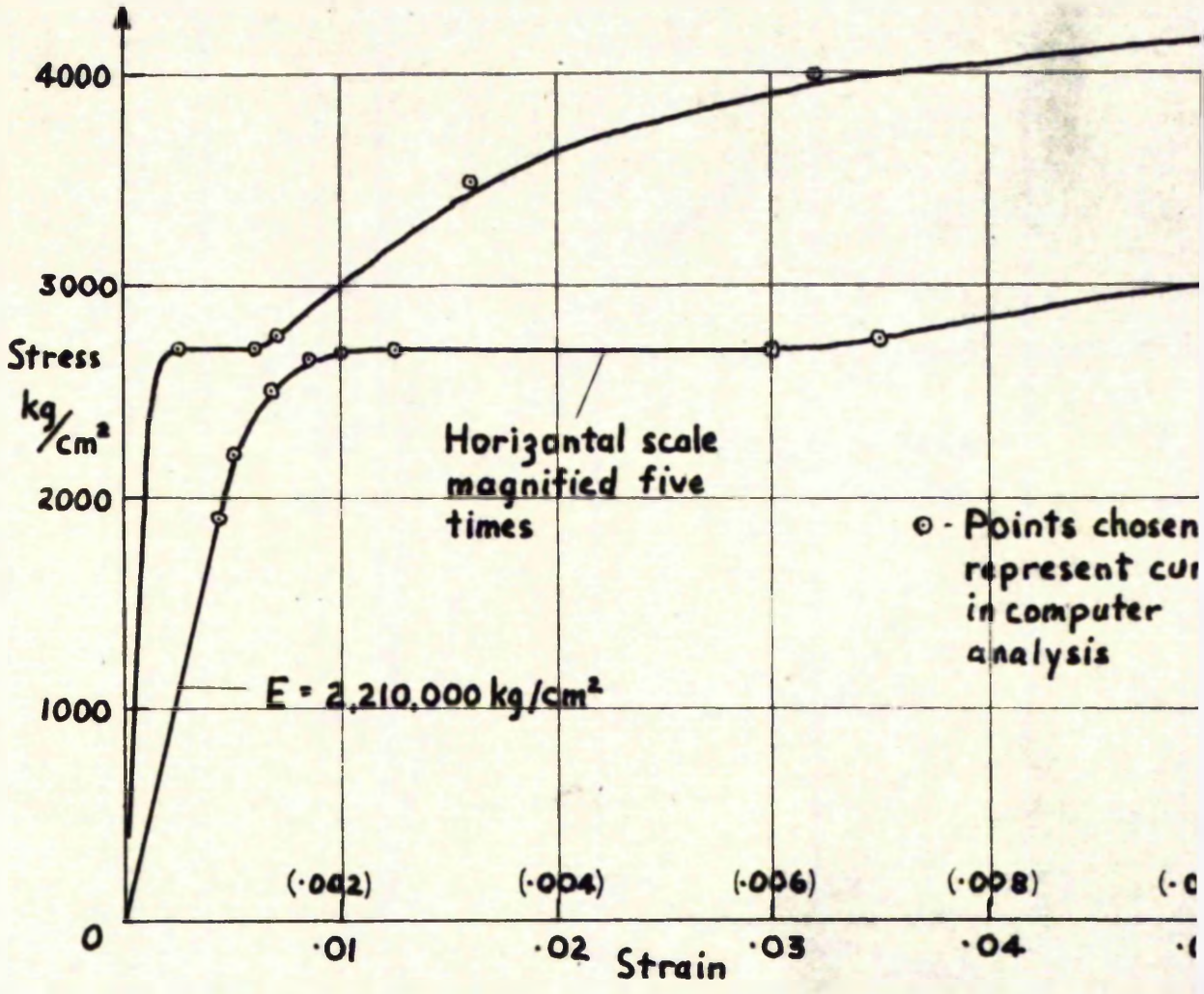

FIG. 3.6. STRESS-STRAIN CURVE USED BY CHWAL

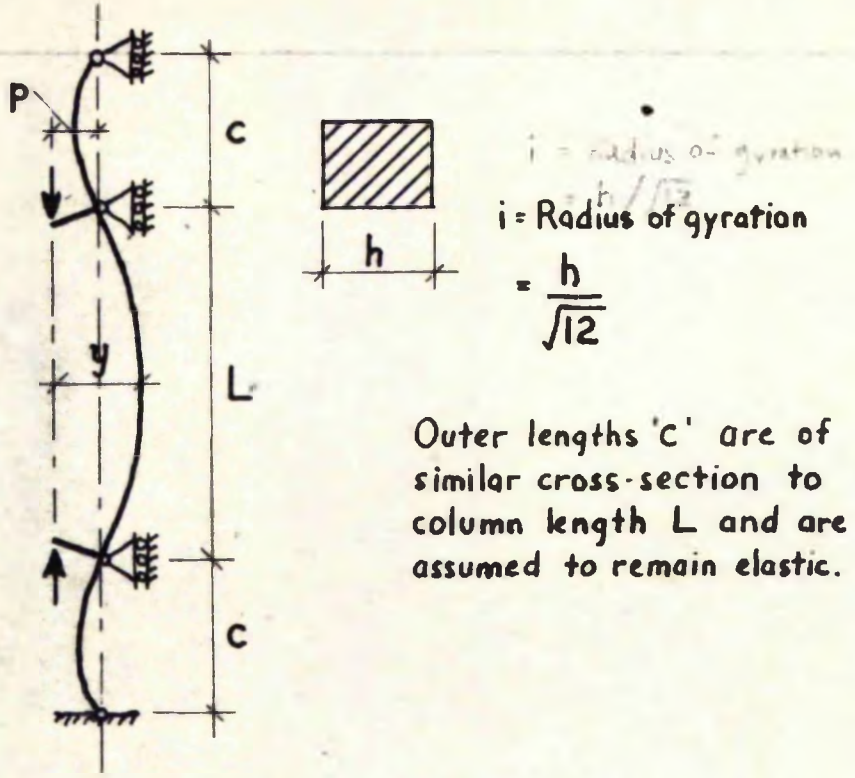

(a) System analysed

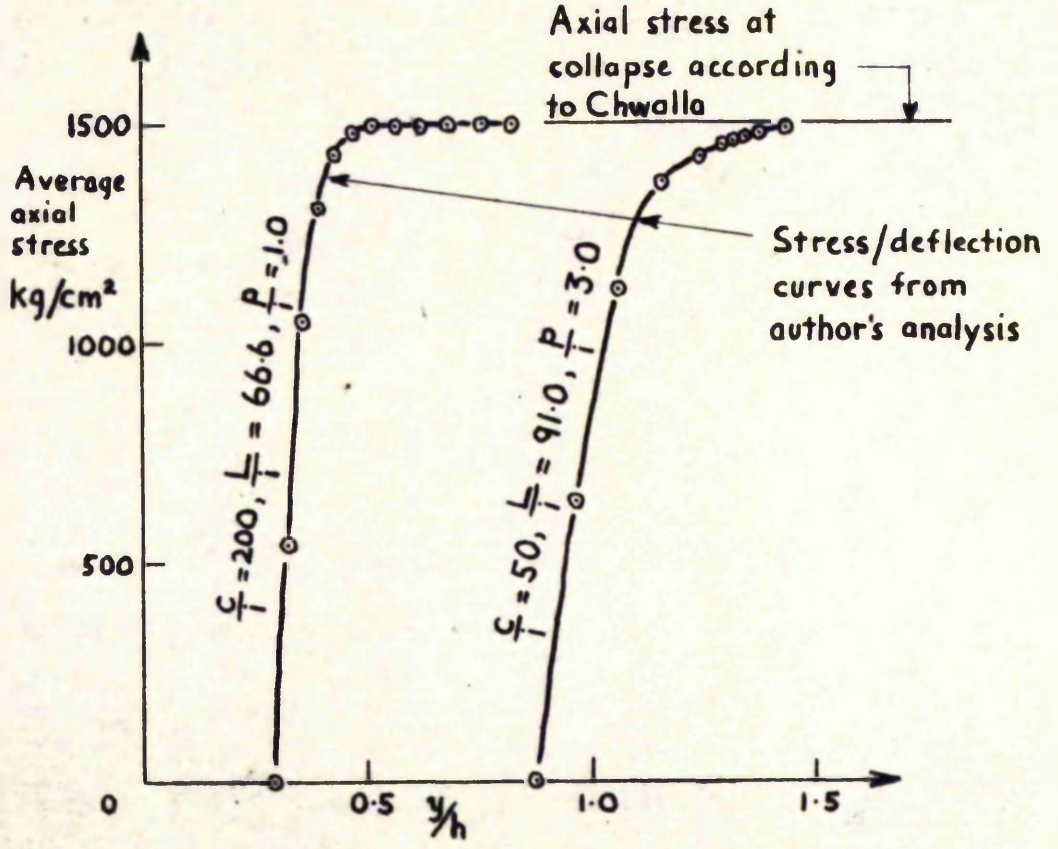

(b) Stress/deflection curves

FIGS.7. RESTRAINED COLUMNS ANALYSED BY CHWALLA

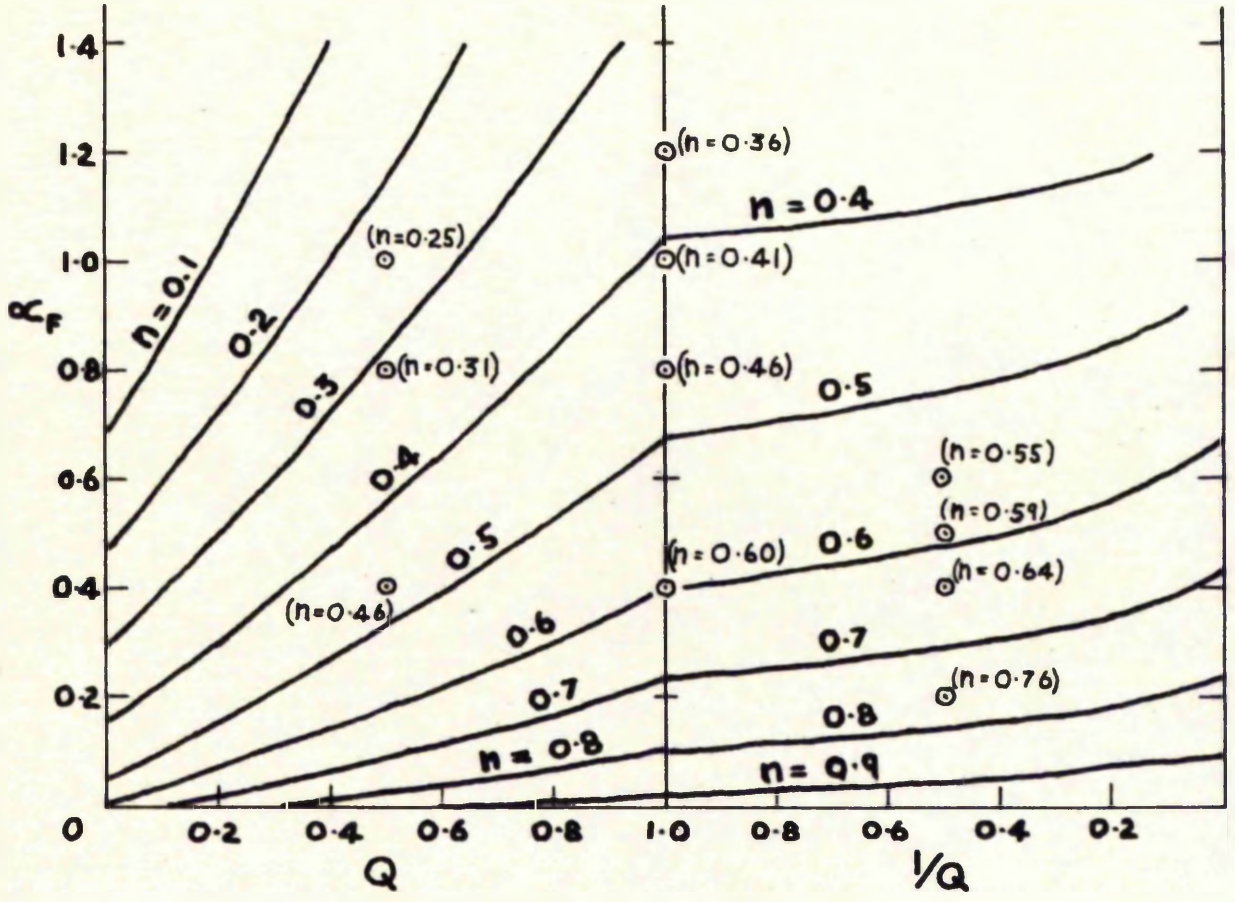

$$n = \frac{\text{Mean axial stress at collapse}}{\text{Yield stress}}$$

$$\alpha_F = \frac{\text{Fixed end beam moment}}{M_p \text{ for stanchion}}$$

$$Q = \frac{\text{Stiffness of beam}}{\text{Stiffness of stanchion}}$$

/ - Curves from "The Steel Skeleton" Fig. 14.19(a), p. 290.

⊙ - Points derived from collapse loads obtained using the author's analysis on columns with appropriate α_F and Q values.

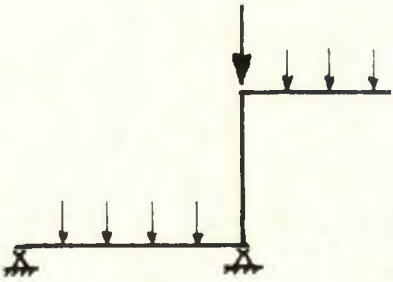

System analys

FIG. 3.8. COLLAPSE LOADS OF PLANE RECTANGULAR STANCHIONS BE
IN SYMMETRICAL SINGLE CURVATURE FOR A SLENDERNESS
RATIO OF $4\sqrt{E/f_L}$.

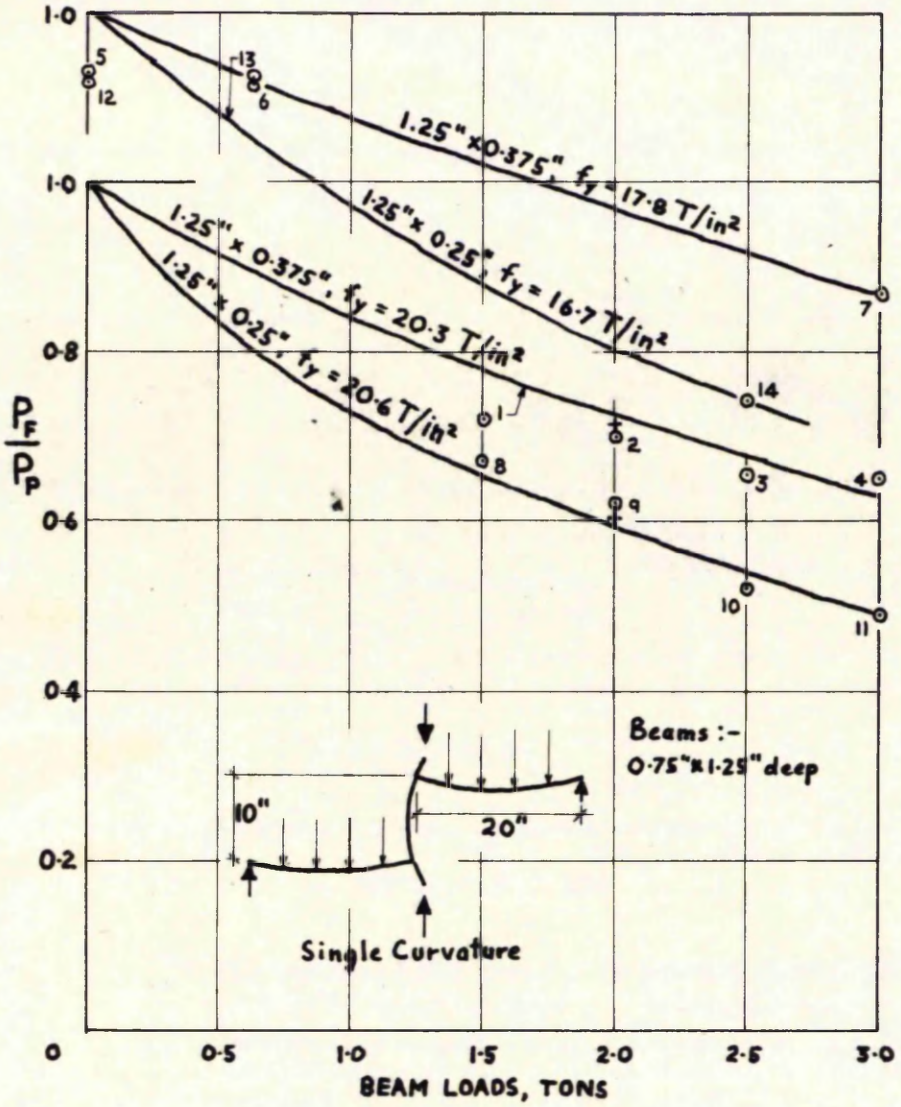

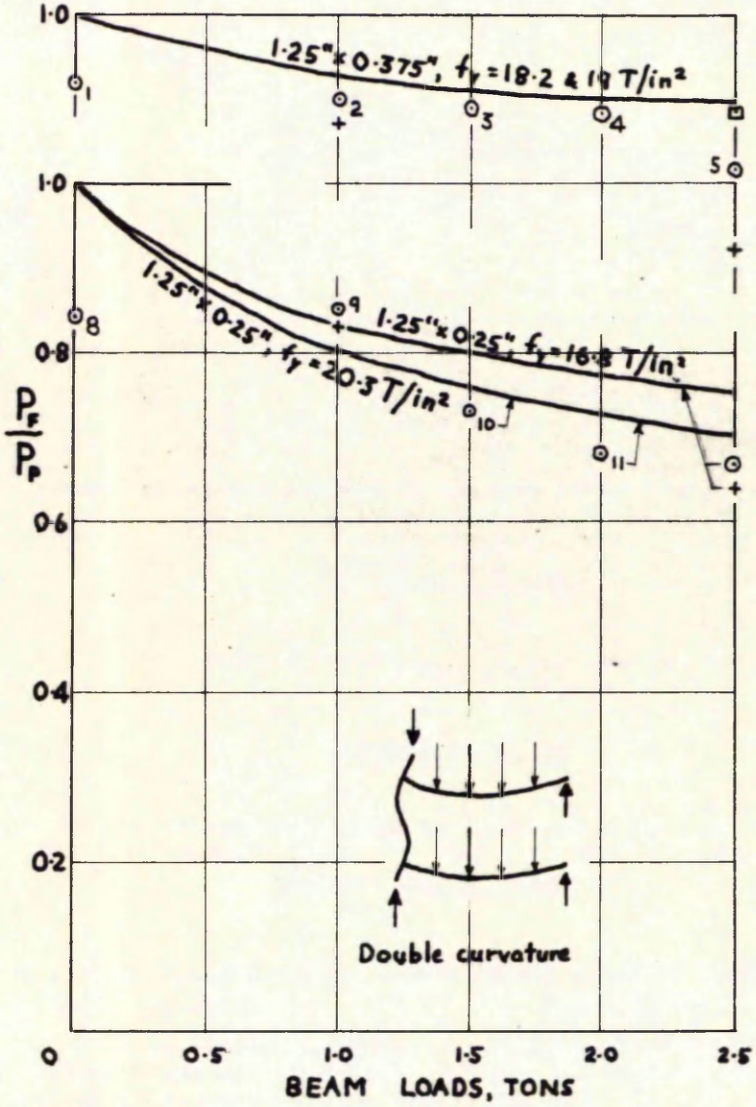

\ - Curves interpolated from results of author's analysis presented in Chapter 5, taking unloading into account.

⊙ - Denotes experimental result, the number beside it being taken from "The Steel Skeleton", Tables 13.1 and 13.2.

\+ Denotes calculated result from rigorous theory neglecting unloading taken from "The Steel Skeleton," Tables 13.1 and 13.2.

⊡ Denotes calculated result from rigorous theory considering unloading taken from "The Steel Skeleton", Table 13.2.

FIG. 3.9. TESTS ON RESTRAINED COLUMNS BY BAKER AND RODERICK

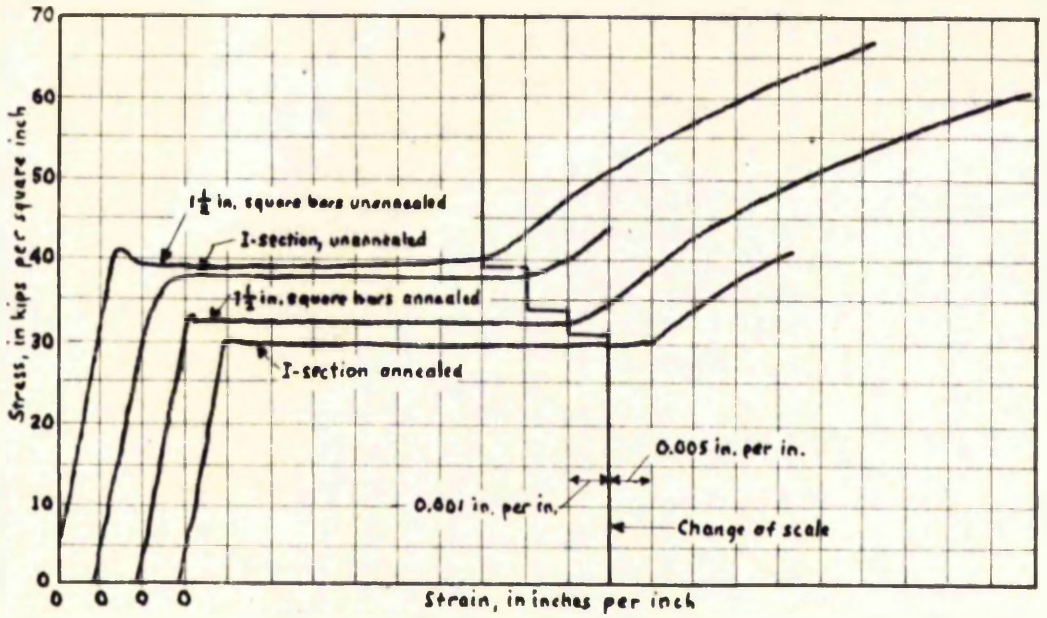

(a) Experimental curves

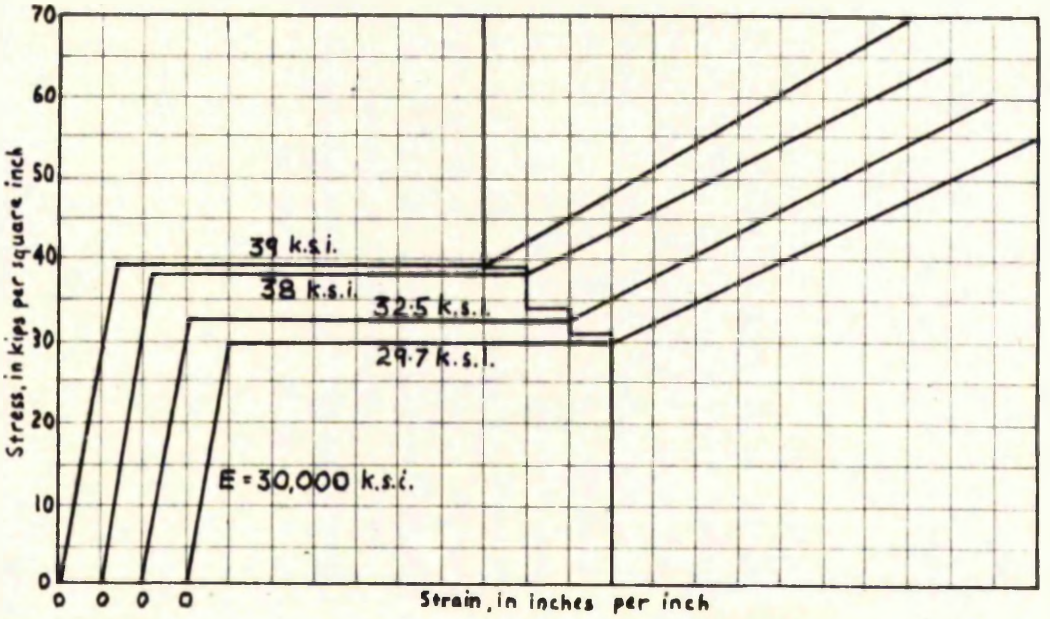

(b) Curves used in author's computer analysis of tests

FIG. 3.11 STRESS/STRAIN CURVES FOR COLUMNS TESTED BY BIJLAARD, FISHER AND WINTER.

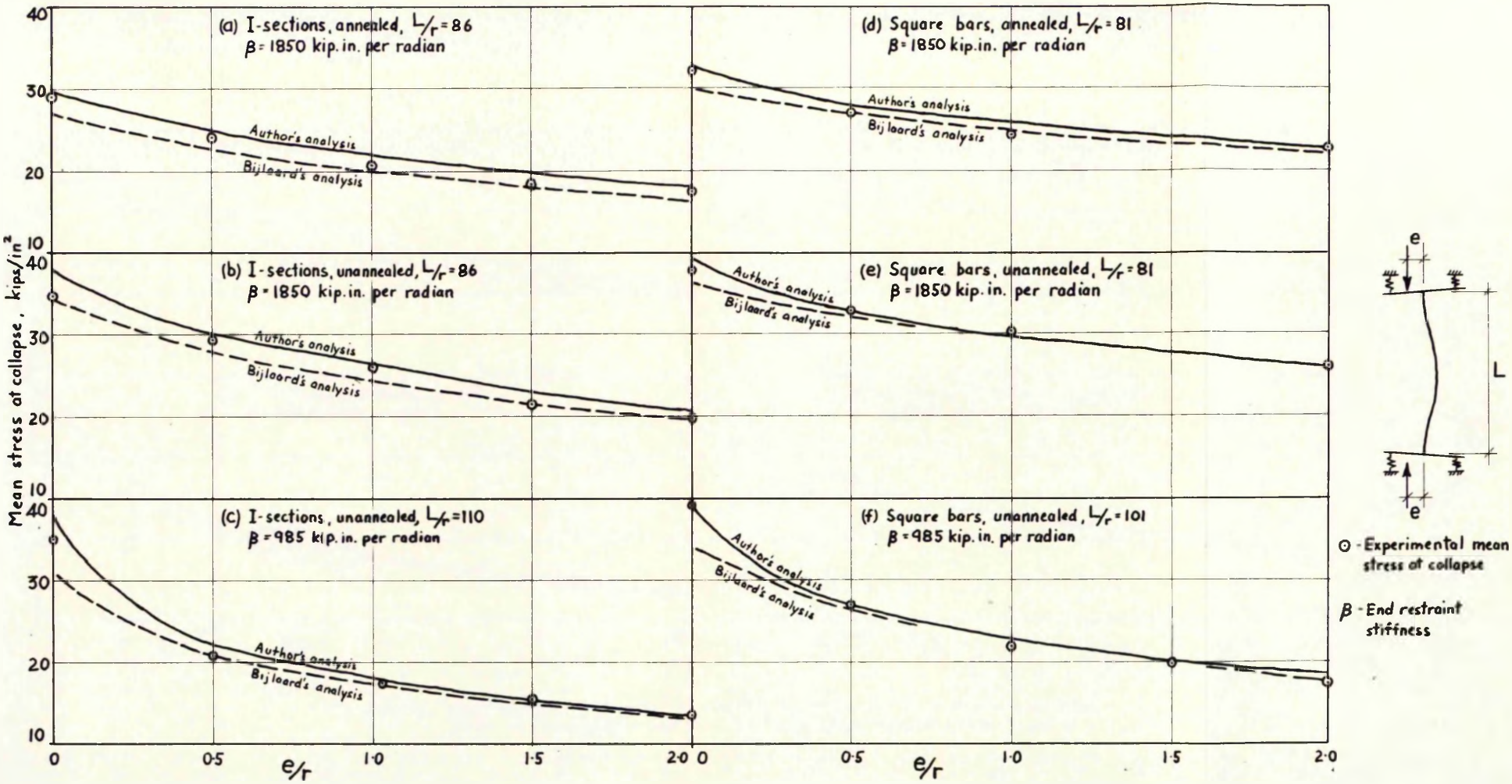

FIG. 3.11 COMPARISON BETWEEN THEORETICAL AND EXPERIMENTAL COLLAPSE LOADS FOR COLUMNS TESTED BY BIJLAARD, FISHER, AND WINTER

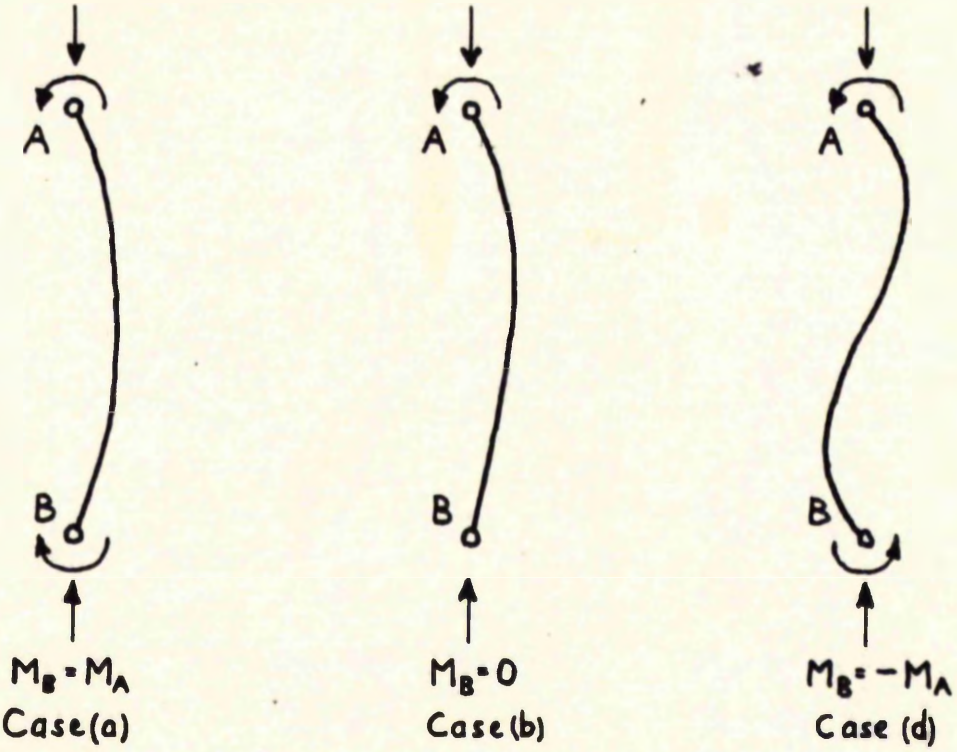

FIG. 4.1. LOADING CONDITIONS FOR PINNED TESTS.

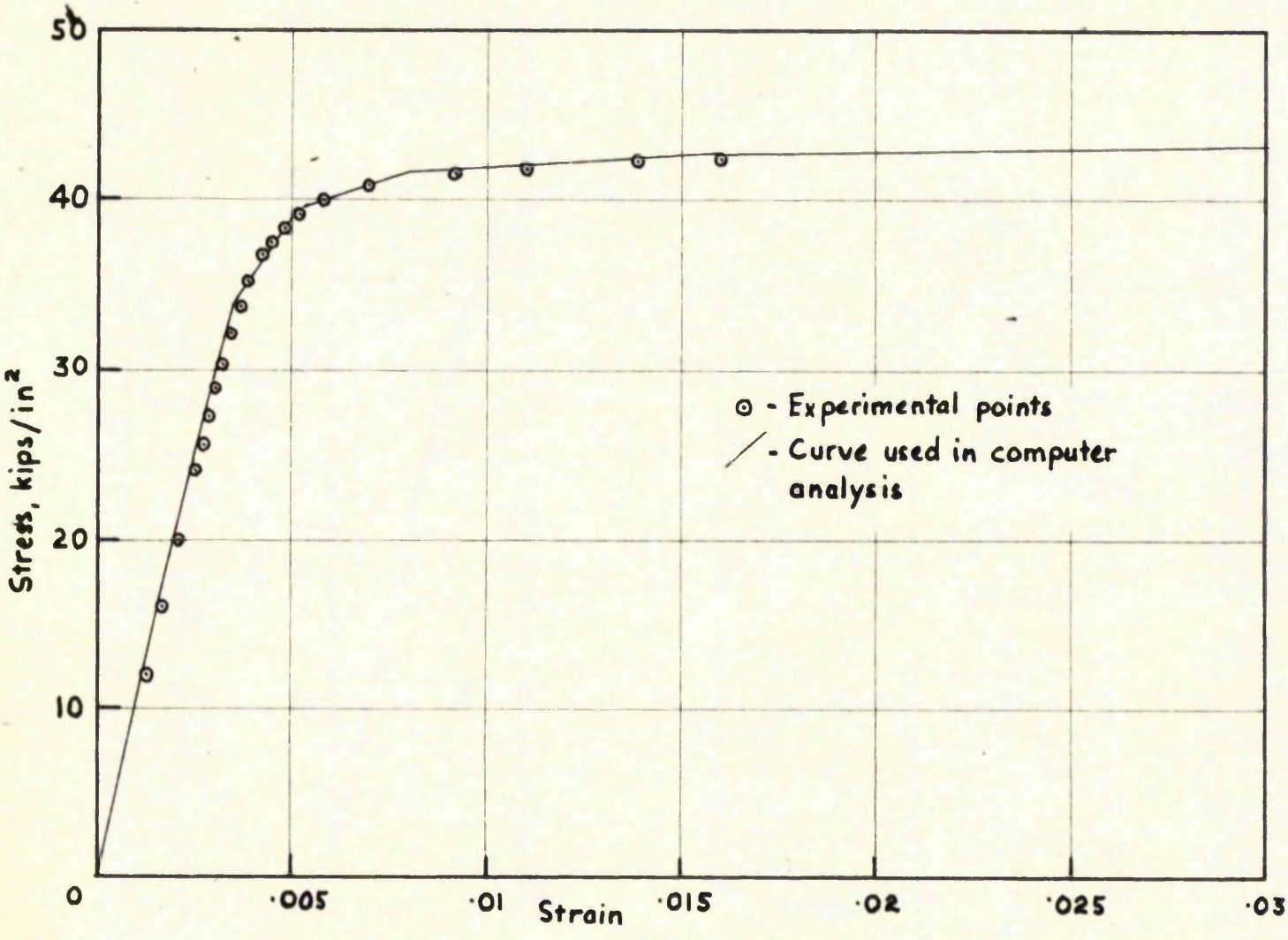

FIG. 4.3. STRESS-STRAIN CURVE FOR HE30WP ALUMINIUM ALLOY.

DRWG. No. WX. S.L.D.O.

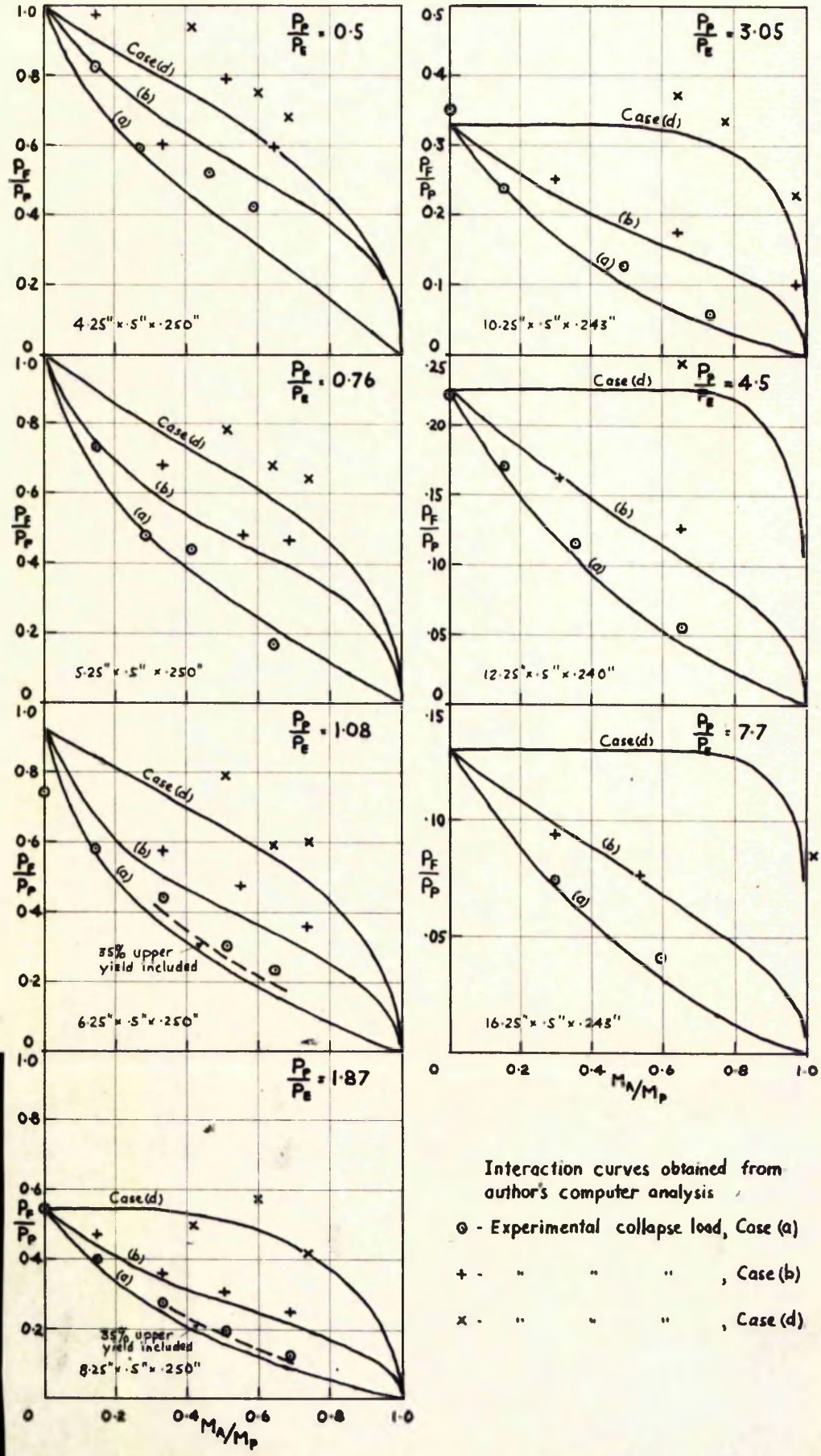

Interaction curves obtained from author's computer analysis

⊙ - Experimental collapse load, Case (a)

\+ - " " " , Case (b)

× - " " " , Case (d)

FIG. 42. COLLAPSE LOADS OF PINNED STEEL COLUMNS

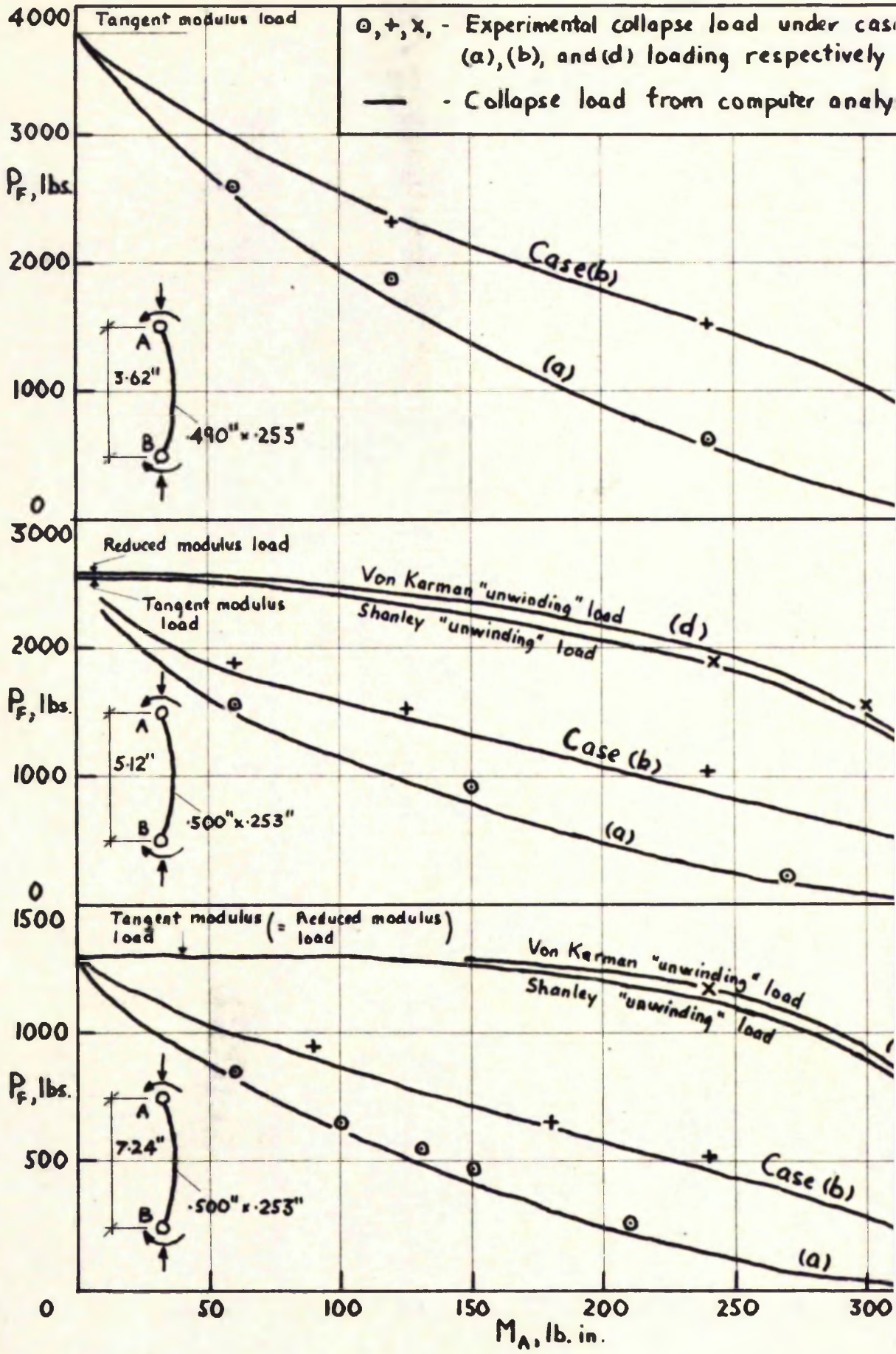

FIG 4.4. COLLAPSE LOADS OF PINNED HE 30 WP ALUMINIUM ALLOY COLUMNS.

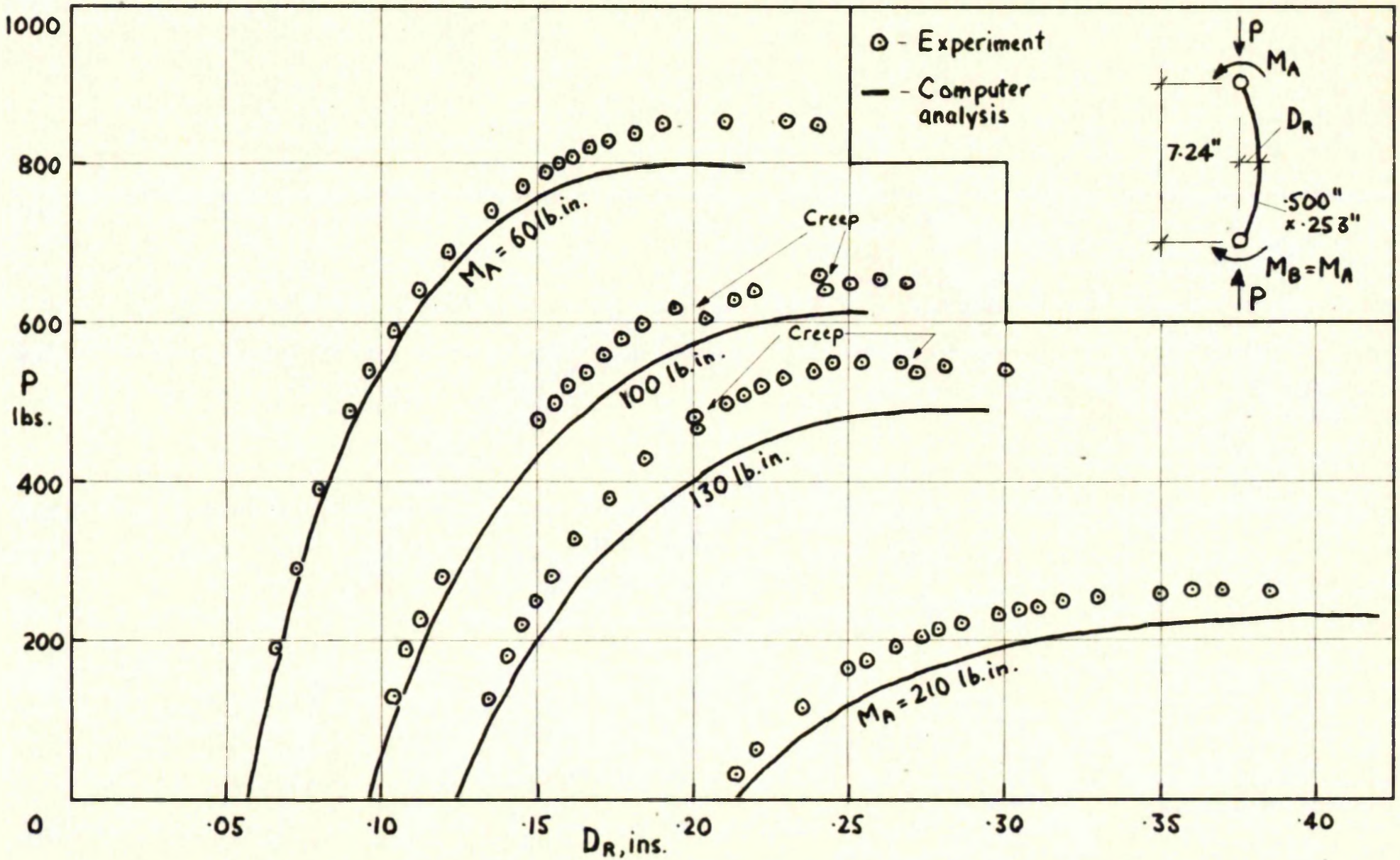
1000
800
600
400
200
0
P
lbs.
·05
·10
·15
·20
·25
·30
·35
·40
D_R, ins.
⊙ - Experiment
— - Computer analysis
P
M_A
D_R
7·24"
·500"
x·258"
$M_B = M_A$
P
M_A = 60 lb.in.
100 lb.in.
130 lb.in.
M_A = 210 lb.in.
Creep
Creep

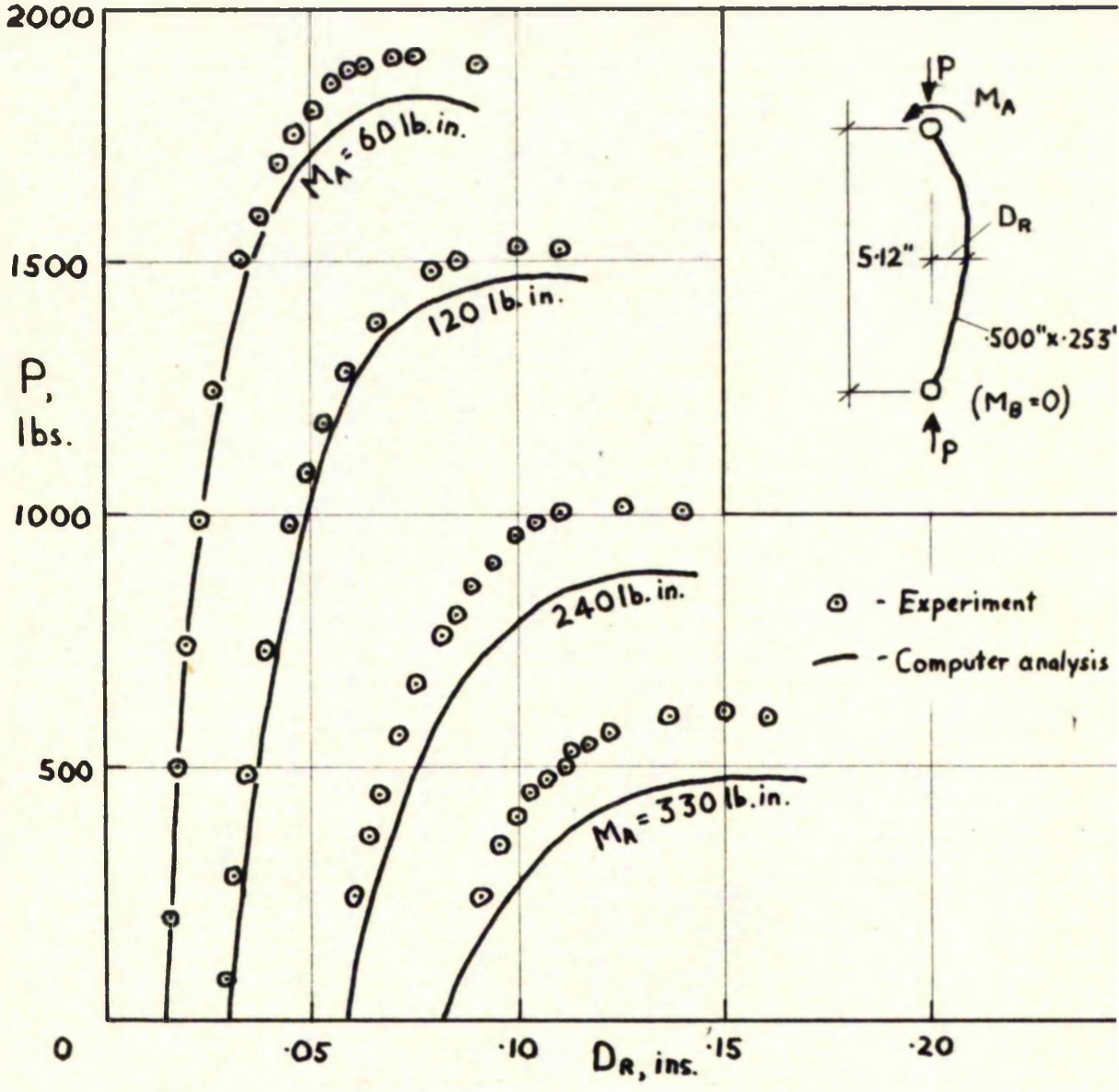

FIG. 4.6. LOAD-DEFLECTION CURVES FOR PINNED HE30WP ALLOY COLUMNS.

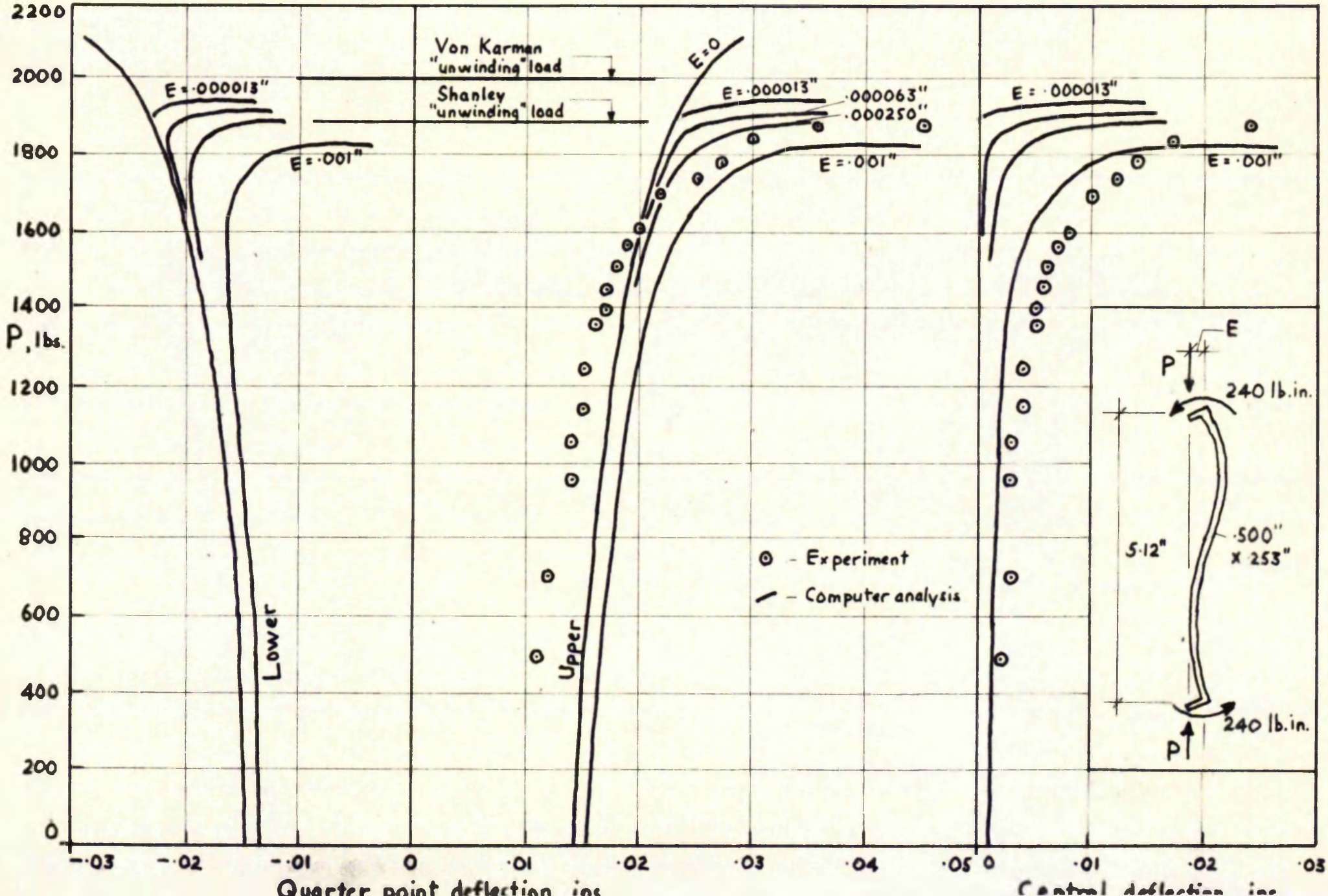
2200
2000
1800
1600
1400
1200
1000
800
600
400
200
0
P, lbs.
Von Karman "unwinding" load
Shanley "unwinding" load
E = ·000013"
E = ·001"
E = 0
E = ·000013"
·000063"
·000250"
E = ·001"
E = ·000013"
E = ·001"
Lower
Upper
⊙ - Experiment
— - Computer analysis
E
P
240 lb.in.
5·12"
·500" x ·253"
240 lb.in.
P
-·03
-·02
-·01
0
·01
·02
·03
·04
·05
Quarter point deflection, ins.
Central deflection, ins.

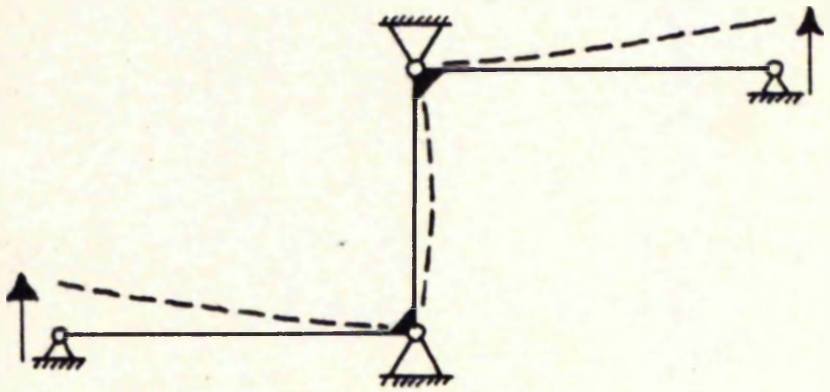

Case (a)

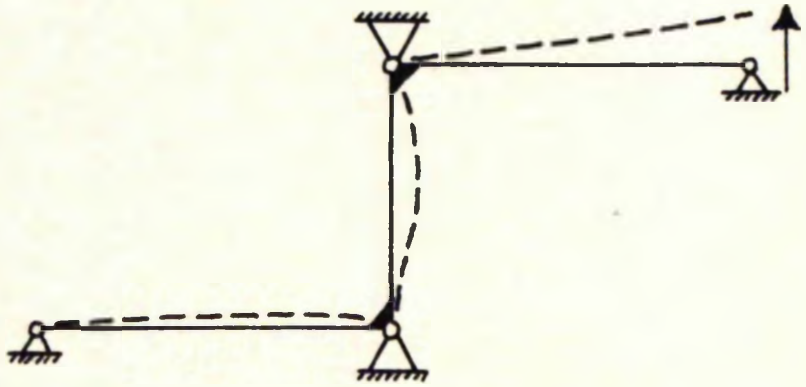

Case (b)

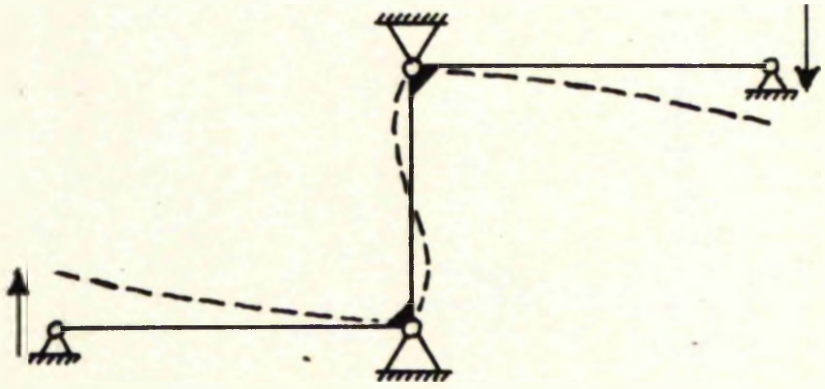

Case (d)

FIG. 4.8. APPLICATION OF MOMENT LOADING FOR TESTS ON RESTRAINED COLUMNS

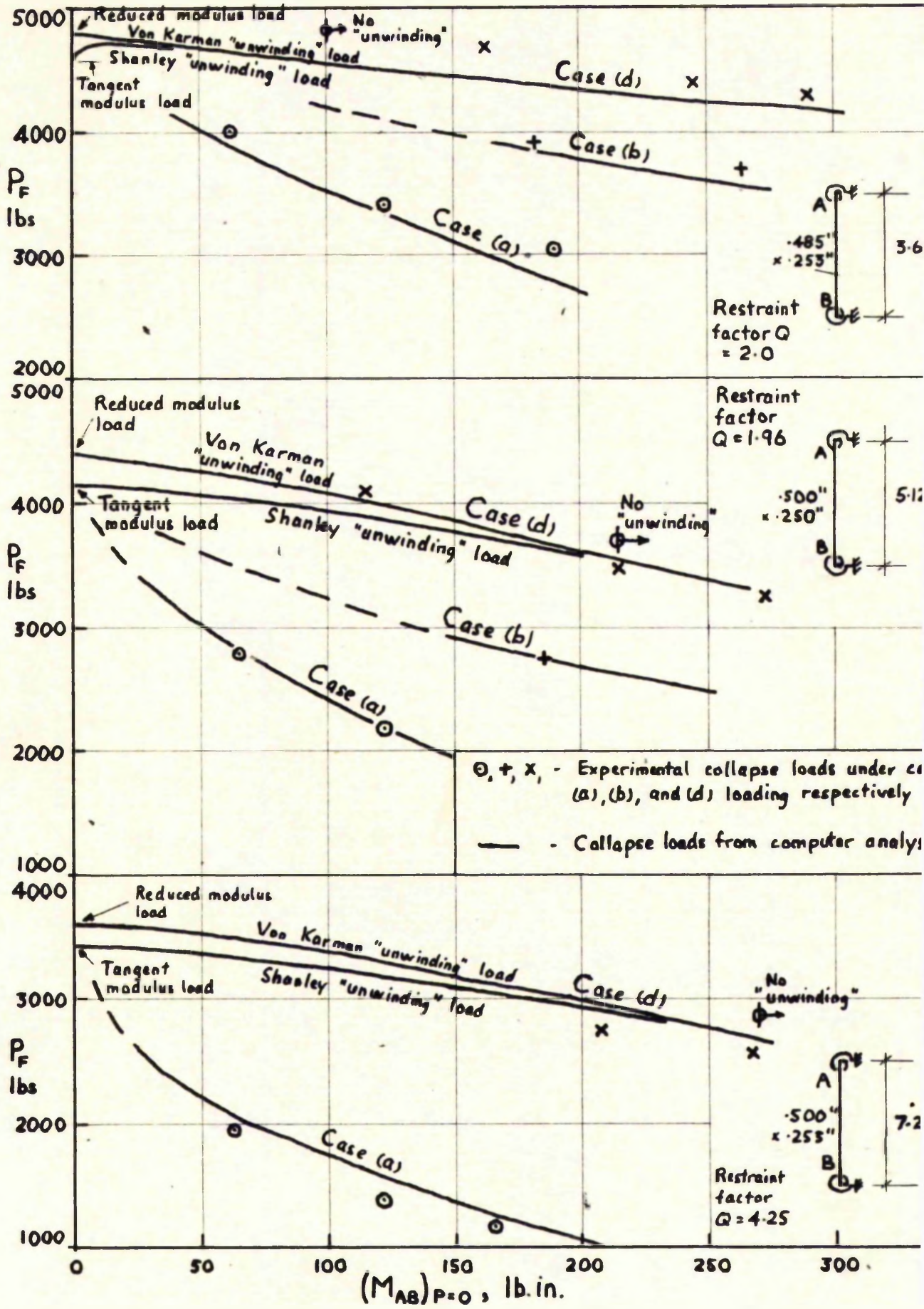

FIG. 4.9. COLLAPSE LOADS OF RESTRAINED HEDGOW ALUMINIUM ALLOY COLUMNS.

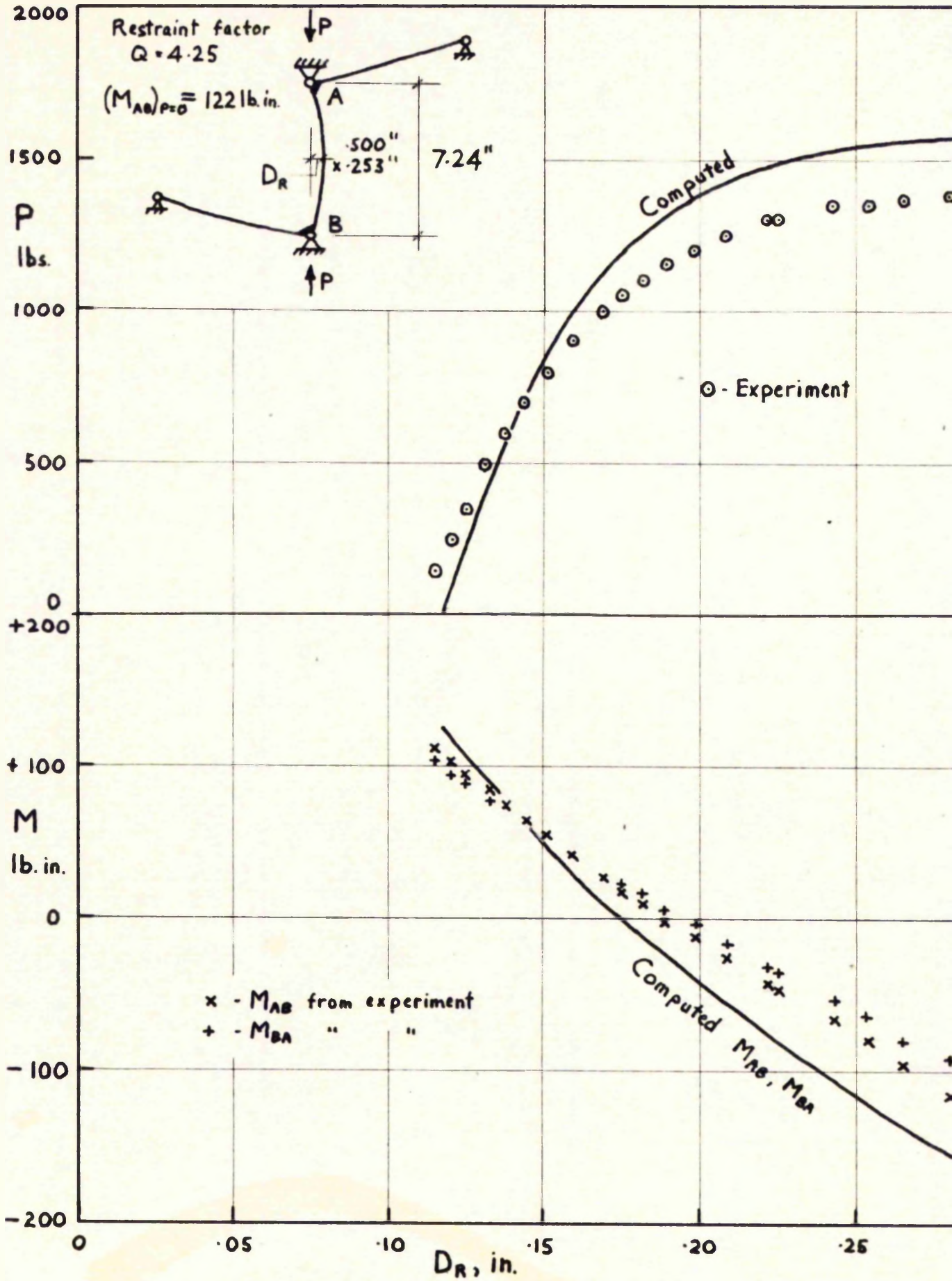

FIG. 4.10. TYPICAL TEST OF RESTRAINED HEDONIA ALUMINIUM ALLOY COLUMN UNDER CASE (A) LOADING.

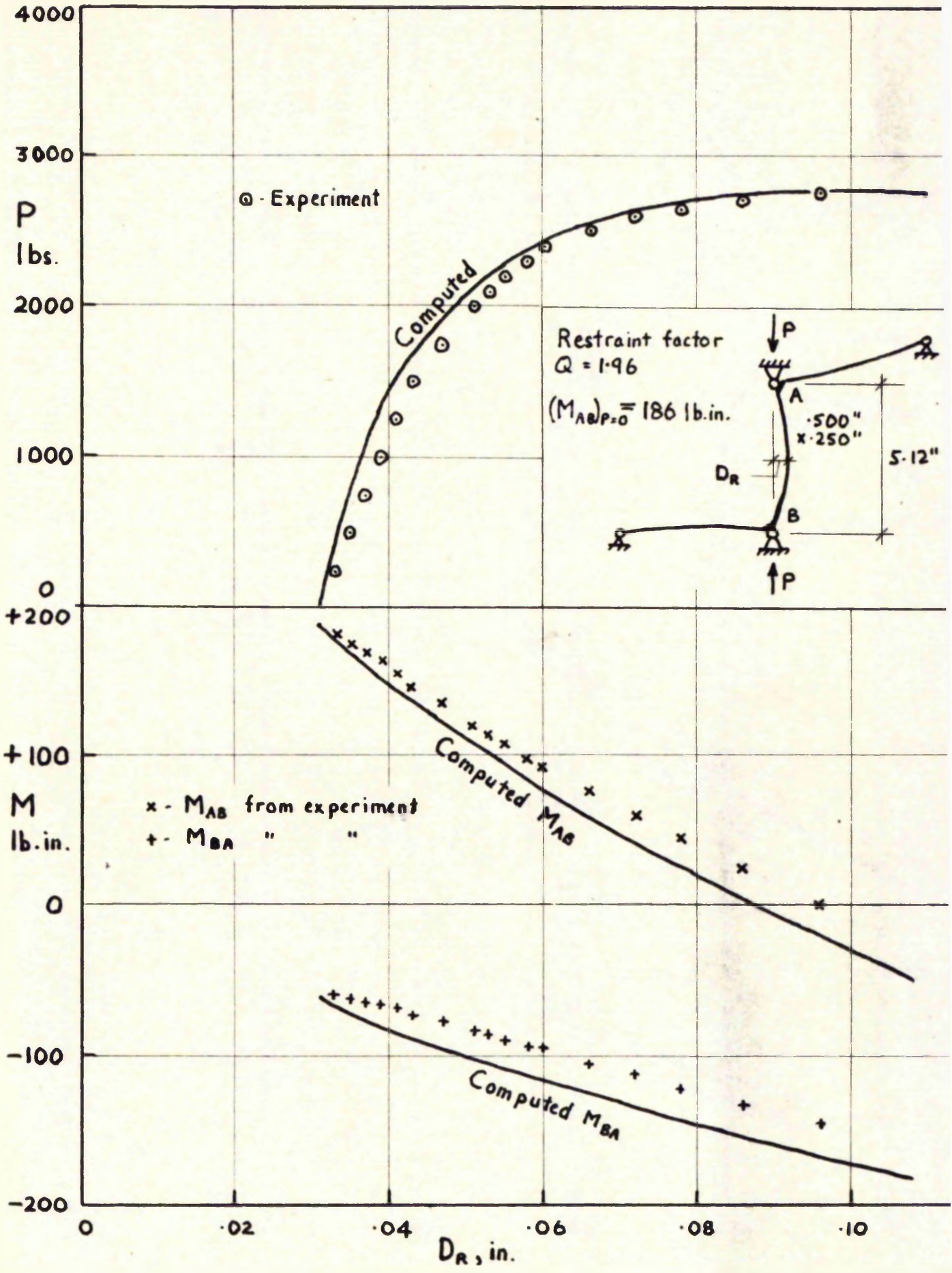

FIG. 4.11. TYPICAL TEST OF RESTRAINED MESOMP ALUMIN ALLOY COLUMN UNDER CASE (B) LOADING.

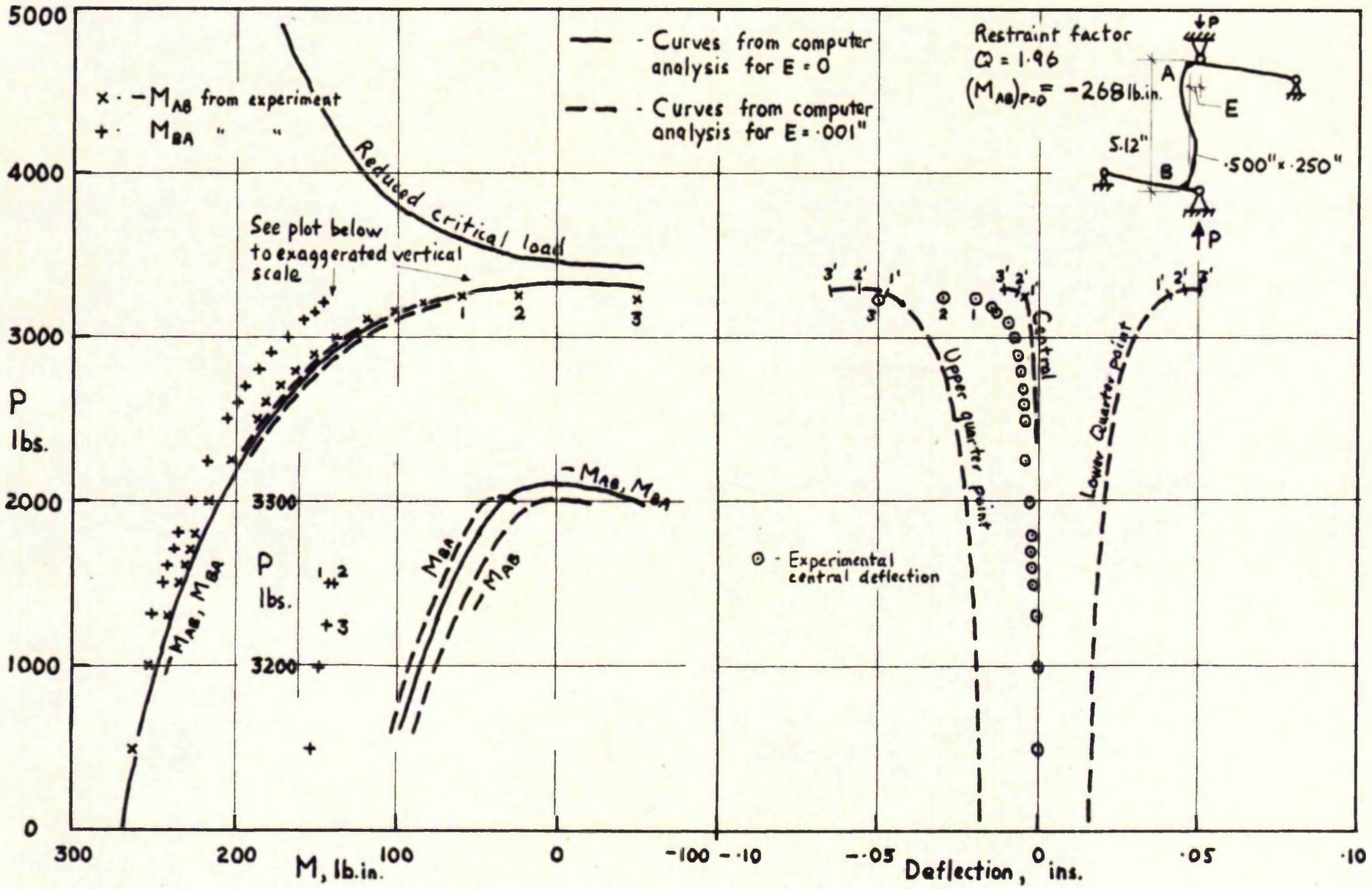

FIG. 4.12. TYPICAL TEST ON RESTRAINED RESOLVE ALUMINIUM

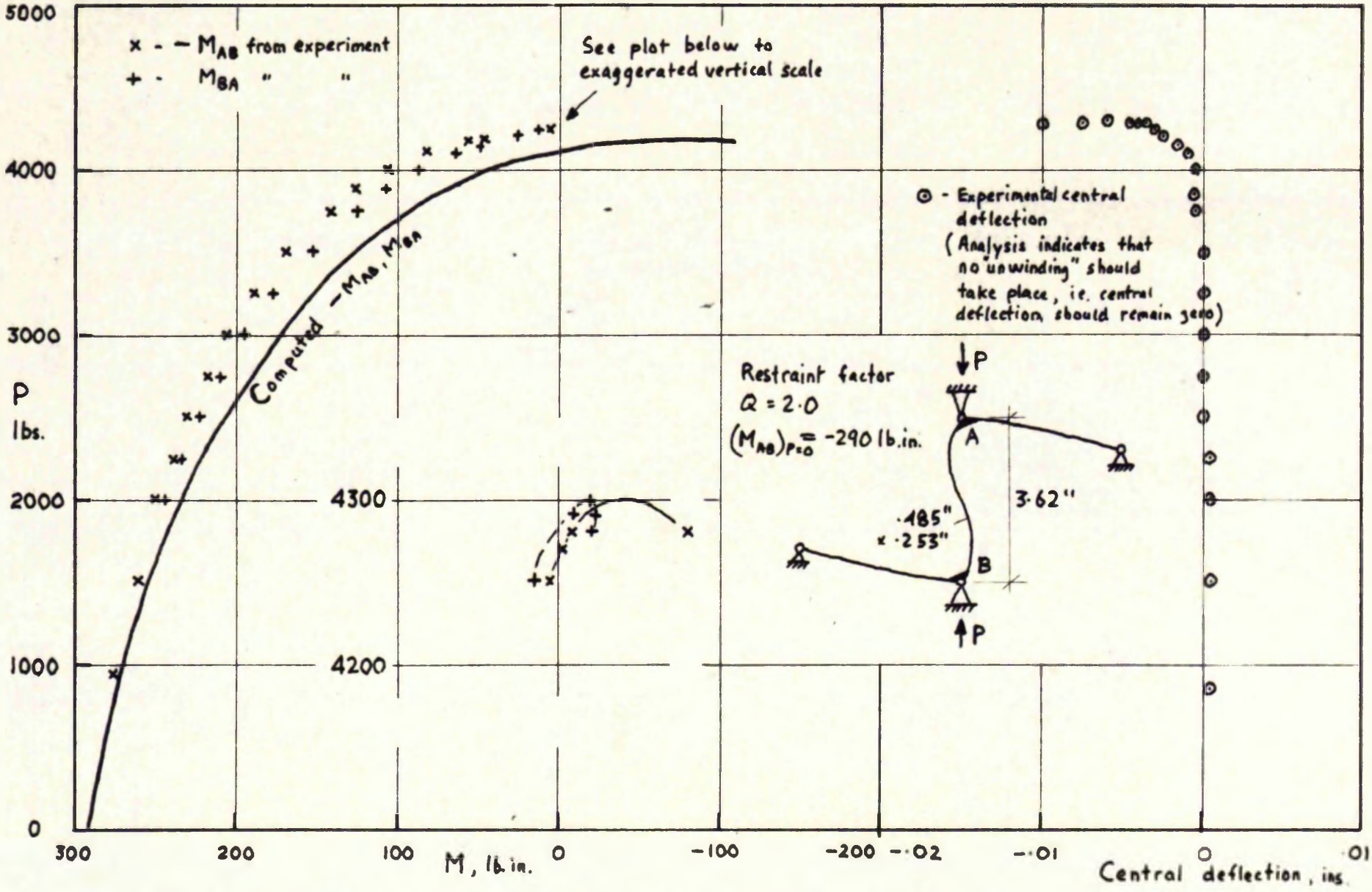

FIG. 4-13. TYPICAL TEST OF RESTRAINED HEDGEHOP ALUMINIUM ALLOY

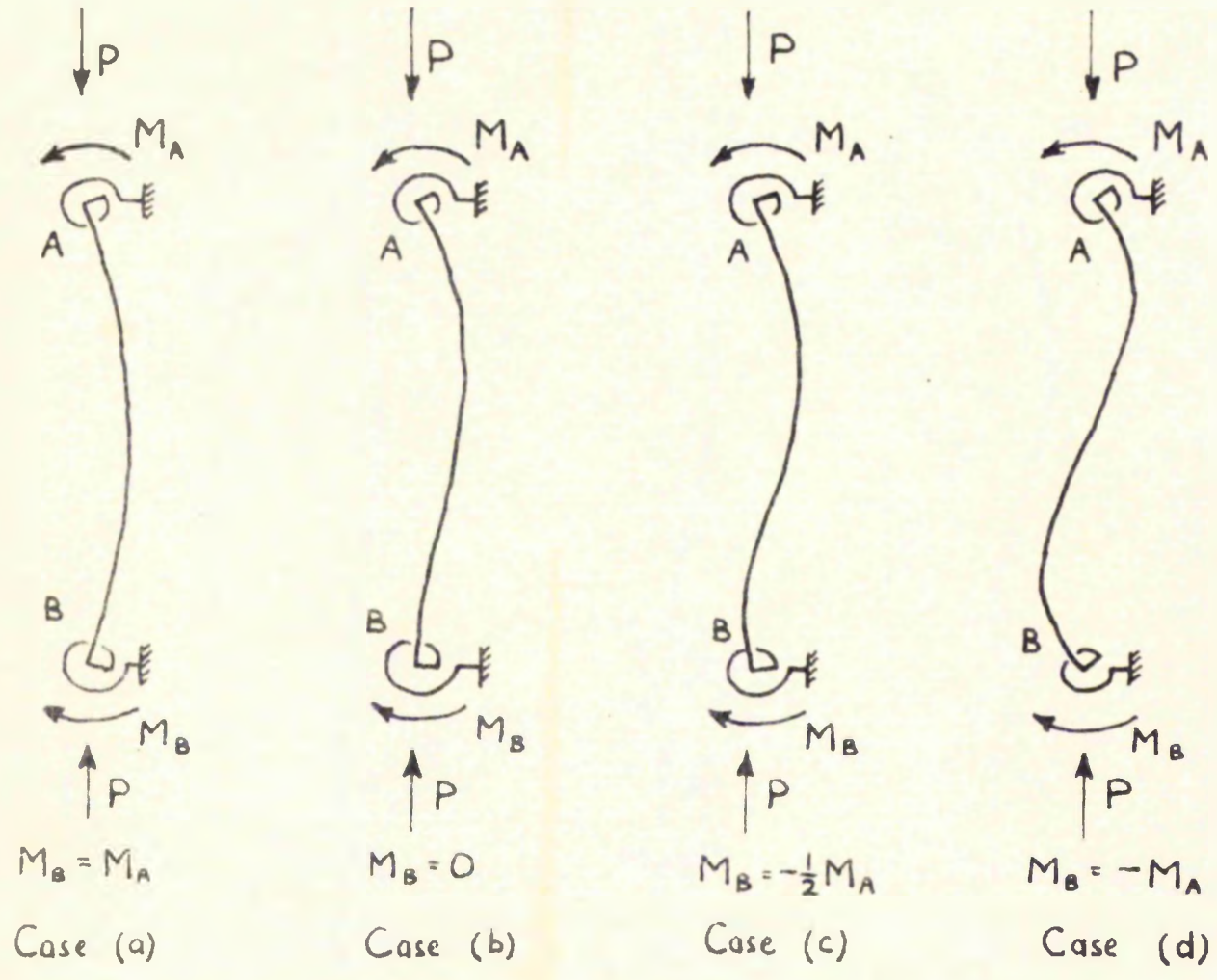

FIG. 5.1 MOMENT LOADING CONDITIONS CONSIDERED IN ANALYSIS OF IDEAL ELASTIC - PLASTIC COLUMNS.

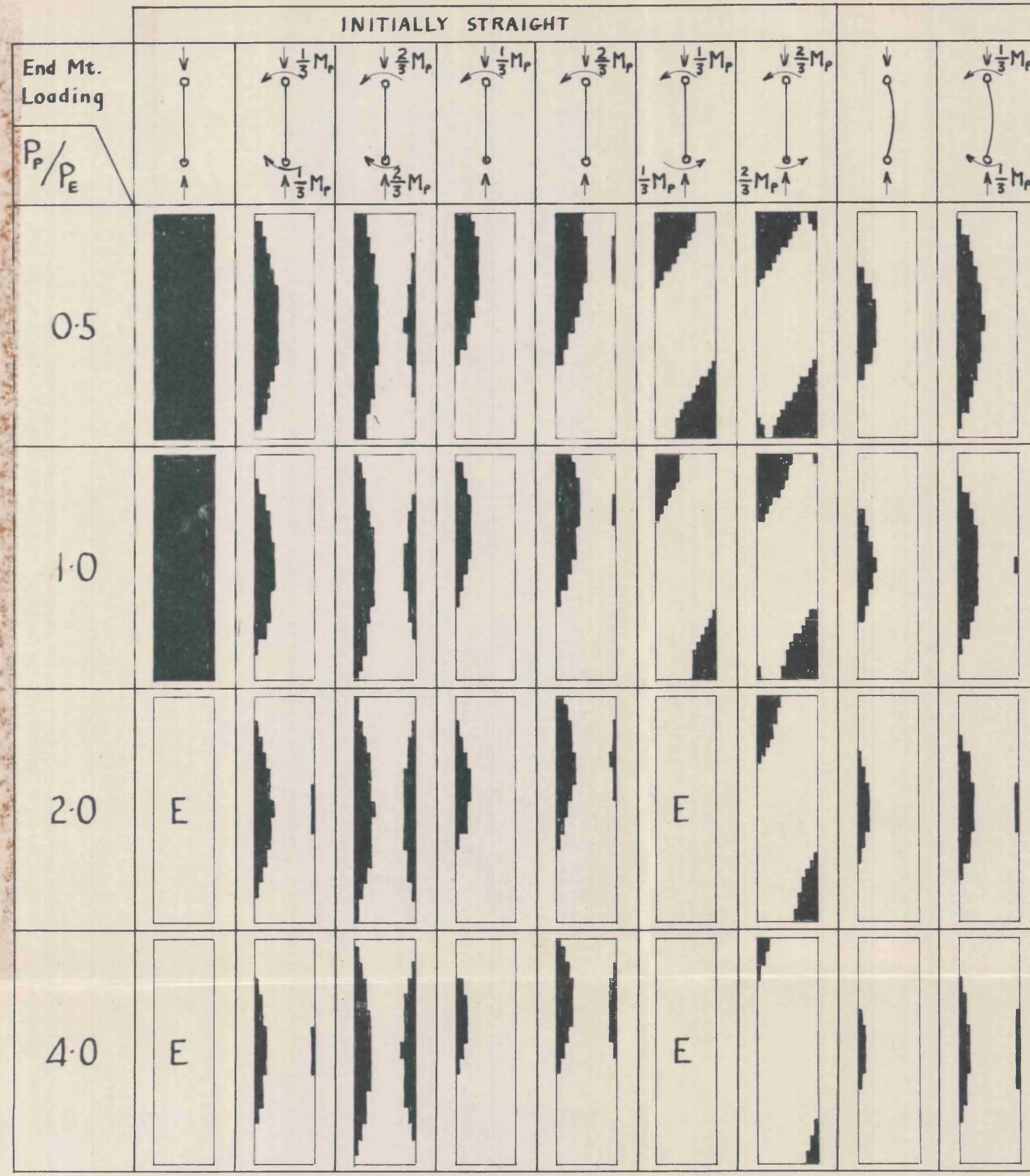

FIG. 12 PLASTIC ZONES IN BEAMS CARRYING AT COLLAPSE

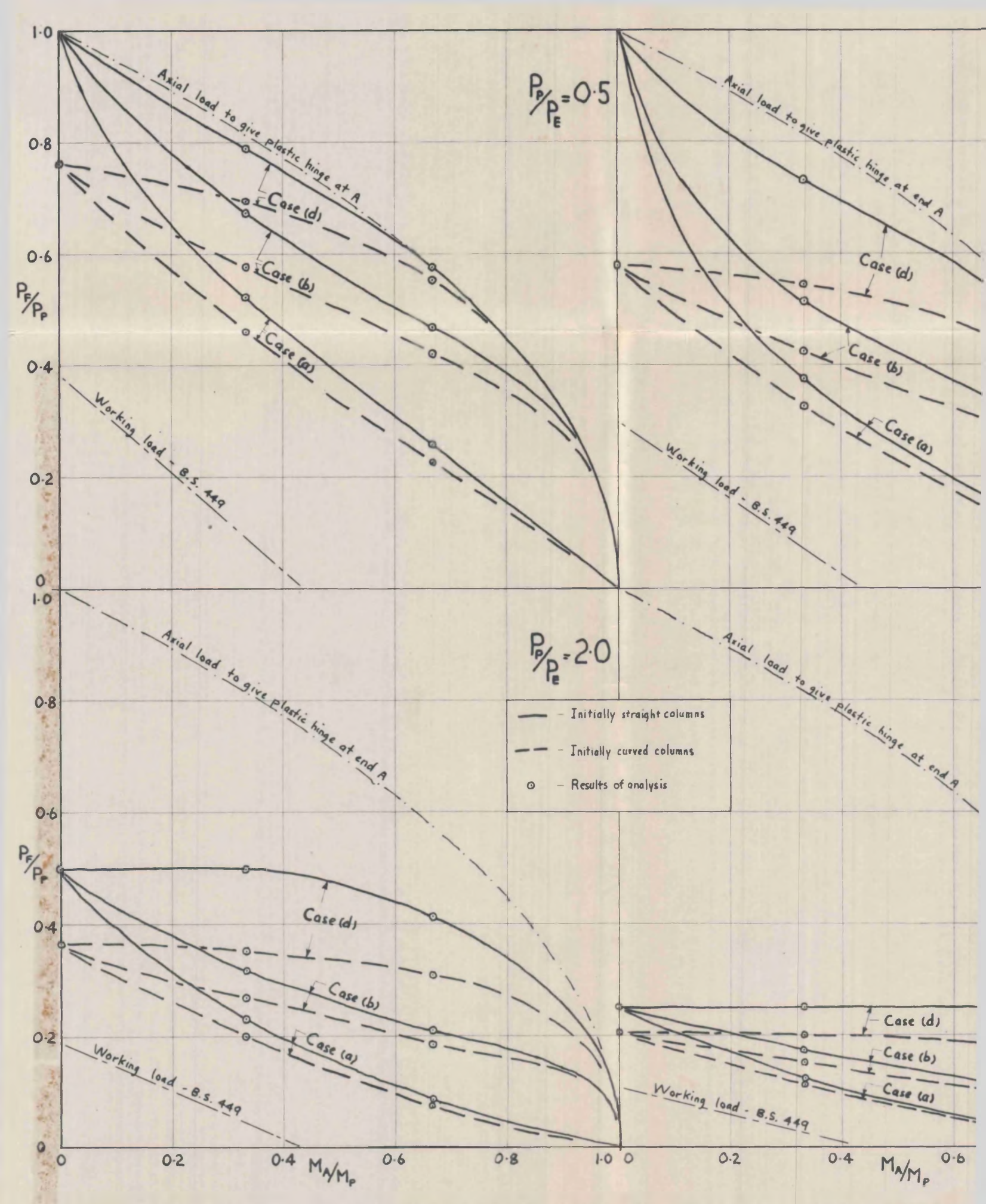

FIG. 5.2. ANALYTICAL COLUMN CURVES FOR PINNED COLUMNS OF IDEAL ELASTIC-PLASTIC MATERIAL

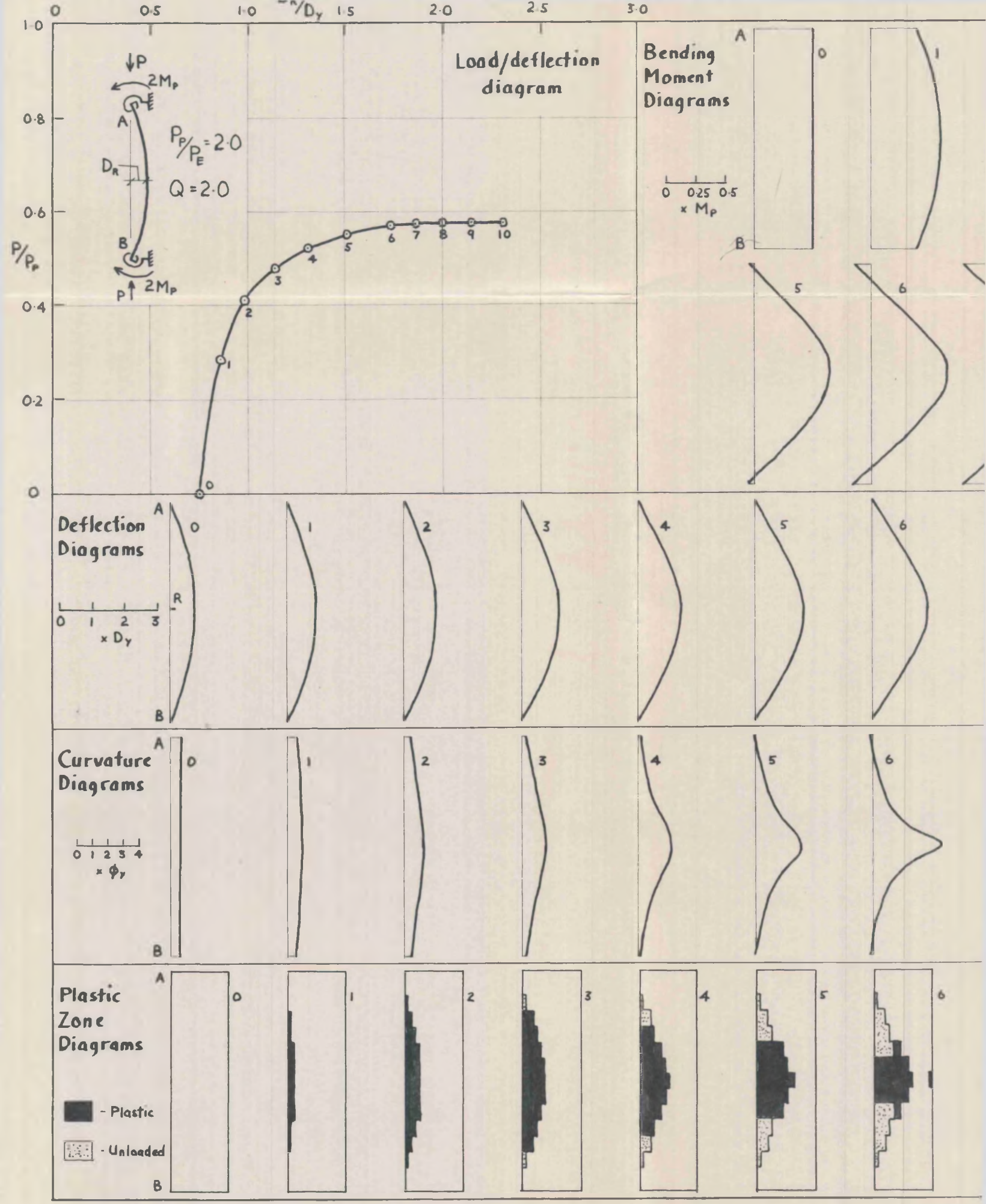

FIG. 5.4. BEHAVIOUR OF RESTRAINED COLUMN

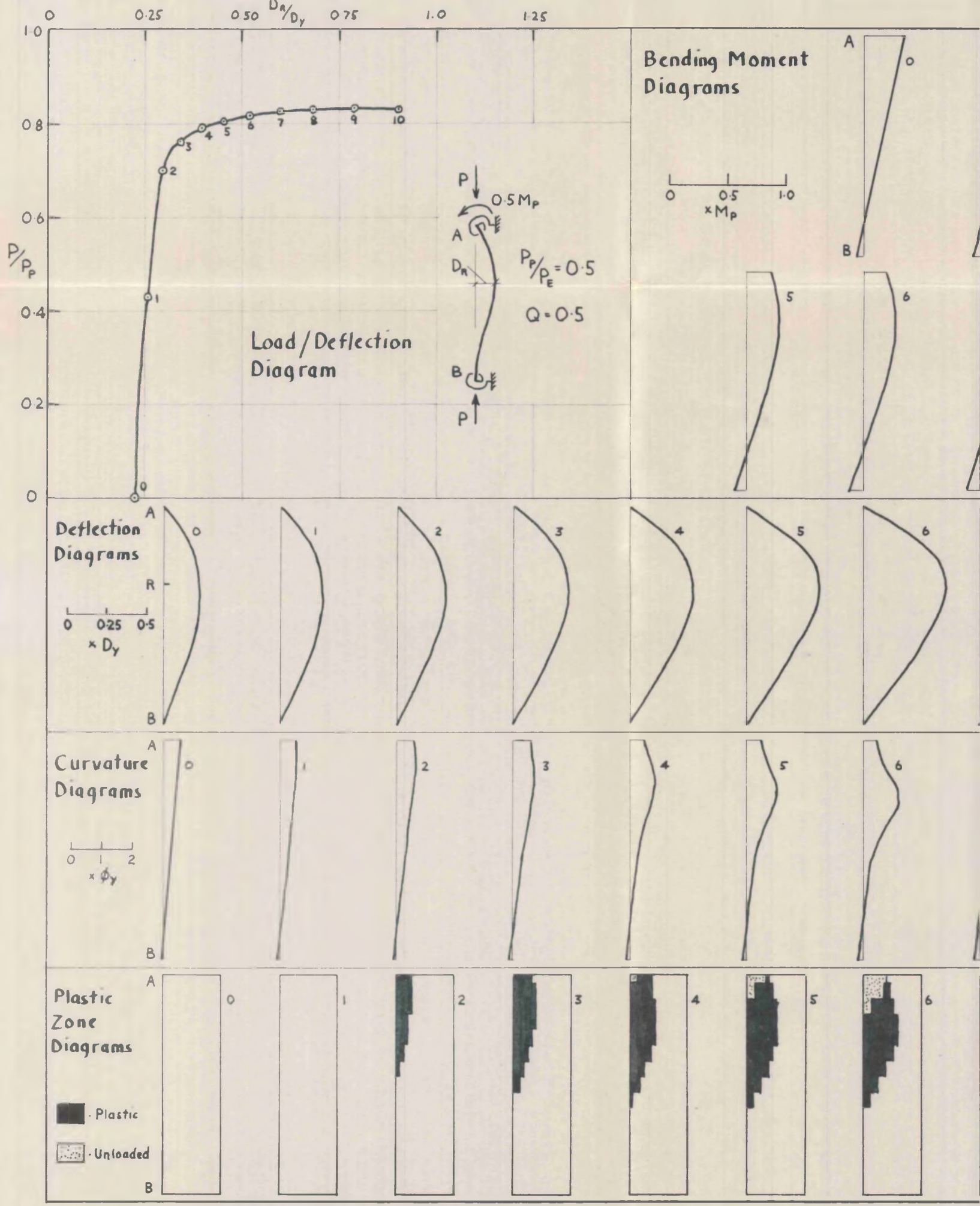

FIG 5.5. BEHAVIOUR OF RESTRAINED COLUMNS - TYPICAL CASE

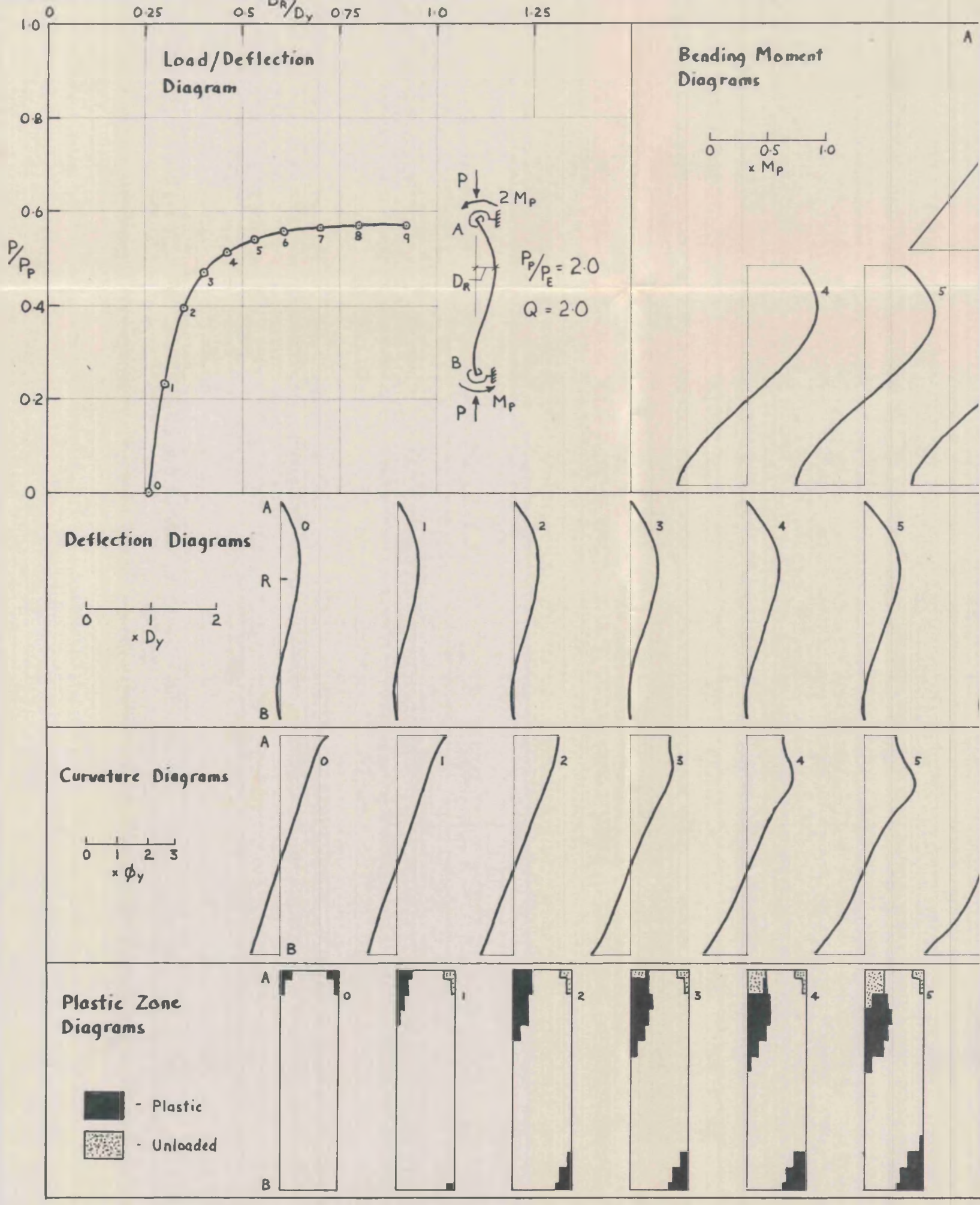

FIG. 7.6 BEHAVIOUR OF RESTRAINED COLUMNS - TYPICAL CASE OF LOADING.

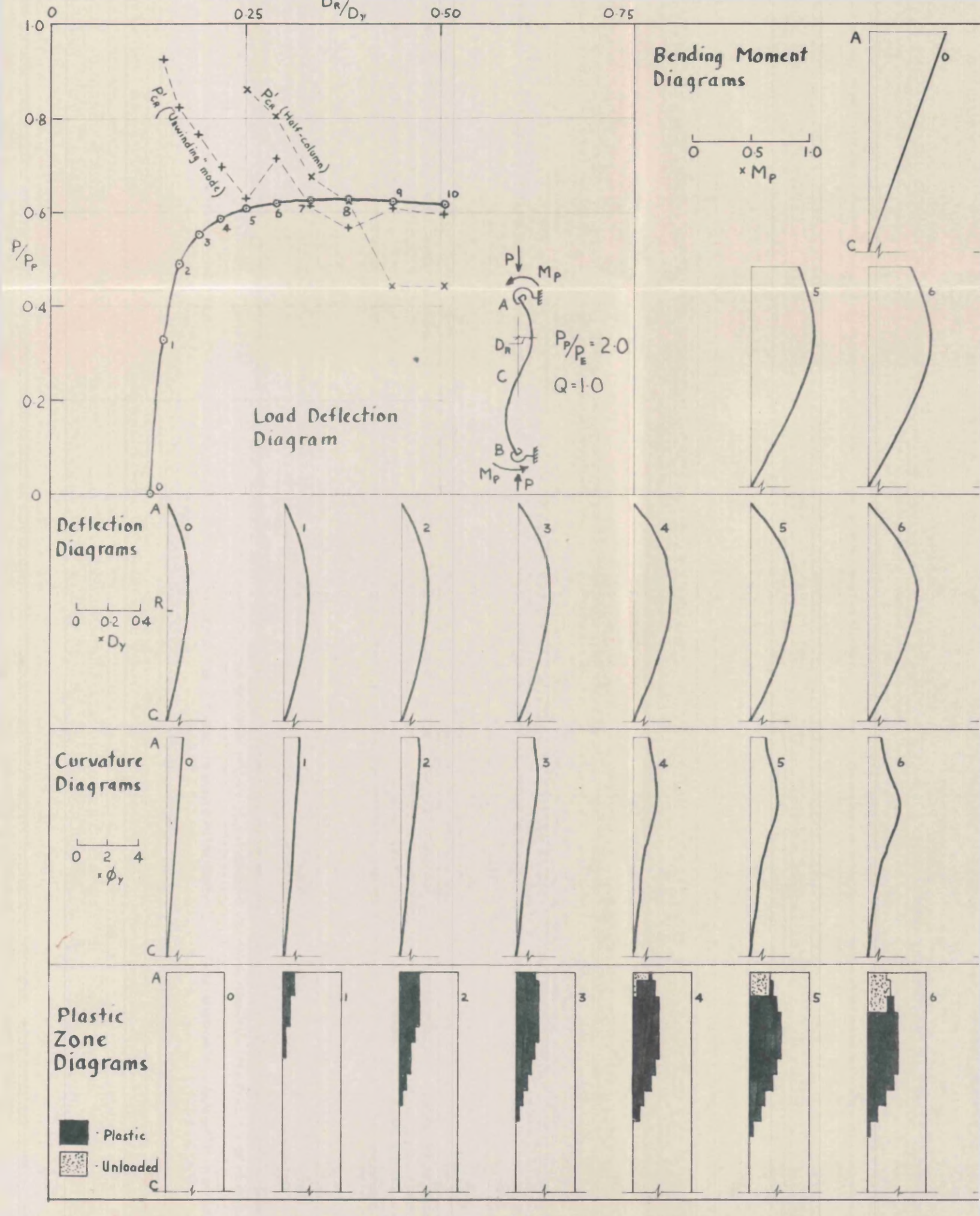

FIG 5.2 DETAILED

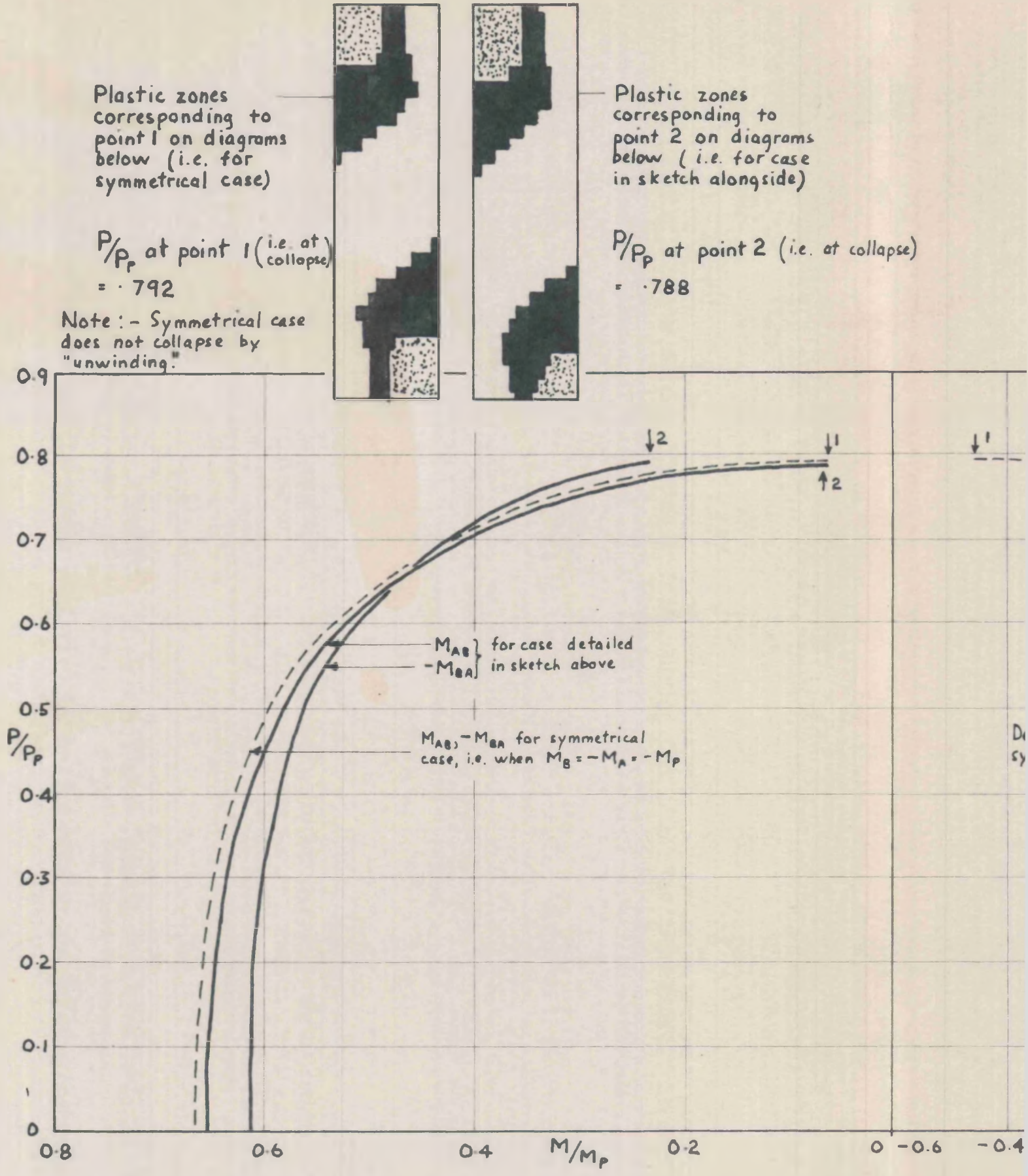

FIG. 5.8. - BEHAVIOUR OF PARTICULAR CASE WHERE

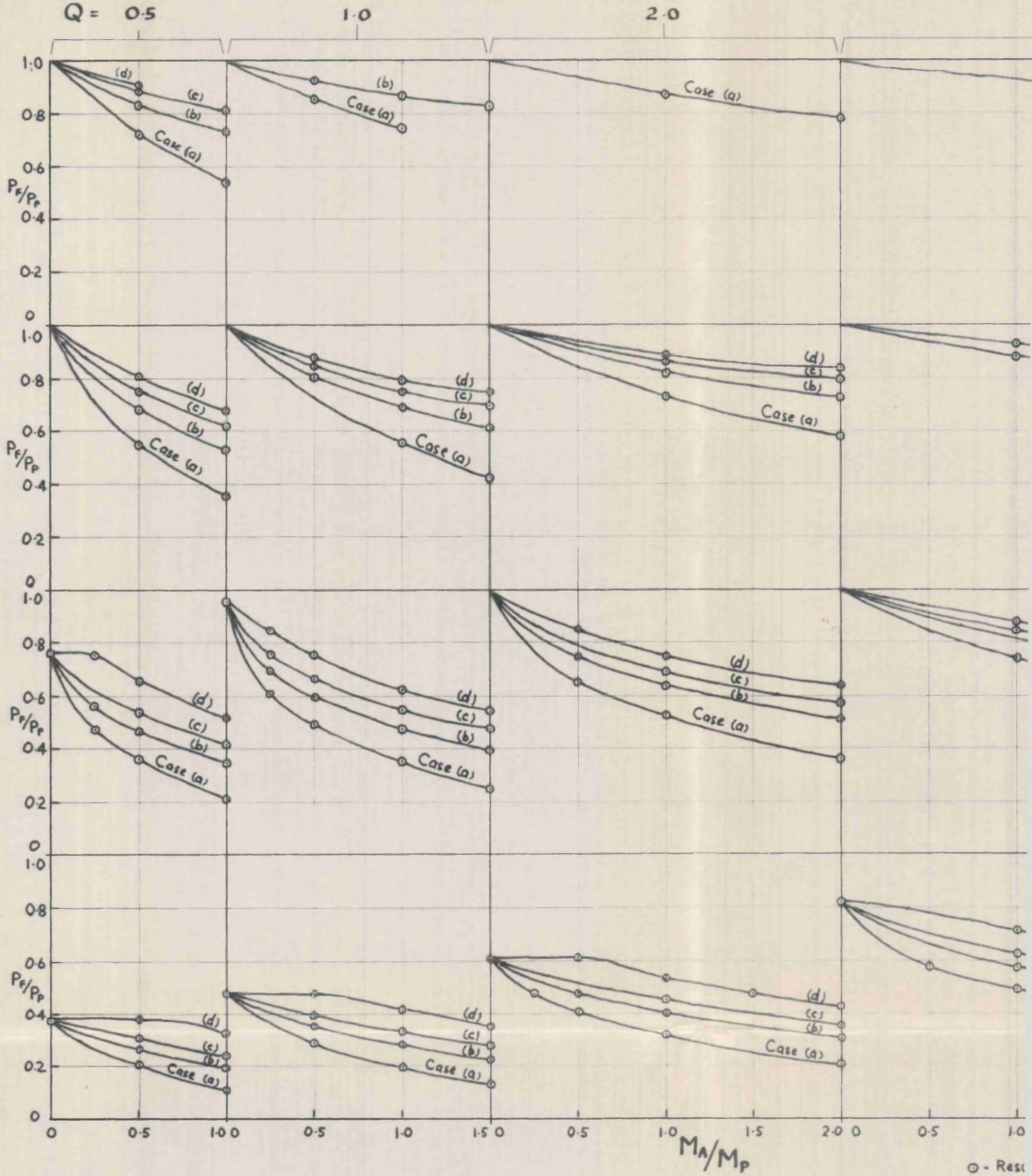

FIG 5.9. - COLLAPSE LOADS OF RESTRAINED COLUMNS OF IDEAL ELASTIC PLASTI

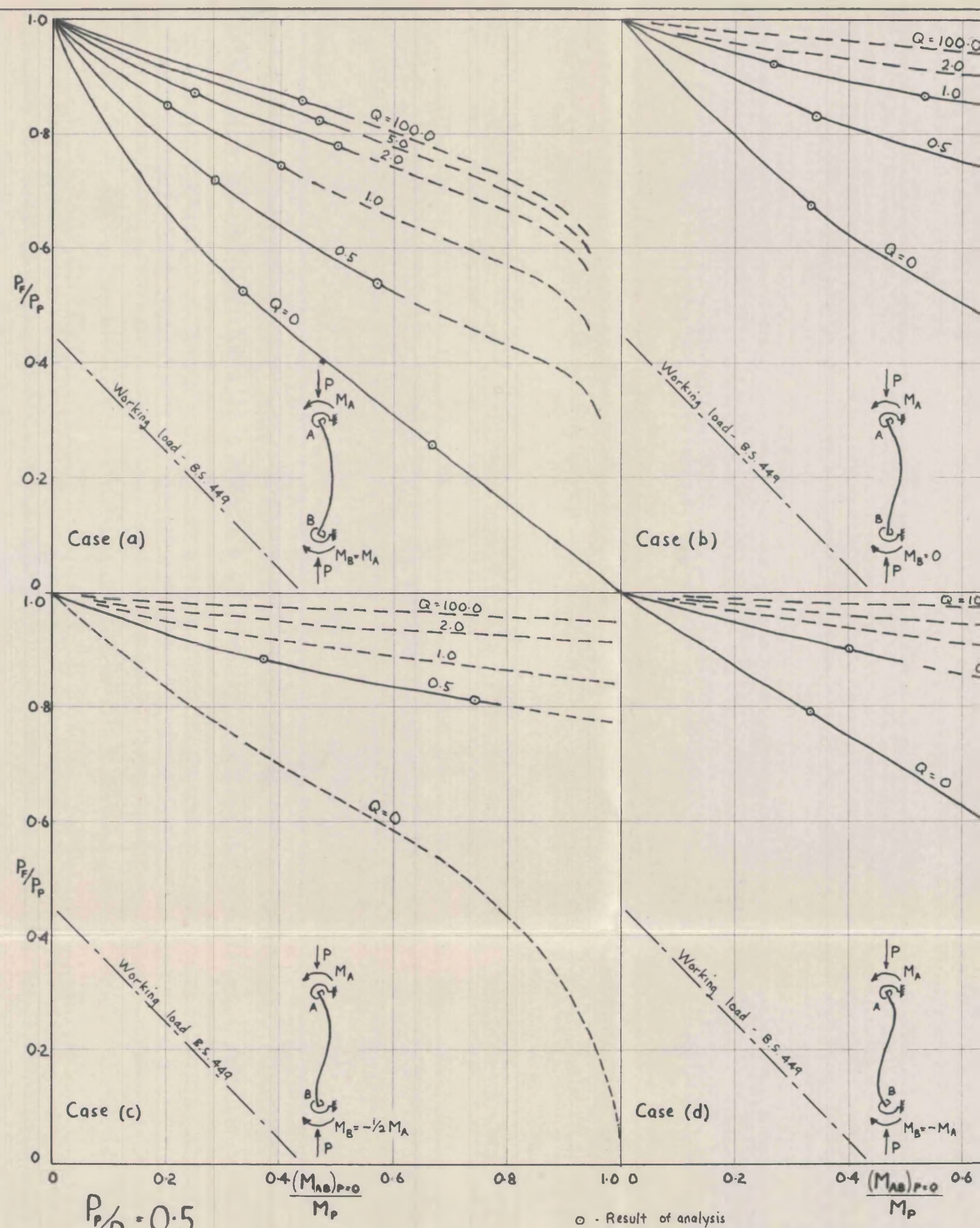

$P_p/P_E = 0.5$

o - Result of analysis

— — — - Curve obtained by extrapolation or interpolation

FIG. 5(b). COLLAPSE LOADS OF RESTRAINED COLUMNS OF IDEAL ELASTIC-PLASTIC MATER

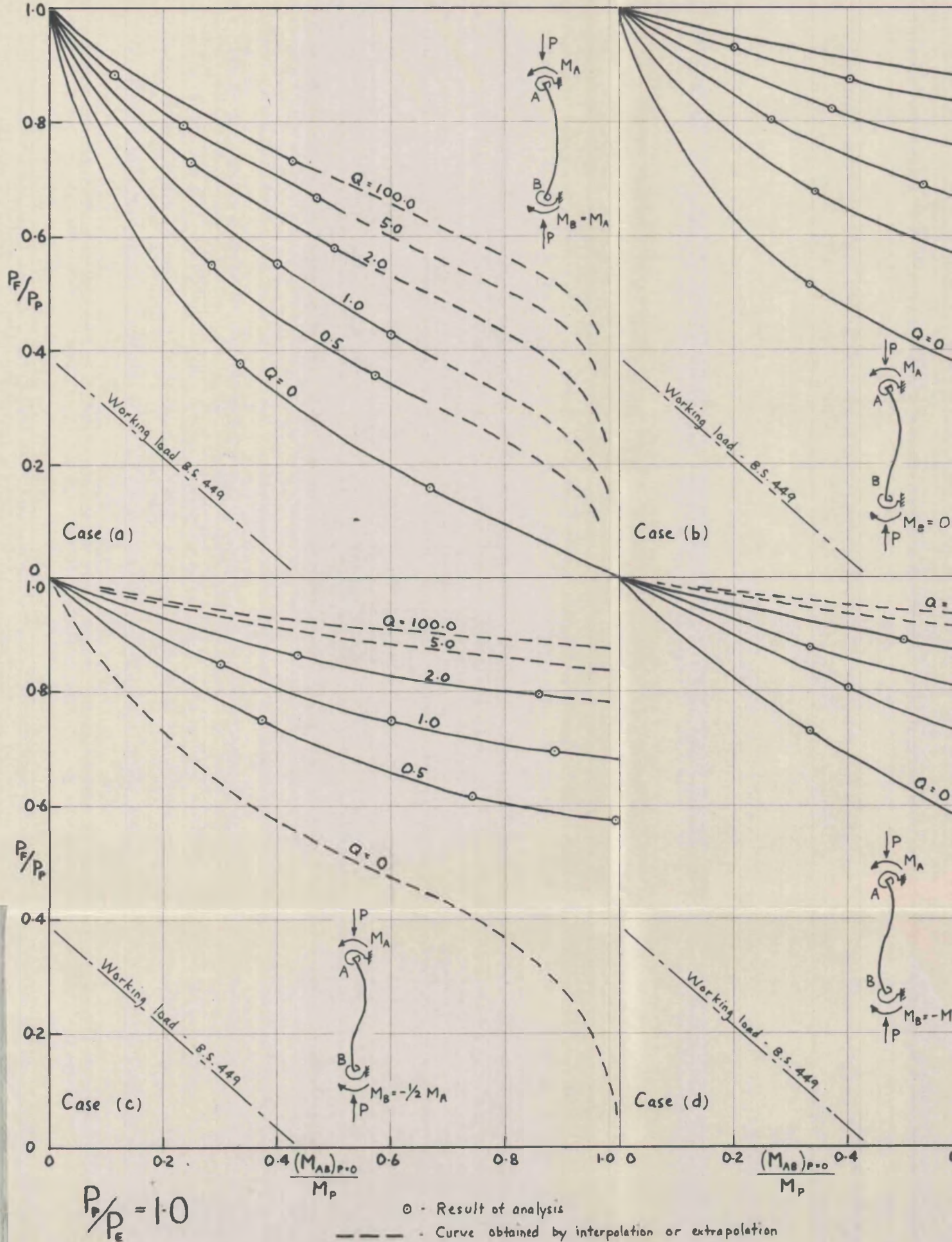

FIG. 5.11. COLLAPSE LOADS OF RESTRAINED COLUMNS OF IDEAL ELASTIC-PLASTIC MA

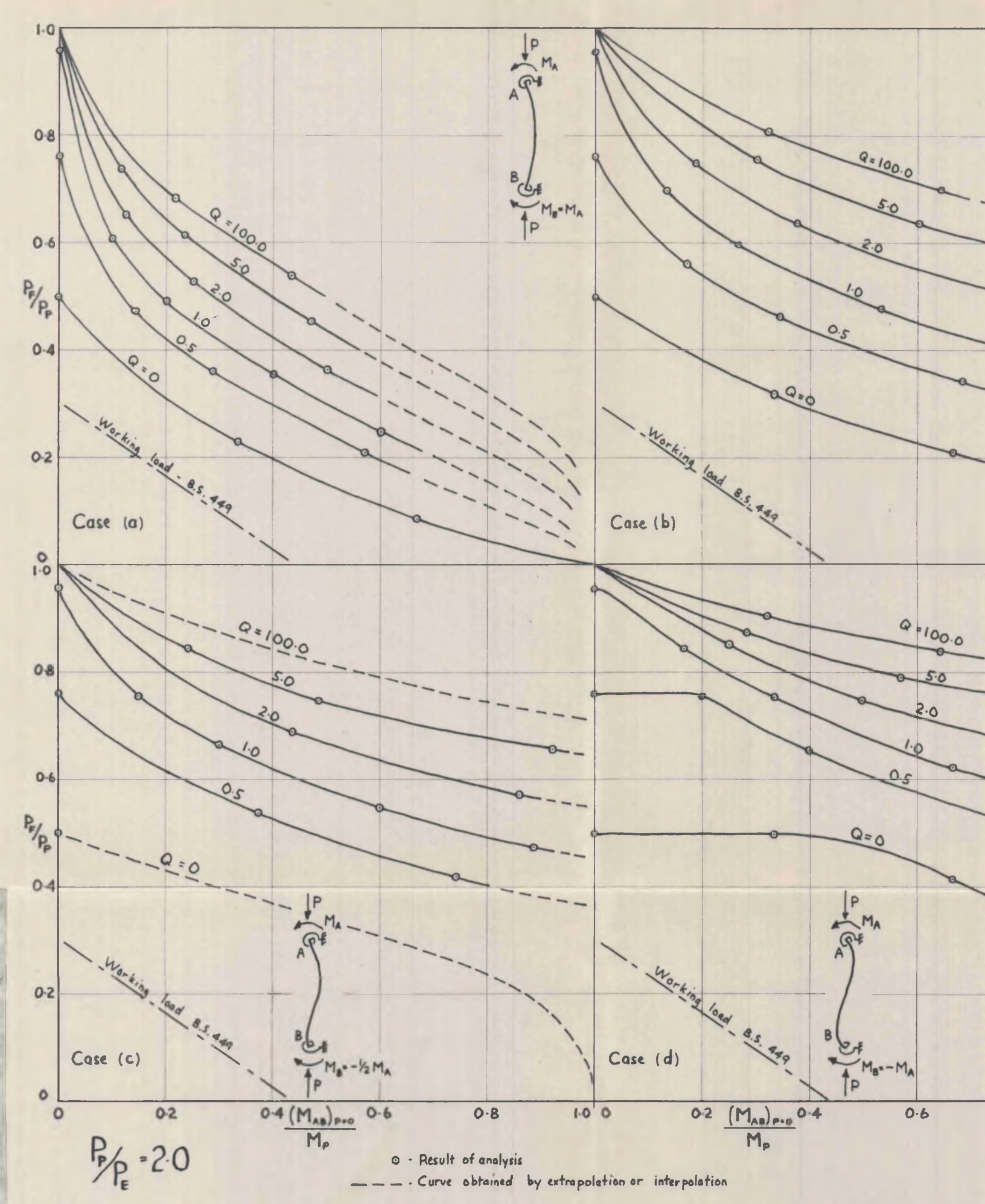

FIG. 5.12. COLLAPSE LOADS OF RESTRAINED COLUMNS OF IDEAL ELASTIC-PLASTIC MA

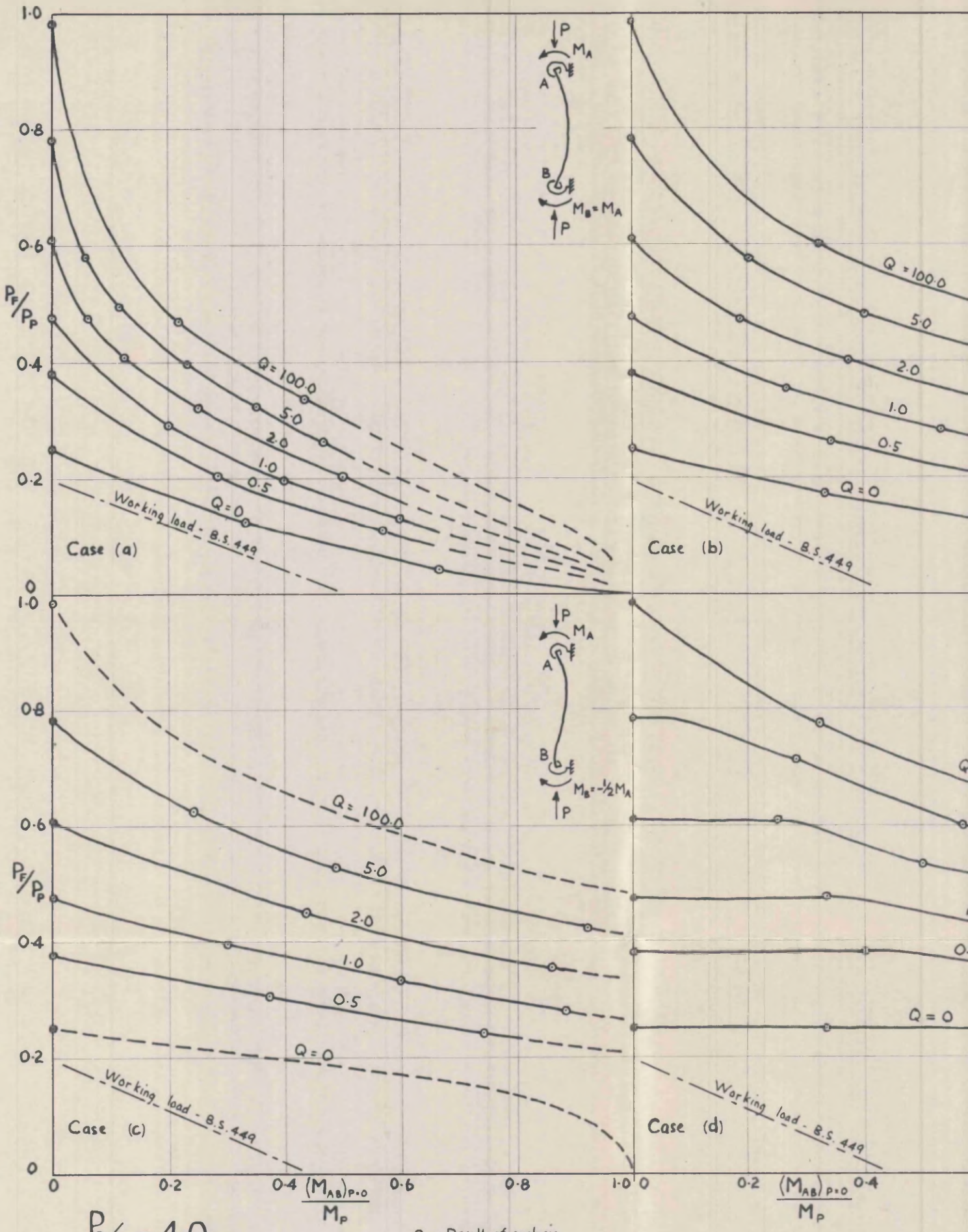

$P_P/P_E = 4·0$

o - Result of analysis

— — - Curve obtained by extrapolation or interpolation

FIG. 5.13 COLLAPSE LOADS OF RESTRAINED COLUMNS OF IDEAL ELASTIC-PLASTIC MA

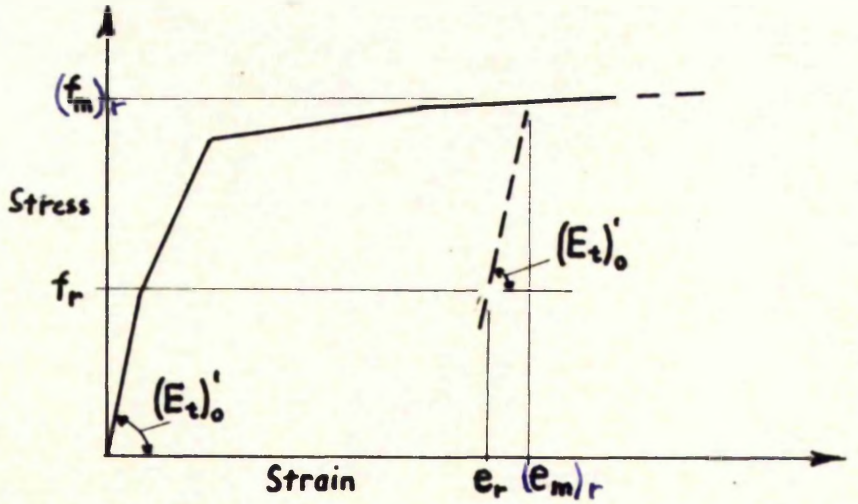

FIG A2.1. CALCULATION OF STRESS UNDER UNLOADING CONDITIONS.

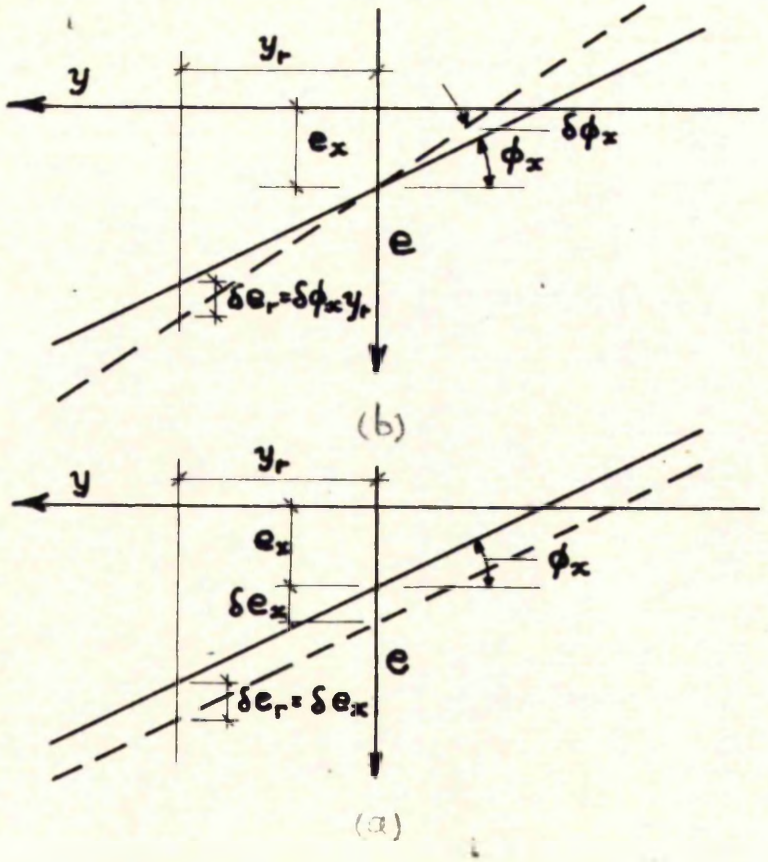

FIG A2.2 EFFECTS OF SMALL CHANGES IN AXIAL STRAIN AND CURVATURE.

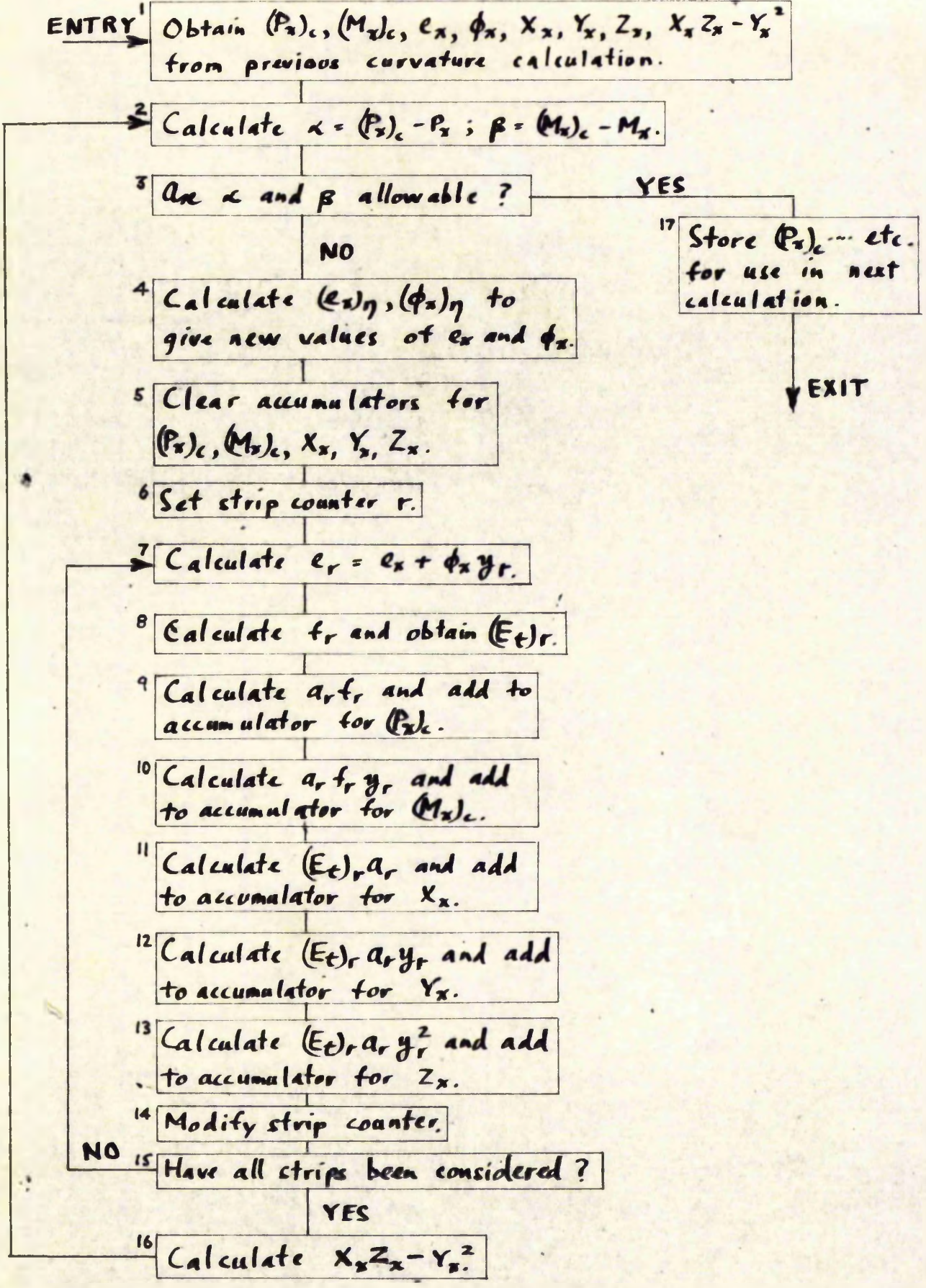

FIG. ~~A.3~~ A2.3

FLOW DIAGRAM FOR CURVATURE CALCULATION.

ENTRY

1 Calculate γ_A, γ_B based on $M_{AB} = M_{BA} = 0$
i.e. $\gamma_A = -M_A k_A$; $\gamma_B = -M_B k_B$.

2 Calculate $\frac{X_x}{X_x Z_x - Y_x^2}$ for each division point.

3 Calculate $(d\phi_x)_{dM_{AB}=1} = \frac{\left(1 - \frac{x}{N}\right) X_x}{X_x Z_x - Y_x^2}$ for each division point.

4 Integrate $(d\phi_x)_{dM_{AB}=1}$ to give $(d\theta_A)_{dM_{AB}=1} = \frac{\partial(\theta_A)_c}{\partial M_{AB}}$; $(d\theta_B)_{dM_{AB}=1} = \frac{\partial(\theta_B)_c}{\partial M_{AB}}$

5 Calculate $(d\phi_x)_{dM_{BA}=1} = \frac{\frac{x}{N} X_x}{X_x Z_x - Y_x^2}$ for each division point.

6 Integrate $(d\phi_x)_{dM_{BA}=1}$ to give $(d\theta_A)_{dM_{BA}=1} = \frac{\partial(\theta_A)_c}{\partial M_{BA}}$; $(d\theta_B)_{dM_{BA}=1} = \frac{\partial(\theta_B)_c}{\partial M_{BA}}$

7 Set up coefficients of L.H. sides of equations A2.21 and solve to obtain $(M_{AB})_1$ and $(M_{BA})_1$. Hence obtain new values of M_{AB} and M_{BA}.

8 Are values of M_{AB} and M_{BA} to be read manually ?

YES → 16 Read values of M_{AB}, M_{BA}, over-writing values obtained above.

NO

9 Calculate bending moment at each division point.

10 Calculate curvature at each division point

11 Integrate curvatures to give calculated deflections and end rotations $(\theta_A)_c$, $(\theta_B)_c$.

12 Calculate $\gamma_A = (\theta_A)_c - (M_A - M_{AB}) k_A$
$\gamma_B = (\theta_B)_c - (M_B - M_{BA}) k_B$
giving R.H. sides of equations A2.21

NO ← 13 Are γ_A and γ_B sufficiently small ?

YES

14 Store data required for later stages in the analysis.

15 Punch out results

EXIT

FIG. A2.4

FLOW DIAGRAM FOR ANALYSIS UNDER MOMENT LOADING ONLY.

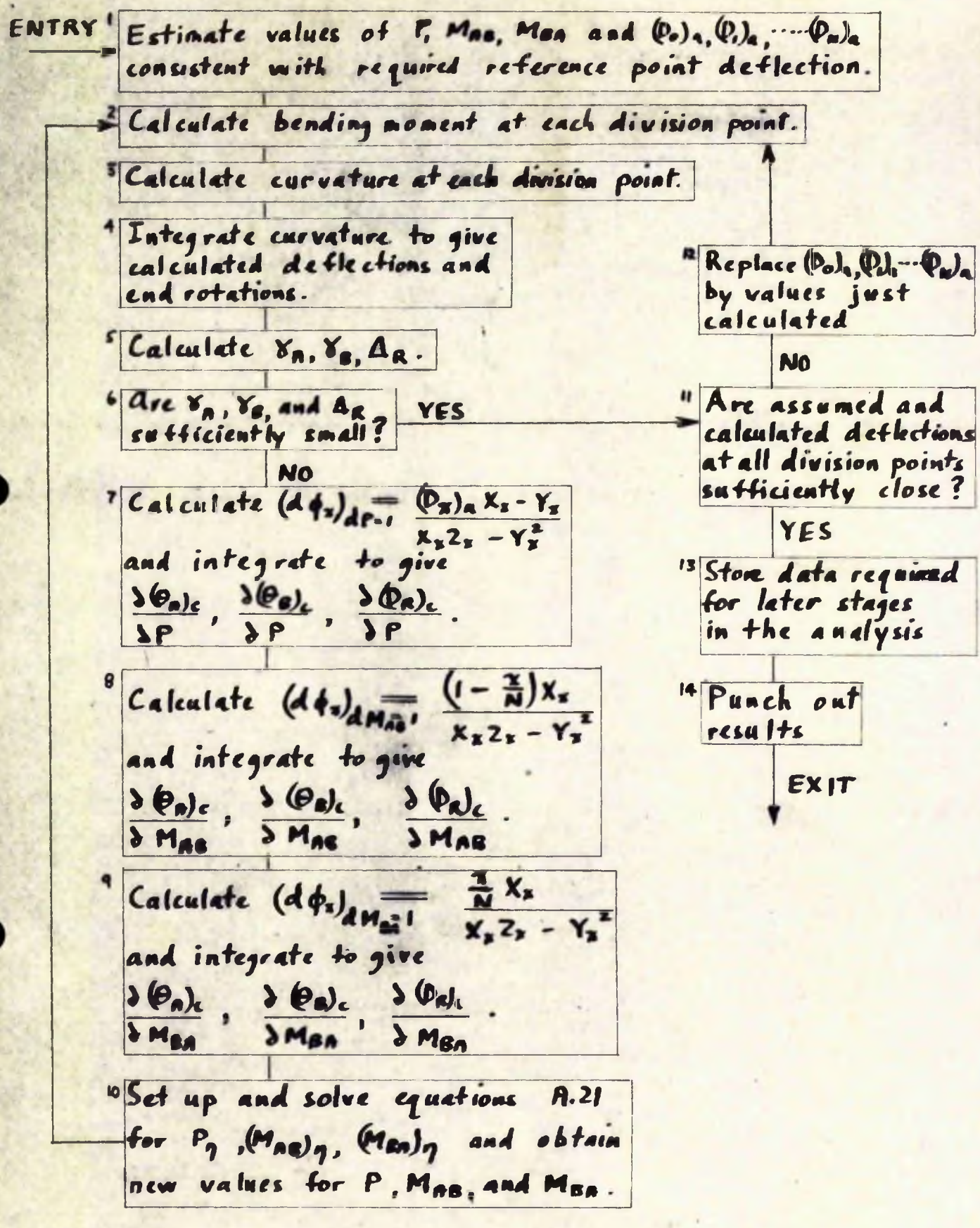

FIG. A.5

FLOW DIAGRAM FOR ANALYSIS UNDER END MOMENT LOADING AND AXIAL LOAD.

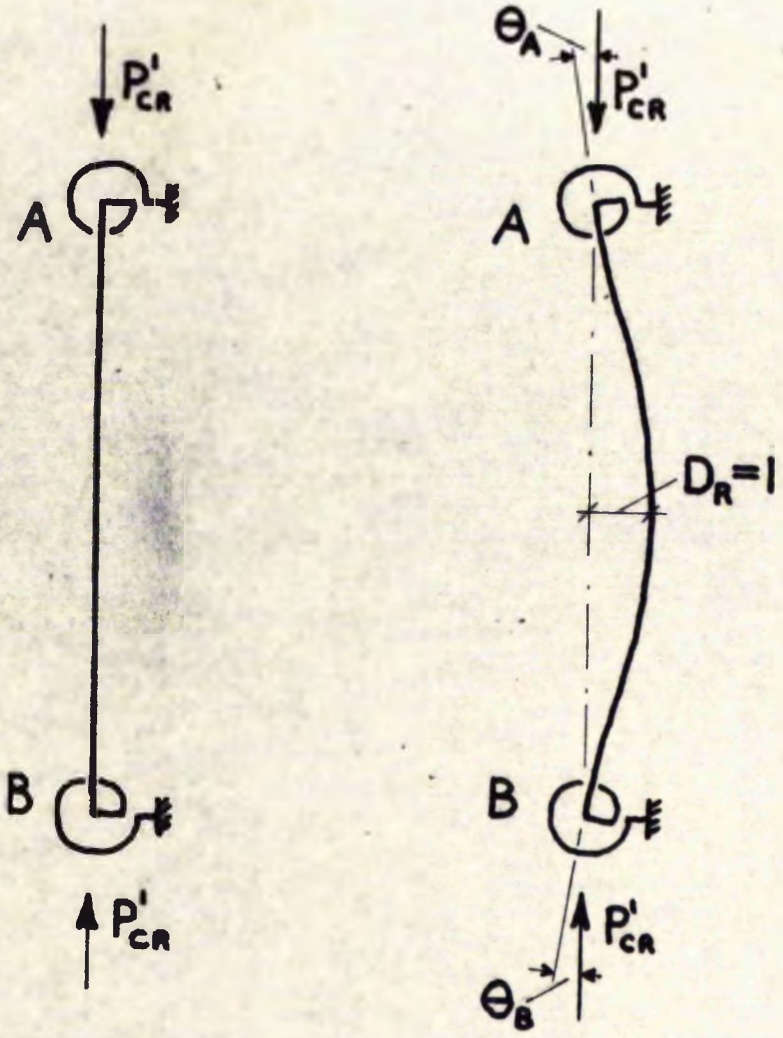

FIG A2.6. SYSTEM ANALYSED IN REDUCED CRITICAL LOAD CALCULATION.

ENTRY

1 Calculate stiffness $\frac{1}{(EI)'_x} = \frac{X_x}{X_x Z_x - Y_x^2}$ at each division point.

2 Obtain values of $P'_{CR}, (M_{AB})_{CR}, (M_{BA})_{CR}$, and $D_0, D_1, D_2, \cdots D_N$, from previous calculation to serve as initial trial.

3 Calculate bending moment at each division point.

4 Obtain appropriate stiffness value, i.e. $\frac{1}{(EI)'_x}$ if bending moment is in the same direction as the actual bending moment on the column, otherwise $\frac{1}{(EI)_x}$.

5 Calculate curvature at each division point.

6 Integrate curvature to give calculated deflections and end rotations.

7 Calculate $\gamma_A, \gamma_B, \Delta_R$.

8 Are γ_A, γ_B, and Δ_R sufficiently small?

YES → 13 Are assumed and calculated deflections at all division points sufficiently close?

NO → 14 Replace $(D_0)_a, (D_1)_a \cdots (D_N)_a$ by values just calculated. → 3

13 NO

YES → 15 Store $P'_{CR}, (M_{AB})_{CR}$ $(M_{BA})_{CR}$ and $D_0, D_1, \cdots D_N$ for use as trial for next calculation

16 Punch out results.

EXIT

8 NO

9 Calculate $(d\phi)_{dP'_\eta}$ and integrate to give $\frac{\partial(\theta_A)_c}{\partial P'}, \frac{\partial(\theta_B)_c}{\partial P'}, \frac{\partial(D_R)_c}{\partial P'}$.

10 Calculate $(d\phi_x)_{dM_{AB}}$ and integrate to give $\frac{\partial(\theta_A)_c}{\partial M_{AB}}, \frac{\partial(\theta_B)_c}{\partial M_{AB}}, \frac{\partial(D_R)_c}{\partial M_{AB}}$.

11 Calculate $(d\phi_x)_{dM_{BA}}$ and integrate to give $\frac{\partial(\theta_A)_c}{\partial M_{BA}}, \frac{\partial(\theta_B)_c}{\partial M_{BA}}, \frac{\partial(D_R)_c}{\partial M_{BA}}$.

12 Set up and solve equations A247 for $P'_\eta, (M_{AB})_\eta, (M_{BA})_\eta$ and obtain new values for $P'_{CR}, (M_{AB})_{CR}, (M_{BA})_{CR}$. → 3

FIG. ~~A37~~ A2.7

FLOW DIAGRAM FOR ANALYSIS TO OBTAIN REDUCED CRITICAL LOAD (VON KARMAN CRITERION).

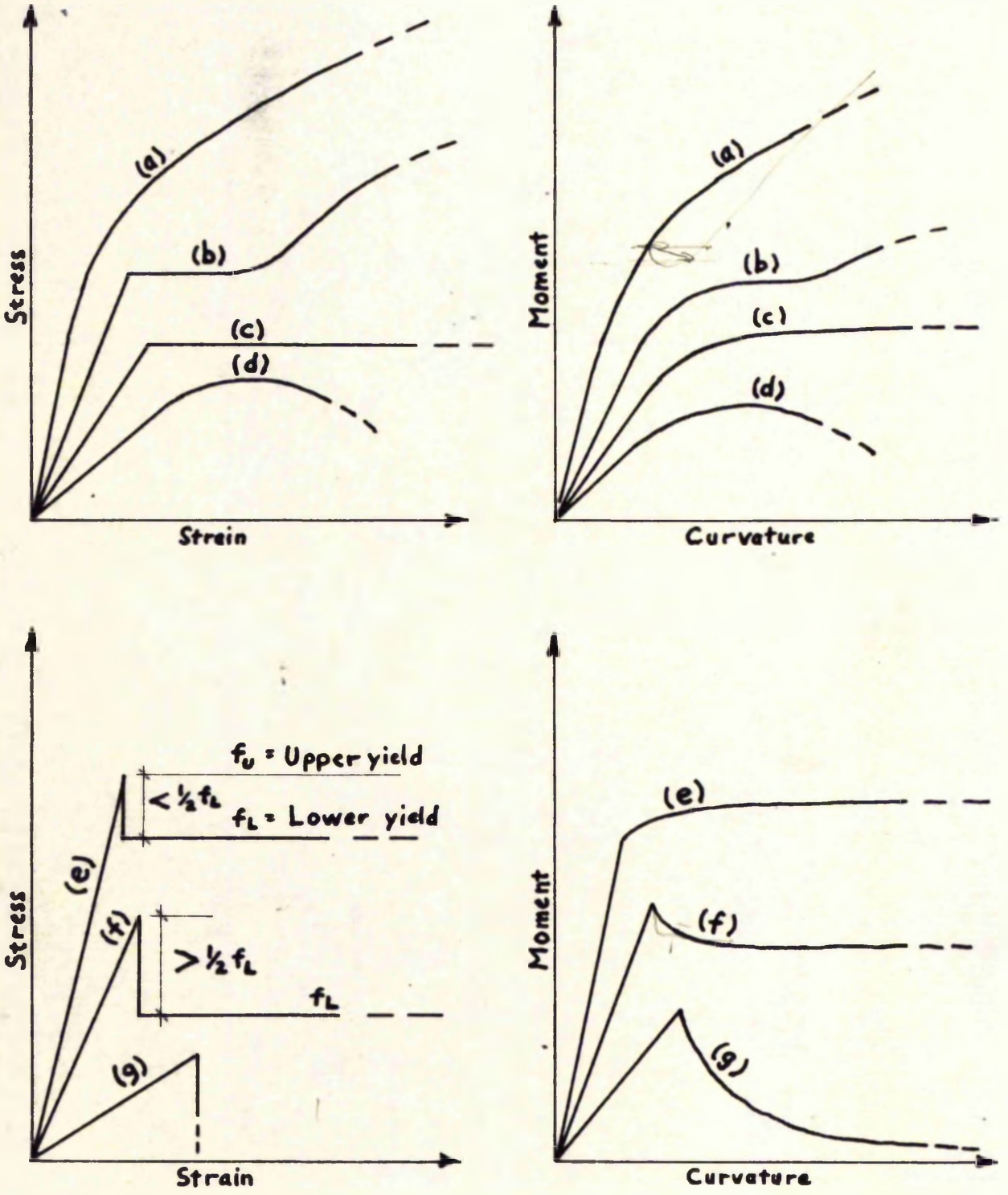

FIG A2.8. STRESS-STRAIN CURVES WITH CORRESPONDING MOMENT CURVATURE RELATIONS.

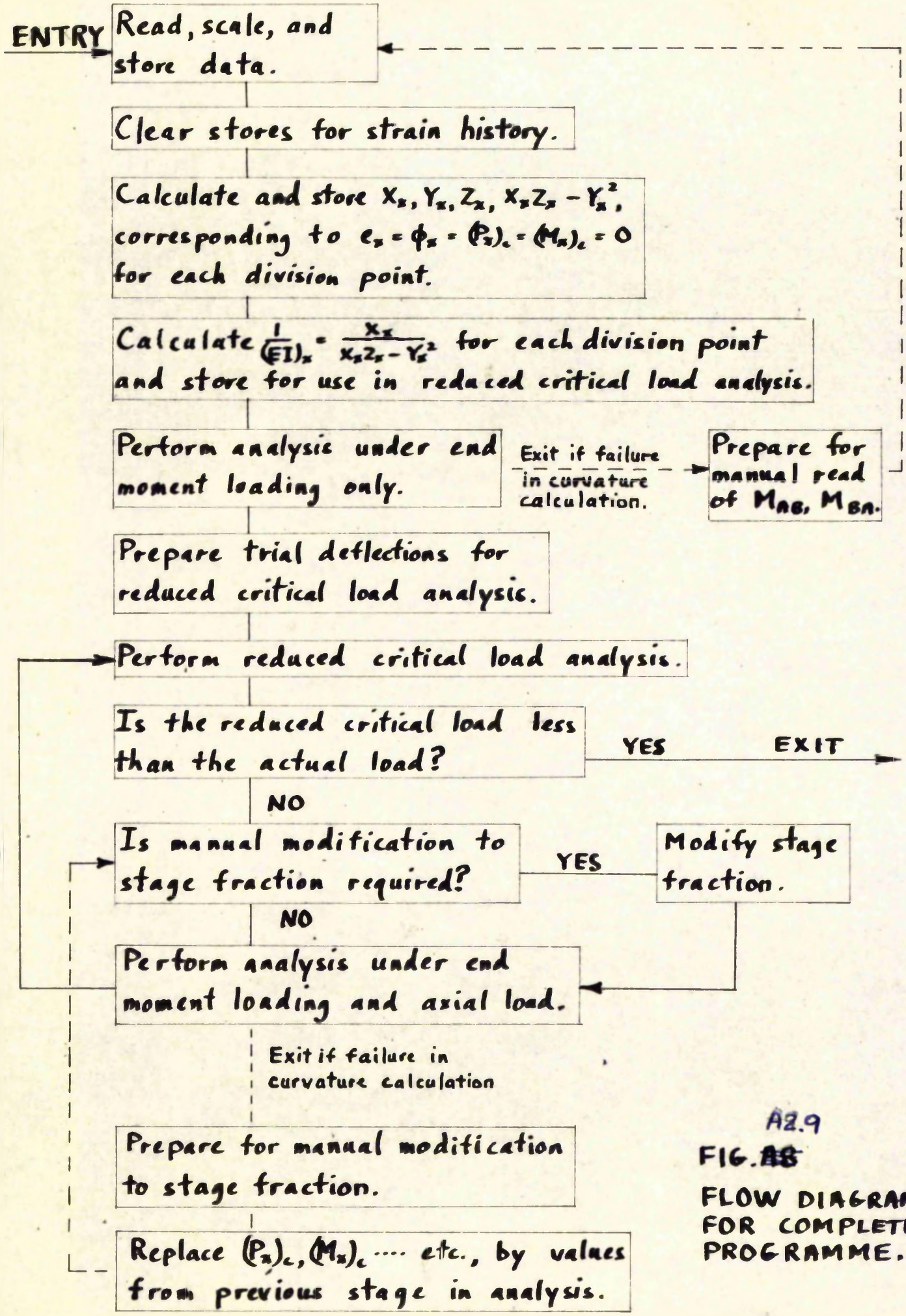

A2.9

FIG. ~~A8~~

FLOW DIAGRAM FOR COMPLETE PROGRAMME.

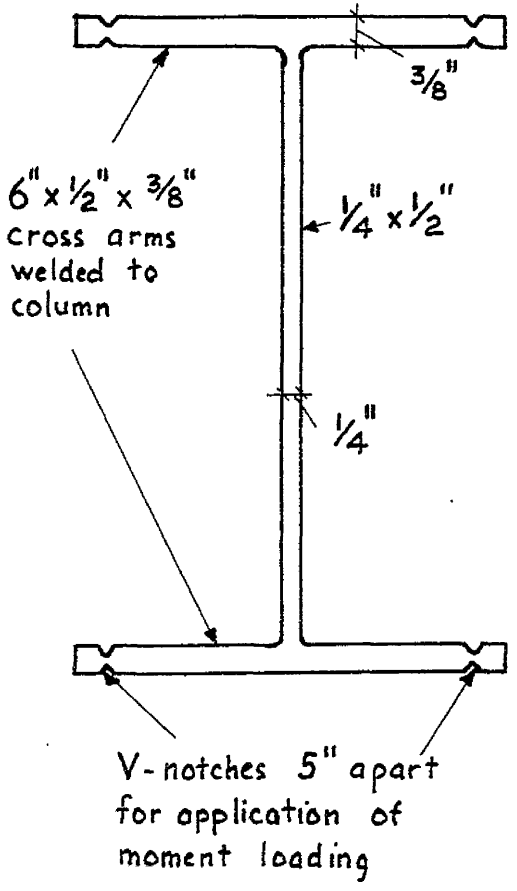

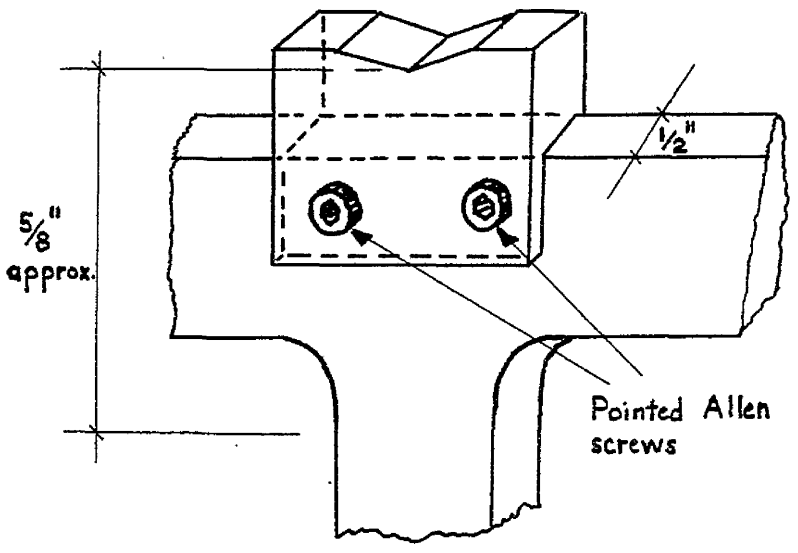

Sketch of case-hardened
steel saddle

FIG A3.1. TEST COLUMN DETAILS

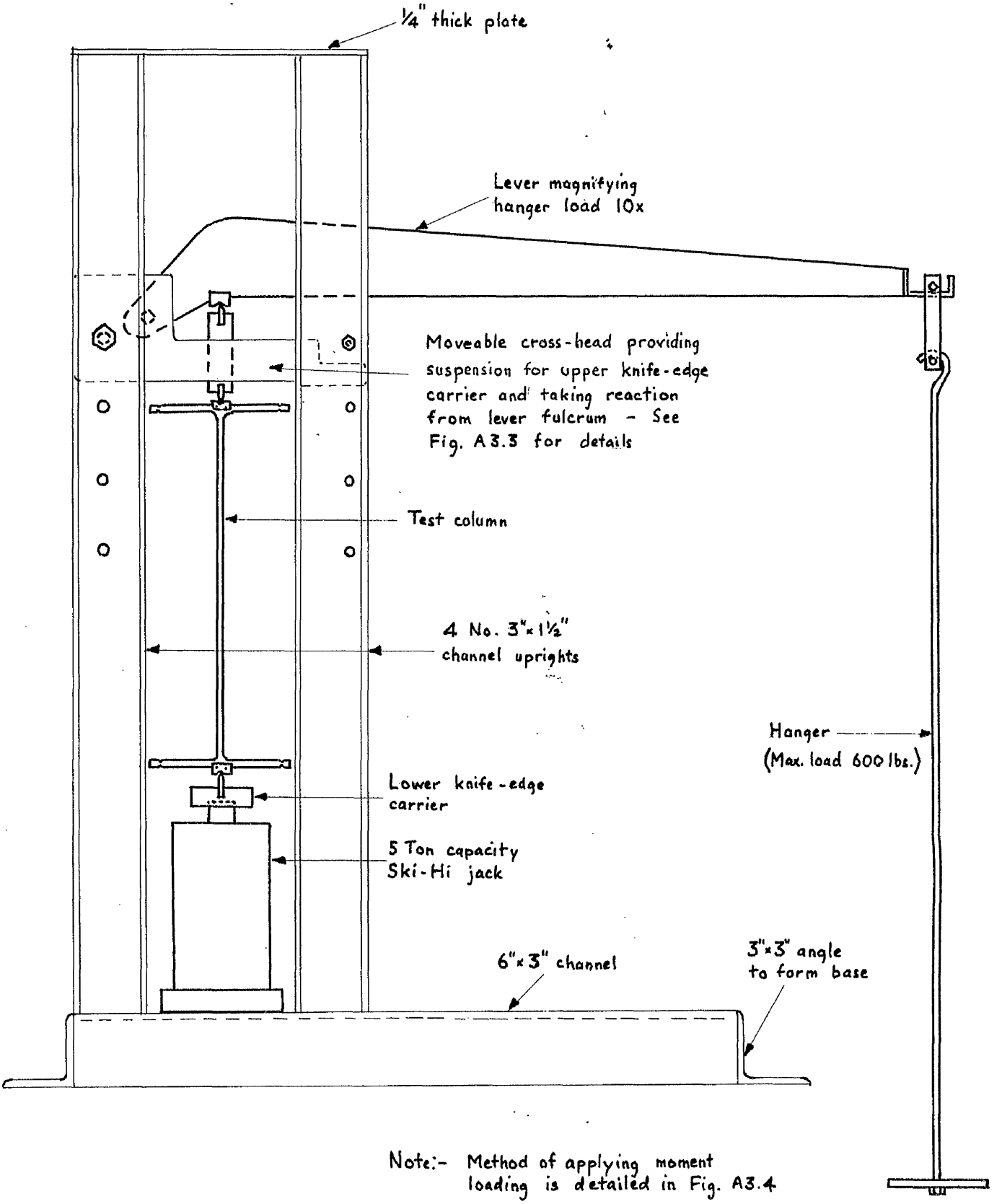

Note:- Method of applying moment loading is detailed in Fig. A3.4

FIG A3.2. OUTLINE OF TEST FRAME SHOWING METHOD OF APPLYING AXIAL LOAD

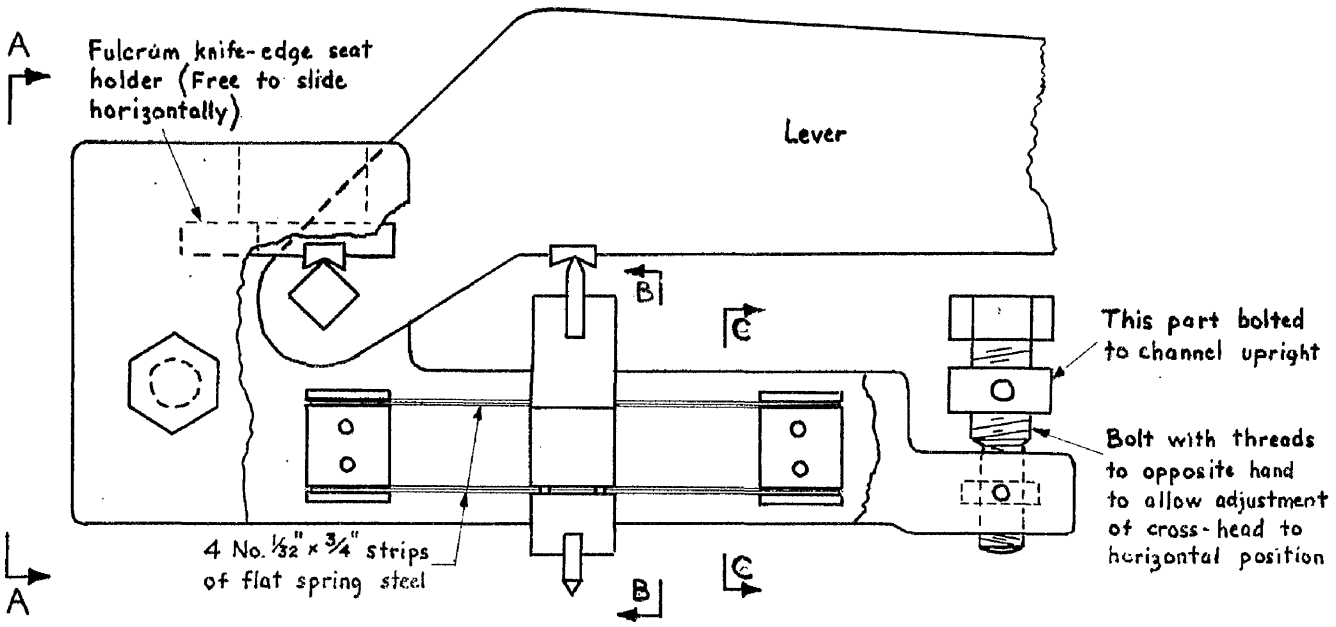

ELEVATION

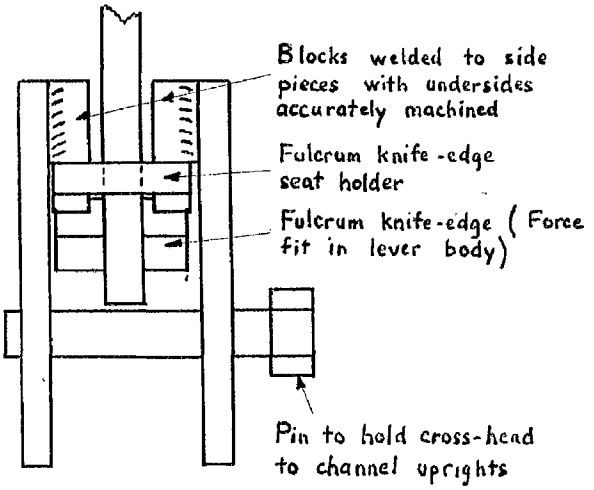

VIEW ON A-A

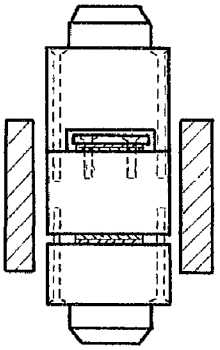

SECTION B-B

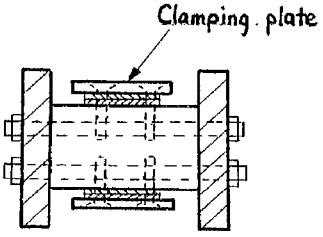

SECTION C-C

FIG A3.3. DETAILS OF CROSS-HEAD

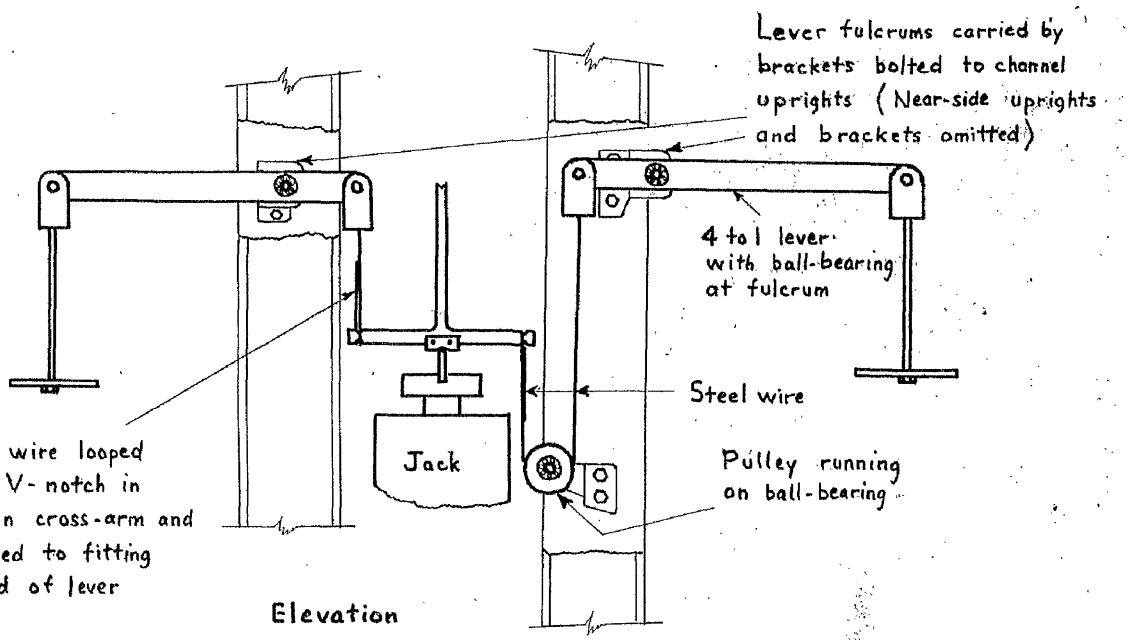

(a) Lower moment loading

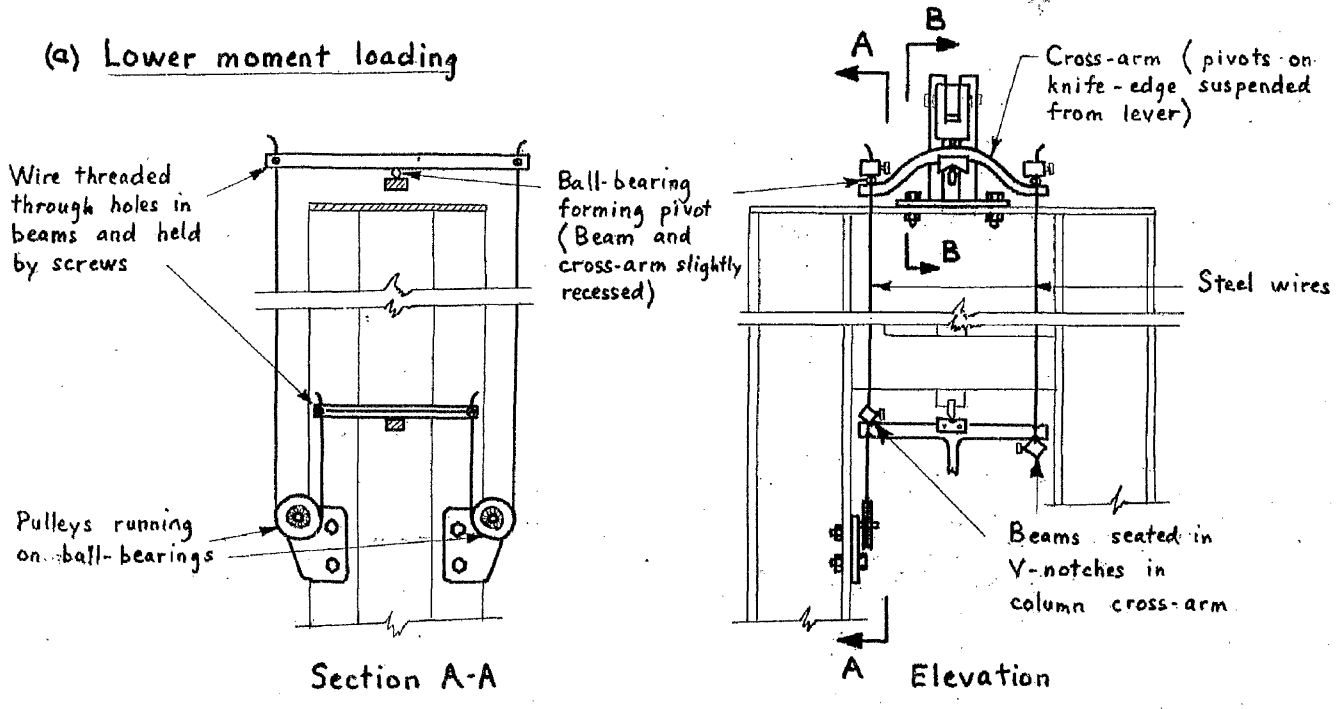

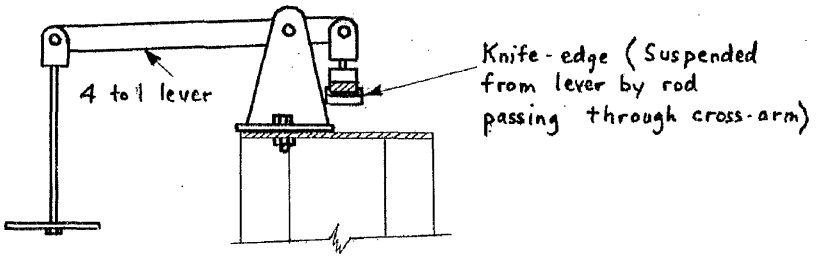

(b) Upper moment loading

FIG. A3.4. METHOD OF APPLYING MOMENT LOADING

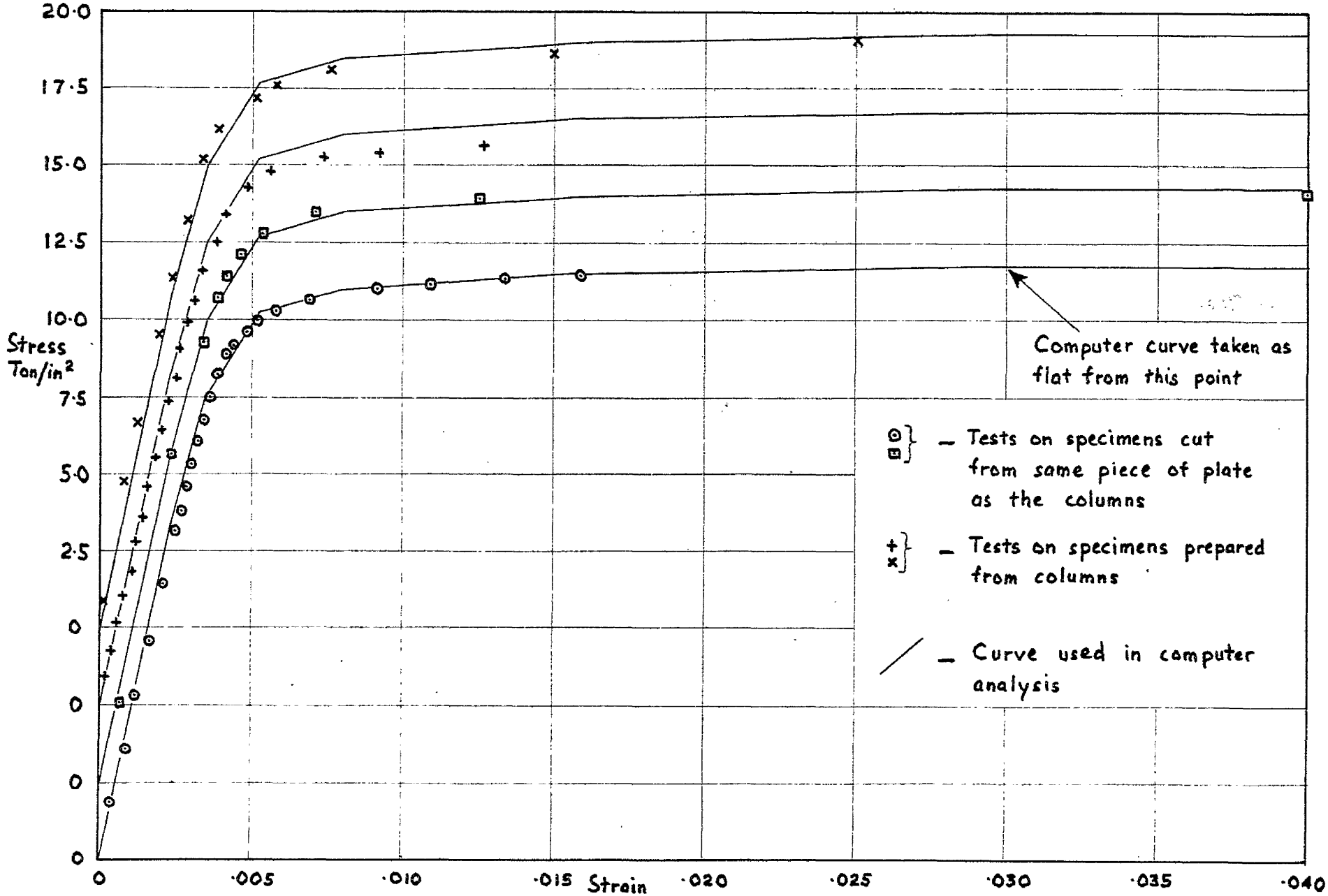

FIG. A3.5. STRESS STRAIN CURVES FOR HE30WP ALUMINIUM ALLOY

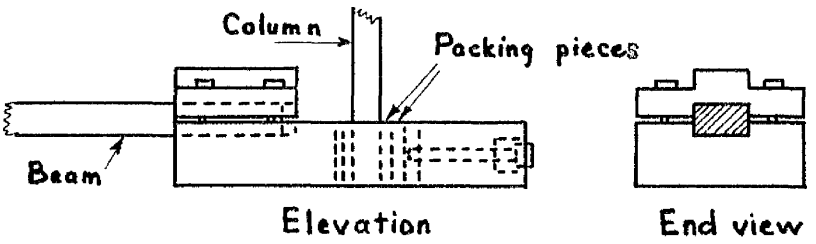

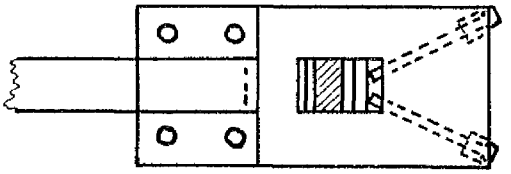

(a) End fitting

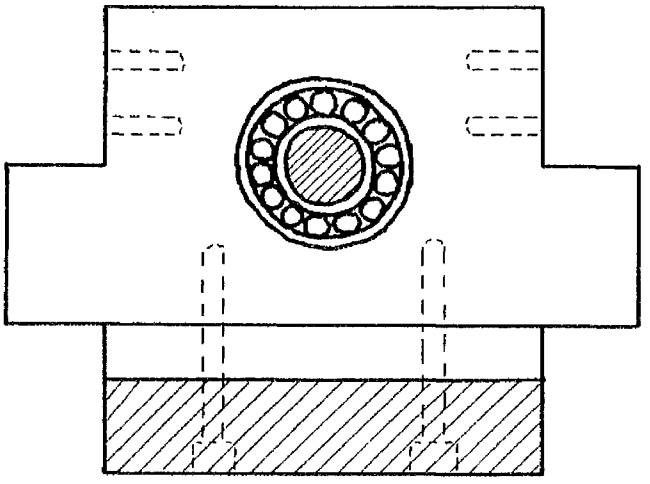

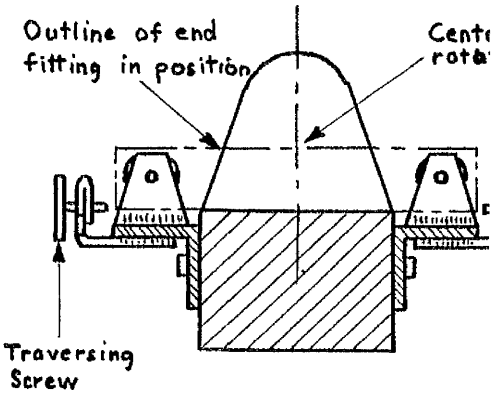

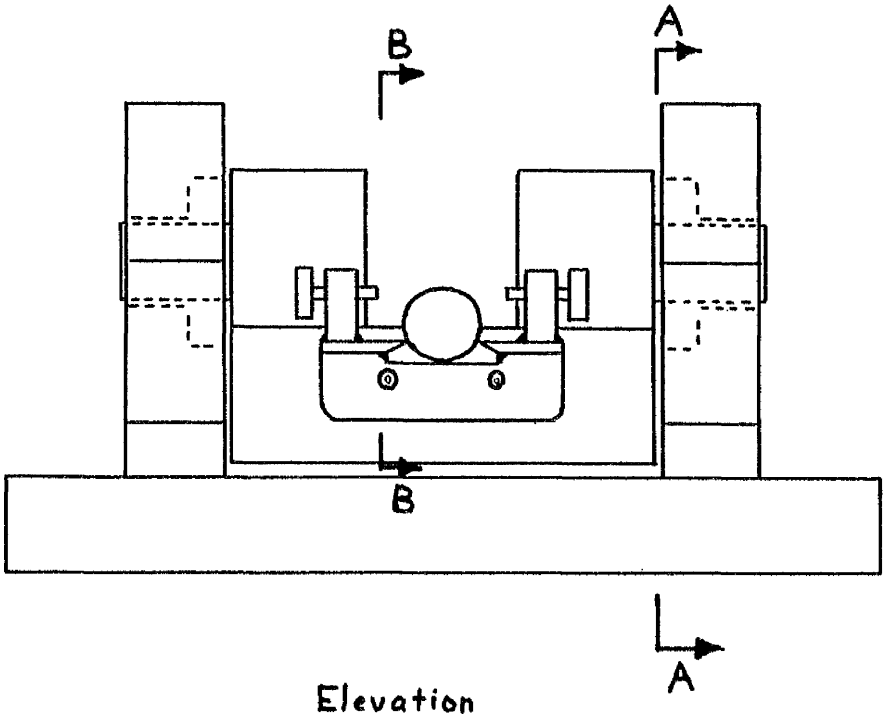

(b) Loading head

FIG. [illegible] DETAILS OF TEST RIG FOR ALUMINIUM COLUMNS

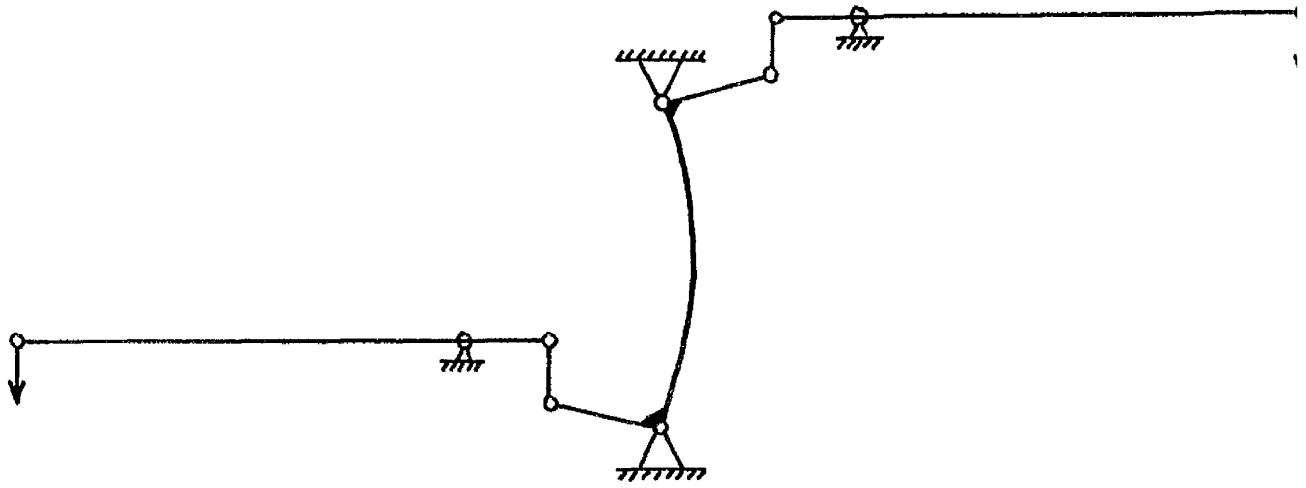

Case (a) loading

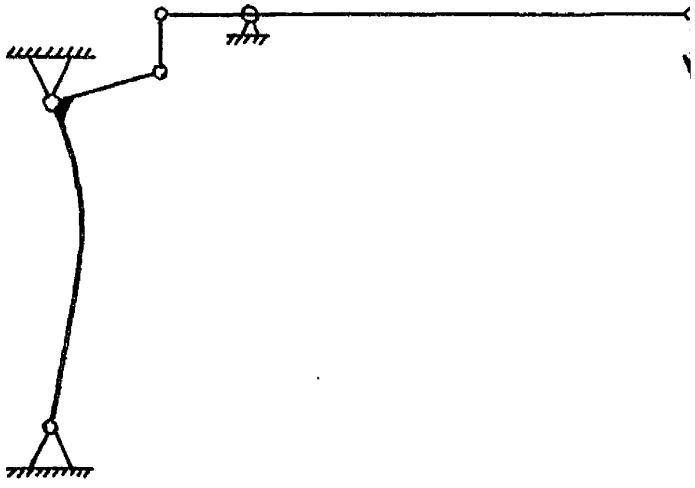

Case (b) loading

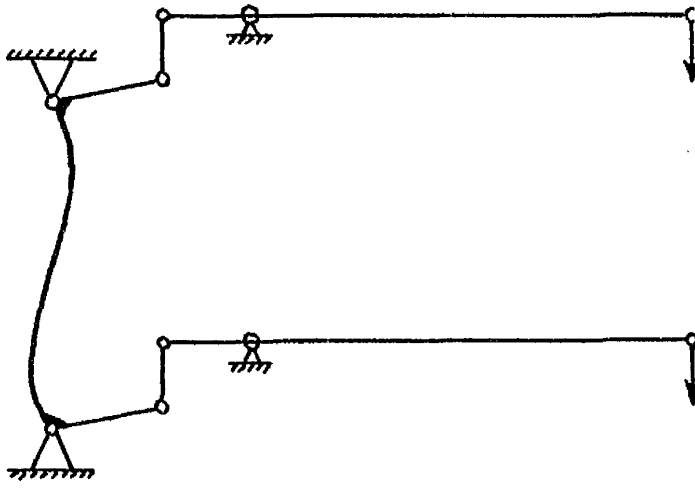

Case (d) loading

FIG. A5.7. ARRANGEMENT OF LEVERS FOR TESTS ON PINNED ALUMINIUM COLUMNS.